RETINOBLASTOMA-RELATED regulates cell size of mitotic and post-mitotic cells under standard and elevated temperatures in *Arabidopsis thaliana*

Ph.D. Dissertation

Shiekh Rasik Bin Hamid

Supervisor: **Dr. Magyar Zoltán**

Doctoral School of Biology

University of Szeged

Institute of Plant Biology

HUN-REN Biological Research Centre, Szeged, Hungary.

Szeged, 2025

Table of contents

ABBREVIATIONS

ACD- Asymmetric cell divisions

ARF6- Auxin response factor 6

AtSMOS1-AP2 TYPE transcription factor, Arabidopsis relative of the rice SMALL ORGAN SIZE 1

bHLH- basic-helix-loop-helix

BZR1- Brassinazole resistant 1

bZIP- basic leucine zipper transcription factor

CDK- CYCLIN-DEPENDENT KINASE

CDKB2- CYCLIN DEPENDENT KINASE B2

CKI – CDK inhibitor proteins

CO- CONSTANS

CRY2- Cryptochrome circadian regulator 2

DEL- DELLA transcriptional regulator

DP- DIMERIZATION PARTNER

DREAM- DP-RBR-E2Fs-And MUVB

E2F- E2FA, E2FB, E2FC transcription factors.

EDU- 5′ - ethynyl - 2′ - deoxyuridine

ELF3- EARLY FLOWERING 3

EEN- INO80-EIN6 ENHANCER

FCA- Flowering control locus A

FLM- Flowering locus M

FLP- FOUR LIPS

FT- Flowering locus T

G-phase- Gap phase of the cell cycle

GC- Guard cells

GFP- Green fluorescent protein

GMC- Guard mother cell

HY5- Elongated hypocotyl 5

IAA19- Indole -3- acetic acid inducible 19

IAA29- Indole -3- acetic acid inducible 29

JMJ14- JUMONJI 14

KN- KNOLLE

KRPs- KIP RELATED PROTEINS

LLPS- Liquid-liquid phase separation

M-phase- Mitotic phase

MIP- Myoinhibiting peptide precursor

MuvB- Multi-vulval class B

ORC2- Origin recognition complex 2

PHOT- Phototropin

PhyA- Phytochrome A

PhyB- Phytochrome B

PIF4- Phytochrome interacting factor 4

PIF7- Phytochrome interacting factor 7

PRC2- Polycomb repressive complex 2

QC- Quiescent centre

qRT-PCR- Quantitative Reverse Transcription Polymerase Chain Reaction

RAM- Root apical meristem

RB- RETINOBLASTOMA

RBR- RETINOBLASTOMA-RELATED

(RUP1-2)- Repressor of UV-B Photomorphogenesis 1 and 2

S-phase- Synthesis phase

SAM- Shoot apical meristem

SCD- Symmetric cell divisions

SCL28- SCARECROW-LIKE28

SCRM- SCREAM

SMRs- SIAMESE RELATED PROTEINS

SOC1- SUPPRESSOR OF OVEREXPRESSION OF CONSTANS

SPCH- SPEECHLESS

SVP- SHORT VEGETATIVE PHASE

TSF- TWIN SISTER OF FT

UVR8- UV resistance locus 8

YUC- YUCCA genes (YUC1,2,8,9)

1. INTRODUCTION

1.1 Plants response to warm temperatures: THERMOMORPHPOGENESIS

Climate change presents a significant challenge to current and future crop production efficiency and food security (Ray *et al.* 2019; Ortiz-Bobea *et al.* 2021; Mirón *et al.* 2023). In addition to the anticipated increase in the frequency of extreme weather events (Arnell *et al.*, 2019; Mirón *et al.*, 2023), a consistent rise in the average global temperature poses a substantial concern. Temperature exerts a considerable influence on plant development, growth, metabolism, and defence mechanisms (Lippmann *et al.*, 2019), thereby significantly affecting the distribution of optimal crop production regions (Anderson *et al.*, 2020).

Plants are sessile organisms that lack homeostatic mechanisms to regulate body temperature. They have evolved sophisticated regulatory mechanisms to adapt to varying temperatures, ensuring enhanced survival and reproduction, as well as maintaining growth and development (McClung et al., 2016). A non-stressful but significant increase in average temperatures not only accelerates the metabolism and growth of plants but also activates adaptation processes. These adjustments to the vegetative body plan are mediated by a phytohormone-dependent pathway known as thermo-morphogenesis, which is crucial for plant fitness and yield (Crawford et al., 2012, Casal and Balasubramanian, 2019). Characteristic features of thermomorphogenesis include elongation of the hypocotyl, stem, petiole, and primary root, as well as hyponasty of leaves with decreased surface area (Quint *et al.*, 2016; Casal and Balasubramanian, 2019; Lippmann *et al.*, 2019; Wang and Zhu, 2022), which collectively contribute to enhanced evaporative leaf cooling (Crawford *et al.*, 2012; Bridge *et al.*, 2013; Park *et al.*, 2019). Thermomorphogenesis research has initially

addressed and continues to elucidate two central questions: How do plants sense subtle changes in ambient temperature, and how are these changes translated into well-defined morphological alterations? The majority of our knowledge regarding the molecular players involved in this process derives from studies of hypocotyl elongation in Arabidopsis seedlings grown at 27-29°C (thermomorphogenesis) in comparison to 22-24°C (typical morphogenesis). These investigations have demonstrated that ambient light and temperature signalling share common pathways (Casal and Qüesta, 2018; Romero-Montepaone *et al.*, 2021; Qi *et al.*, 2022; Wang and Zhu, 2022; Legris, 2023; Wu *et al.*, 2023).

1.1.1 Sensing warm temperatures

1.1.2 Light sensors function as thermo-sensors: the involvement of phytochromes

To initiate an appropriate response to fluctuating temperatures, plants require precise temperature change detection mechanisms. Multiple recent studies have revealed different ambient temperature sensors and their mechanisms for temperature sensing in plants. Phytochrome B (PhyB), a photoreceptor comprising an open-chain tetrapyrrole chromophore, has been identified as a temperature sensor that regulates various aspects of thermomorphogenesis acceleration during flowering, senescence, and architectural changes (Jung et al., 2016; Quint et al., 2016). Photoreceptor PhyB also functions as a thermosensor in plants (Jung *et al.* 2016). Its identification was based on biochemical properties and its association with chromatin (Legris et al., 2016). Phytochromes (including five members; PhyA to PhyE) exist in two photo-interconvertible isoforms (Burgie et al., 2014). Phytochromes are sensitive light receptors synthesized in the red light (R)-absorbing inactive form (Pr) and far-red (FR)-absorbing active form (Pfr). These sensitive photoreceptors absorb light via the phytochromobilin chromophore. The (Pr) form is

converted into the (Pfr) form of PhyB upon exposure to red light. Consequently, the percentage of the Pfr form is controlled by the R/FR ratio (Rockwell et al., 2006), whereas exposure to FR light initiates reversion to the (Pr) inactive form (Hayes, 2020; Fig. 1). Thermal reversion of Pfr to Pr is a light-independent process that can occur in both dark and light environments and promotes thermomorphogenesis (Fig. 1). Pfr is known to translocate from the cytoplasm to the nucleus, where, in conjunction with its interacting proteins, it forms photobodies (Pardi and Nusinow, 2021; Kim *et al.*, 2023). PhyB, due to its intrinsically disordered N-terminal extension, spontaneously undergoes liquid-liquid phase separation (LLPS) to assemble these liquid-like droplets (Chen *et al.*, 2022). It has been demonstrated that PhyB can differentiate between light and temperature cues owing to conformational changes and phase separation, respectively (Chen *et al.*, 2022).

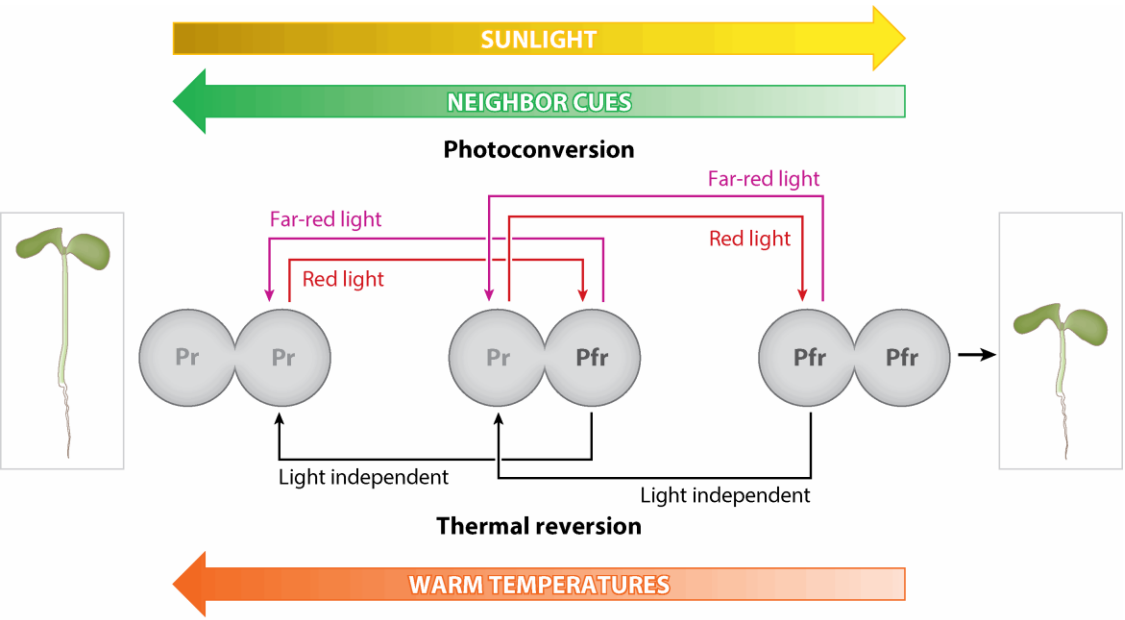

Figure 1. Temperature and light sensing by PhyB. The steady state of the active conformer of PhyB, the Pfr-Pfr homodimer, depends on light and thermal reactions. Abbreviations: Pfr, far red light -absorbing phytochrome B; Pr, red light-absorbing phytochrome. (Casal, J. J., & Balasubramanian, S. (2019), Thermomorphogenesis. *Annual review of plant biology*, *70*, 321-346).

PhyB is not the sole photosensor for plants that exhibit temperature sensitivity. Hypocotyl growth (Jung et al., 2016) and flowering (Sanchez-Lamas et al., 2016) responses to temperature present in *phyb* mutant are absent in the quintuple phytochrome mutant, suggesting that other phytochromes either sense temperature or are necessary to establish the conditions for a temperature response.

1.1.3 Additional plant thermo-sensors

In addition to the phytochromes, the various blue light photoreceptors (the cryptochromes, phototropins, and ZEITUPLE protein) and the UV-B sensor *UVR8* also exhibit temperature-dependent changes in their activity and thus may influence the thermomorphogenic response (Ma *et al.*, 2016; Hayes *et al.*, 2017, 2021; Saitoh *et al.*, 2021; Jung *et al.*, 2023). In the liverwort *Marchantia polymorpha*, the blue-light photoreceptor phototropin (Phot) shows temperature-dependent (Low temperature) alterations in its activity (Fujii et al., 2017). In Arabidopsis, temperature signalling by phototropins (Phot1-2, Fig. 2) has recently been implicated, and warm temperatures that induce stomatal opening are dependent on phototropins and blue light (Kostaki et al., 2020). This indicates that warm temperatures promote the action of phototropin in guard cells of Arabidopsis. In the absence of light, *UVR8* exists as a homodimer; however, upon absorption of UV-B, it undergoes monomerization. In a process mediated by the Repressor of UV-B Photomorphogenesis 1 and 2 (RUP1-2), active *UVR8* monomers are converted into inactive dimers. RUP-mediated reversion of the active UVR8 monomer to the UVR8 dimer appears to be influenced by temperature (Findlay and Jenkins, 2016). However, there is currently insufficient evidence to conclude that cryptochrome and *UVR8* functions are sensitive to temperature and further research is required in this area. RNA secondary structures have been identified as

thermosensors in bacteria and animals (Vu et al., 2019). In a recent study, a discrete RNA-based thermo “switch” was also discovered in plants. Ribosome profiling was employed to identify genes that showed elevated translational efficiency upon exposure to warm ambient temperatures (27°C; Chung et al. 2020). Notably, among numerous genes, *PHYTOCHROME INTERACTING FACTOR 7* (*PIF7*) was one of the genes that displayed an elevated translation (Fig. 2). PIF7 is a key transcription factor that regulates morphological changes at high temperatures (Chung et al. 2020, Fiorucci et al., 2020). Among the mRNAs identified by Chung et al., (2020), several possessed a hairpin structure within their 5’ prime UTR, shortly upstream of their AUG translational start codon. Importantly, a structural change in the *PIF7* 5’ prime UTR hairpin was observed between 22°C and 27°C. This alteration in hairpin structure was proposed to enhance PIF7 translation at a warm ambient temperature (Chung et al. 2020). The regulation of PIF7 translation is not solely attributed to the presence or absence of the hairpin. Consequently, the authors believe that in response to warm temperatures, structural information in the hairpin is essential for the dynamic regulation of translation (Chung et al., 2020). The ELF3 (Early flowering 3) protein is a component of the evening complex (EC) in Arabidopsis. *In vitro* studies show that its DNA-binding activity is stronger at 4°C and weaker at 27°C (Silva et al., 2020). ELF3 has been reported to form "nuclear speckles" when interacting with ELF4 (Herrero et al., 2012). Recent research suggests that these speckles result from liquid-liquid phase separation (LLPS). A prion-like domain (PrD) in ELF3 drives this process, particularly under high temperatures (30–35°C), facilitating the transition of ELF3 from an active to an inactive state. Thus, the PrD of ELF3 acts as a temperature-sensitive thermosensor (Jung et al., 2020).

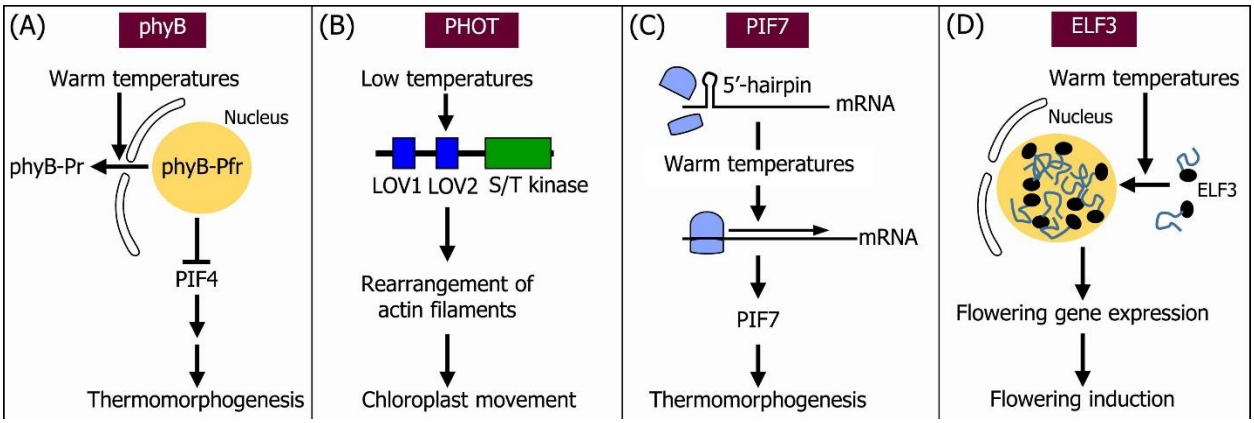

Figure 2. Thermosensory Molecules and Mechanisms in Plants. **A**) Phytochrome B (PhyB). Warm temperatures accelerate the Pfr-to-Pr conversion of PhyB in darkness and, accordingly, the number of phyB -containing photobodies is reduced. As a result, the PHYTOCHROME INTERACTING FACTOR 4 (*PIF4*) function is derepressed, leading to induction of thermomorphogenic hypocotyl growth. **B**) Phototropin (PHOT). In the phototropin receptors, the activated status of the light, oxygen, voltage 2 (LOV2) domain is sustained for longer at low temperatures, and the hyperactivated phototropins trigger the rearrangement of actin filaments, causing chloroplast movement. **C**) *PIF7* mRNA conformer. The 5'-end sequence of *PIF7* mRNA harboring a hairpin conformation senses temperature changes. Under warm temperatures, the hairpin structure is disrupted, and the *PIF7* mRNA is readily translated. PIF7 triggers auxin biosynthesis, leading to thermomorphogenic hypocotyl elongation. **D**) EARLY FLOWERING 3 (ELF3). The prion domain of *ELF3* has intrinsically disturbed regions and acts as a biophysical thermosensor by forming nuclear condensates via phase separation, which mediates the thermal control of flowering induction. It is notable that *ELF3* molecules, and possibly also PhyB, undergo phase separation, forming membrane less compartments. Given the sensitivity of biomolecular condensates to protein concentrations, the nearby presence of other biomolecules, temperature, ionic strength, pH, and metabolic ingredients and status, it is anticipated that the dynamic formation of thermosensory biomolecular condensates is profoundly influenced by internal and metabolic cues in plant cells, contributing to reshaping thermomorphogenesis under changing environments.

1.1.4 Regulation of Hypocotyl Elongation Under Elevated Temperature Conditions

1.1.5 PIF4 a central hub for plant thermomorphogenesis (Transcriptional and Translational regulation)

A significant advancement in understanding the mechanism of thermomorphogenesis in response to moderately increased temperatures was the identification of the basic helix-loop-helix (bHLH) transcription factor PHYTOCHROME INTERACTING FACTOR 4 (PIF4), a crucial transcription factor that facilitates thermomorphogenesis (Koini et al., 2009; Sun et al., 2012). PIF4 belongs to subfamily 15 of the basic (bHLH) superfamily. Parallel light- and thermosensing by photoreceptors are integrated by the PIF4 transcription factor in aboveground plant organs (Koini et al., 2009; Stavang et al., 2009; Bian et al., 2022). *PIF4* is subject to both transcriptional and post-translational regulation in response to light and thermal stimuli, which fine-tune its level and activity (Ma et al., 2016; Martínez et al., 2018*b*; Han et al., 2019; Lee et al., 2020; Qiu, 2020; Qiu et al., 2021; Saitoh et al., 2021; Xu and Zhu, 2021; Zhao and Bao, 2021; Verma et al., 2023). Furthermore, its thermomorphogenesis-promoting activity is gated by the circadian clock (Martínez et al., 2018*b*; Sun et al., 2019; Zhang et al., 2021; Hendrix, 2022; Seo et al., 2023) and confined to the epidermis of the hypocotyl (Kim et al., 2020). *PIF4* reorganizes the transcriptome in concert with various interacting proteins, including hormone-responsive transcription factors, such as BRASSINAZOLE RESISTANT 1 (BZR1) and AUXIN RESPONSE FACTOR 6 (ARF6, Oh et al., 2014). During ambient temperature-dependent hypocotyl elongation, auxin synthesis and signalling are among the primary targets of PIF4 (Koini et al., 2009; Franklin et al., 2011; Sun et al., 2012; Bianchimano et al., 2023). PIF4 directly upregulates genes encoding *YUCCA8* (*YUC8*), *INDOLE-3-ACETIC ACID INDUCIBLE 19* (*IAA19*), and *INDOLE-3-ACETIC ACID INDUCIBLE 29* (*IAA29*). YUC8 is a rate-limiting auxin biosynthesis enzyme, which plays a central role in

temperature-dependent hypocotyl elongation (Franklin et al., 2011; Sun et al., 2012). Brassinosteroids, via the transcription factor BZR1, have also been shown to act downstream of PIF4 and auxin during temperature-induced growth promotion (Ibañez *et al.*, 2018; Martínez et al., 2018*a*; Nieto et al., 2020). As *BZR1* also interacts with and activates the transcription of *PIF4*, a feed-forward growth regulatory loop forms at elevated ambient temperatures (Oh et al., 2012; Ibañez et al., 2018).

In Arabidopsis, in addition to those dependent on PhyB, temperature-sensing mechanisms involving PHYTOCHROME INTERACTING FACTOR 7 (PIF7) and EARLY FLOWERING3 (ELF3) TFs have also been elucidated (Box et al., 2015; Raschke et al., 2015; Press et al., 2016; Chung et al., 2020; Fiorucci et al., 2020; Burko et al., 2022). ELONGATED HYPOCOTYL 5 (HY5), a basic leucine zipper transcription factor (Delker et al., 2014) is also a negative regulator of *PIF4* expression. At low temperatures, *hy5* mutants exhibit an elevated level of the *PIF4* transcript due to the non-binding of *HY5* to the promoter of *PIF4* (Delker et al., 2014). PIF7 and PIF4 interact with each other and co-regulate thermomorphogenesis-related gene expression, with the predominant effect of PIF7 under shade conditions (Chung *et al.*, 2020; Fiorucci *et al.*, 2020; Burko et al., 2022). PIF7 functions not only as a regulator of gene expression but also as a thermosensor (Chung et al., 2020, and Fig. 2). At elevated temperatures, the *PIF7* mRNA forms a hairpin within its 5′ untranslated region, resulting in increased translation and accumulation of the PIF7 protein (Chung et al., 2020). ELF3 suppresses temperature-induced growth by suppressing *PIF4* expression (Box et al., 2015; Raschke et al., 2015; Murcia et al., 2022). Similar to PhyB, ELF3 acts as a thermosensor due to its prion-like domains, allowing temperature-dependent LLPS (Jung et al., 2020; Murcia et al., 2022 and Fig. 2). As the temperature increases, the transition in the liquid phase reduces the activity of ELF3, thus permitting the accumulation of PIF4.

In addition to the numerous potential thermosensors and transcriptional and post-transcriptional regulators of *PIF4*, various epigenetic mechanisms contribute to the complexity of thermomorphogenesis regulation (Perrella et al., 2022). These include, among others, overall H3K4me3 demethylation by JUMONJI14 (JMJ14) and JMJ15 affecting gene activation and repression underlying the thermomorphogenic response (Cui et al., 2021). *PIF4*-mediated recruitment of the attenuator FLOWERING CONTROL LOCUS A (FCA) to the chromatin of growth-promoting genes including *YUC8* (Lee et al., 2014); histone deacetylation at the *YUC8* locus promoting PIF4-binding at warm temperatures (Tasset et al., 2018; van der Woude et al., 2019); and *PIF4*-interaction with the ATP-dependent chromatin remodelling complex INO80–EIN6 ENHANCER (EEN) to activate transcription of auxin-related genes, including *YUC8* (Xue et al., 2021). Most of these mechanisms have been observed to lead to temperature-dependent H2A.Z eviction of thermoresponsive genes to promote their transcription (Kumar and Wigge, 2010; Tasset et al., 2018; van der Woude et al., 2019; Xue et al., 2021).

1.1.6 THERMO-RESPONSE IN THE ROOTS

In comparison to the hypocotyl and other aboveground plant organs, the thermomorphogenic response of the root has been less investigated (Fonseca de Lima et al., 2021). The primary root may experience an increase in temperature near the soil surface; consequently, it may elongate to reach cooler soil layers that potentially contain more water. Under laboratory conditions, a moderate temperature of 26-29°C is sufficient to stimulate the growth of the primary root of Arabidopsis, a phenomenon that is mainly controlled by auxin (Fonseca de Lima et al., 2021; Ai et al., 2023; Bianchimano et al., 2023); however, in long-term responses, the primary role of brassinosteroids has been implicated (Martins et al., 2017). Thus, roots also exhibit

thermomorphogenic responses, the regulation of which appears to differ from that of the above-ground organs. To date, no root-born thermosensors have been identified, although research has shown that Arabidopsis roots can detect and respond to elevated temperatures independently of shoots (Bellstaedt et al., 2020; Ai et al., 2023). The findings of the study by (Gaillochet et al., 2020) and Borniego et al., (2022) indicated that PhyB, ELF3, and PIF7 are not responsible for root thermosensing, although their action on shoots might indirectly influence root growth. While the thermo-regulated elongation of the Arabidopsis hypocotyl primarily depends on auxin- and brassinosteroid-dependent increases in cell size and less on cell division (Bellstaedt et al., 2020), a recent study has reported that an auxin-mediated increase in meristem cell division activity is primary and predominant in the thermosensory response of the roots (Ai et al., 2023). However, the contribution of auxin and/or brassinosteroid-dependent cell elongation, particularly under prolonged high-temperature conditions, cannot be excluded from the root (Martins et al., 2017; Yang et al., 2017). Due to the limited number of studies conducted with different experimental setups, a comprehensive understanding of root thermomorphogenesis has not yet been established. For instance, reports are contradictory regarding the temperature-dependent change in the size of the root meristem (Hanzawa et al., 2013; Yang et al., 2017; Feraru et al., 2019; Ai et al., 2023). Although most studies underscore the importance of auxin in the thermo-response of the root (Fonseca de Lima et al., 2021), the link between auxin signalling and either upstream, as yet unknown, thermosensors, or downstream targets regulating cell division in the meristem remains to be elucidated.

1.1.7 Developmental acceleration by warm temperatures: early flowering response to ambient temperatures

The transition from the vegetative stage to the reproductive stage is critical for the reproductive success of plants, and is tightly controlled by both internal (gibberellin level) and various environmental signals, such as light quality, photoperiod, and temperature (Amasino, 2010; Pose et al., 2012; Capovilla et al., 2015; Song et al., 2015). Plants employ distinct mechanisms or pathways to induce flowering in response to temperature changes. For instance, numerous plant species utilize prolonged exposure to cold temperatures as a signal for flowering (vernalization). In contrast, a modest increase in temperature can induce floral transitions in Arabidopsis (Balasubramanian et al., 2006). This observation suggests that temperature changes are among the key regulators controlling the timing of flowering. The induction of floral transition is largely ascribed to the increased expression of a major set of flowering-promoting genes known as floral integrators, including FLOWERING LOCUS T (FT), TWIN SISTER OF FT, and SUPPRESSOR OF OVEREXPRESSION OF CO1 (Blazquez et al., 2003; Seo et al., 2009; Lee et al., 2013). These genes are essential for integrating both endogenous and environmental cues to induce flowering in Arabidopsis (Fornara et al., 2010). Light receptors play a crucial role in the thermoresponsive flowering in Arabidopsis. PhyB and CRY2 have both positive and negative effects on the regulation of the thermal transition of flowers (Blázquez et al., 2003; Halliday et al., 2003). Under long-day conditions, PhyB destabilizes CONSTANS (CO), which subsequently induces FT expression to promote flowering, whereas PhyA and CRY2 enhance the stability of CO (Valverde et al., 2004). In addition to the aforementioned genes, MADS-box genes, which constitute a large family of genes in plants, play a crucial role in various aspects of development, including the timing of flowering in plants (Smaczniak et al., 2012). Indeed, type II MADS-box genes, also

known as MICK-type, such as FLOWERING LOCUS M (*FLM*) and SHORT VEGETATIVE PHASE (*SVP*), play a pivotal role in flowering in response to ambient temperature by inhibiting the expression of Florigen genes (Scortecci et al., 2001; Lee et al., 2007). is shown by Both *FLM* and *SVP* demonstrate high sequence similarity; however, the functional range of temperature and molecular mechanisms underlying their temperature-dependent gene regulation differ. The ambient temperature in the *SVP* induces post-translational regulation, whereas in the *FLM*, post-transcriptional regulation occurs (Lee et al., 2013). *SVP* undergoes rapid degradation at high temperatures (27°C), indicating a reduction in SVP protein levels, which contributes to accelerated flowering (Lee et al., 2013). *SVP* can also inhibit flowering by reducing FT and TSF transcription in the leaves and SOC1 in the shoot meristem (Lee et al., 2007; Li et al., 2008; Jang et al., 2009). Temperature-dependent flowering is additionally regulated by CDKS, for instance, through the regulation COOLAIR, an antisense noncoding transcript produced by FLOWERING LOCUS C (Csorba et al., 2014). CDKGs and their similar cyclins (CYCLIN L1; CYCL1) have recently been identified as thermosensitive splicing regulators (Cavallari et al., 2018). The CDKG2-CYCL1 complex contributes to the splicing of *FLM* (Nibau et al., 2020).

1.1.8 The influence of warm temperatures on plant growth and development: proliferation dynamics in plants

Proliferation is concentrated in specific regions of plants known as meristems. The activity of plant meristems is crucial for the plant growth and development. Meristems are groups of cells that promote shoot and root growth, including the growth of new organs, and regulate vascular development throughout the life of a higher plant. Their continuous proliferation must be coordinated with the growth requirements of the plant. The shoot meristem (SAM) contains stem cells at the tip in the central zone (CZ). The surrounding peripheral zone comprises more rapidly

dividing transit amplifying (TA) cells that can enter a differentiation pathway. A limited number of stem cells are maintained, and their progeny are displaced toward the periphery during development.

Similar to the shoot, the root is also a continuously growing organ due to the presence of stem cells localized in the stem cell niche region of the root meristem (RAM). In the *Arabidopsis* root, all cell layers originate from specific initials and are organized in a simple radial pattern of clonal cell files. The root meristem can be divided into three main regions: the proliferating meristematic zone, the elongation zone, and the differentiation zone. The meristematic zone contains the stem cell niche, comprising the rarely dividing quiescent centre (QC) cells, which control the surrounding stem cells (also called initial cells).

Accelerated growth and faster development in response to higher temperatures was long believed to be part of a general response accelerating growth without affecting morphogenesis (Casal and Balasubramanian, 2019). However, the aforementioned involvement of hormonal signalling in the growth response of the root supports the genetic control of meristem functions at warmer temperatures. One may inquire whether warmer temperatures affect the cell division rate in the meristematic region of the root in the same manner as in the shoot. It is well known that warmer ambient temperature accelerates Arabidopsis development resulting in early flowering (Balasubramanian et al., 2006, and Casal and Balasubramanian, 2019). PIF4 has been shown to be involved in the temperature-dependent early flowering response, directly regulating the expression of the *FLOWERING LOCUS T* (*FT*) gene (Kumar et al., 2012). Increased YUC-dependent auxin synthesis in floral primordia has also been reported at warmer temperatures (John et al., 2023). Interestingly, there is a lack of research on the thermoresponsiveness of the shoot meristem at the seedling stage.

In the root, the mechanism by which thermal regulation of auxin signalling is linked to the observed cell division response remains unclear while, in the shoot, the contribution of accelerated cell divisions to the thermomorphogenic response is not considered. If elevated temperatures exert specific and positive effect on meristem activity, it likely pertains to an increased rate of cells entering the cell cycle. It is widely recognized that the regulation of plant cell cycle is controlled by conserved regulatory mechanisms, particularly involving the RETINOBLASTOMA-E2F pathway (Magyar Z., 2008; Berckmans, B., & De Veylder, L. 2009).

1.1.9 The RETINOBLASTOMA-RELATED-E2F pathway in plants and its role in regulating cell cycle progression

Cell cycle entry is controlled by evolutionary conserved molecular mechanisms including the RETINOBLASTOMA (RB) protein that negatively regulates cell cycle progression through its interaction with members of the E2F/DP family of heterodimeric transcription factors (Henley and Dick, 2012). Arabidopsis possesses a single gene encoding the RETINOBLASTOMA-RELATED (RBR) protein, which is believed to connect environmental signals to cell proliferation and differentiation (Harashima and Sugimoto, 2016). The RBR protein interacts with three E2F transcription factors: E2FA, E2FB, and E2FC. Prior to binding to target sequences, E2Fs must form heterodimers with one of the two DIMERIZATION PARTNER proteins (DPA, and DPB – Magyar et al., 2000). Initial overexpression studies classified these E2Fs either activators (E2FA and E2FB) or a repressor (E2FC). E2FA promotes cell proliferation and is prevalent in S-phase cells (De Veylder et al., 2002), whereas E2FB is active throughout the entire cell cycle, facilitating both G1/S and G2/M transitions (Magyar et al., 2005). Similar to the animal activators E2F1-3,

E2FB is capable of inducing cell proliferation in the absence of the plant growth hormone auxin, thereby supporting its role as a cell cycle activator (Magyar et al., 2005).

In contrast, ectopic E2FC functions as a repressor, inhibiting cell division by repressing the expression of mitotic genes (del Pozo et al., 2006). However, further studies revealed that all the three E2Fs can function as repressors when in complex with RBR (Leviczky et al., 2019; Őszi et al., 2020; Gombos et al., 2023). The RBR-E2F transcriptional regulatory mechanism in plants is highly conserved, and exhibits a remarkably similarity to that found in animals (Fig. 3 and Magyar Z., 2007; Desvoyes and Gutierrez 2020). It is widely recognized that RBR is regulated through phosphorylation, resulting in its phosphorylated forms losing the capacity to form complexes with E2Fs, thereby enabling the induction of cell cycle gene expression necessary for cell cycle entry. The CYCLIN-DEPENDENT KINASE A;1 (CDKA;1) serves as the principle CDK in Arabidopsis, demonstrating RBR-kinase activity when it forms complexes with its regulatory CYCLIN D subunits (Boniotti, M. B., & Gutierrez, C. 2001, and Fig. 3). D-type cyclins are induced by both developmental and environmental signals including light, nutrients and plant growth hormones such as auxin and cytokinin (Fig. 3 and Shimotohno et al., 2021). Its activity is inhibited by KIP-RELATED PROTEINS (KRPs), a group of CDK inhibitory proteins (KRP1-7 - De Veylder et al., 2001). Additionally, plants possess another group of CKIs, namely the SIAMESE and SIAMESE-RELATED PROTEINS (SIM-SMRs), which are believed to repress mitotic and plant specific CDKB kinases (Fig. 7 and Nomoto et al., 2022). The RBR protein is crucial for maintaining meristem integrity, as it regulates stem cell maintenance and coordinates cell division, differentiation, and survival in response to environmental and developmental signals. These processes are purportedly governed by multisite phosphorylation (Zamora-Zaragoza et al., 2024). CDK activity on RBR peaks during mid-G1 and G1/S transition phases, as well as in G2 (Nowack

et al., 2012). The role of CDK inhibitors, particularly Kip-related proteins (KRPs), is crucial for regulating CDK activity (Pettkó-Szandtner et al., 2006).

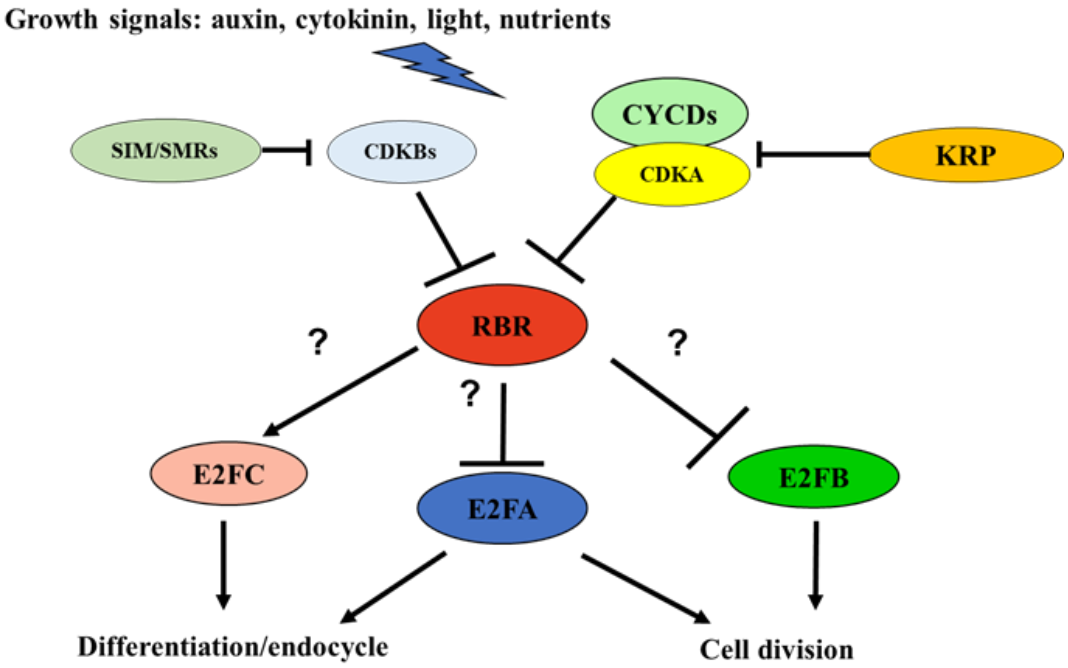

Figure 3. **The model of the plant cell cycle is primarily focused on the regulation by the E2F-RBR pathway.** This regulatory pathway is crucial for both the initiations of cell cycle and the maintenance of quiescence during cellular differentiation. The RBR protein, when complexed with the activator E2Fs (E2FA and E2FB) inhibits cell cycle progression. Conversely, its association with E2FC induces quiescence in committed cells. Notably, the various RBR-E2F complexes may function either as activator or repressor in a manner specific to cell type or developmental stage, as indicated by question marks. Upon receiving mitogenic signals such as the growth hormones auxin and cytokinin, along with environmental cues like light and nutrients, the RBR-kinases are activated. This activation is facilitated by the expression of D-type CYCLINs (CYCDs), which form complexes with the CDKA (CDKA;1) kinase and phosphorylate RBR, thereby releasing E2Fs from repression and permitting cells to enter the cell cycle. However, the precise function of each RBR-E2F complex remains to be elucidated. KIP-RELATED PROTEINs (KRPs) function as CDK inhibitors, targeting CYCDs and CDKA;1 during the G1-S transition, while the plant-specific CDK inhibitory SIAMIESE/SIAMIESE-RELATED (SIM/SMRs) proteins inhibit the activity of CDKB kinases during G2/M

transition. The regulatory subunits of CDKBs are identified as the mitotic cyclins. Additionally, CDKB kinases may phosphorylate the RBR protein when it is in complex with CYCD proteins (Cruz-Ramirez et al., 2012).

The two distinct classes of E2Fs and MYBs with RETINOBLASTOMA (RB) proteins are found to be a part of conserved multiprotein-complex called DP, RB-like, E2F And MuvB (DREAM) and in Drosophilla RBF, E2f2 and Mip complex (dREAM) while in nematodes it is DP, RB and MuvB complex (DRM, Sadasivam S, DeCaprio JA 2013, Latorre et al. 2015, Guiley et al. 2015, Kobayashi et al. 2015). DREAM complexes function as repressors by regulating the expressions of cell cycle genes in phase-dependent manner, and in committed cells to establish quiescence (Sadasivam S. & DeCaprio JA., 2013). In recent studies DREAM-like complexes have been described in Arabidopsis (Magyar et al., 2016, and Fig. 4). Unique to the plants is the presence of two distinct DREAM complexes one with activator type transcription factors (E2FB and MYB3R4) and another with repressor type transcription factors (E2FC and MYB3R3, Kobayashi et al. 2015a, b, Magyar et al. 2016). The activator complex can transition into a repressor when cells exit the cell cycle. In this context, E2FC and MYB3R3 take the place of E2FB and MYB3R4, which leads to the inhibition of G2/M gene expression, promoting quiescence and facilitating a state of differentiation. Additionally, in plants, the repressor DREAM complex serves to suppress mitotic genes outside of the M phase, ensuring that the transcriptional activation waves during the M phase are effectively regulated. (Fig. 4, Kobayashi et al., 2015b, Magyar et al., 2016; Lang et al., 2021).

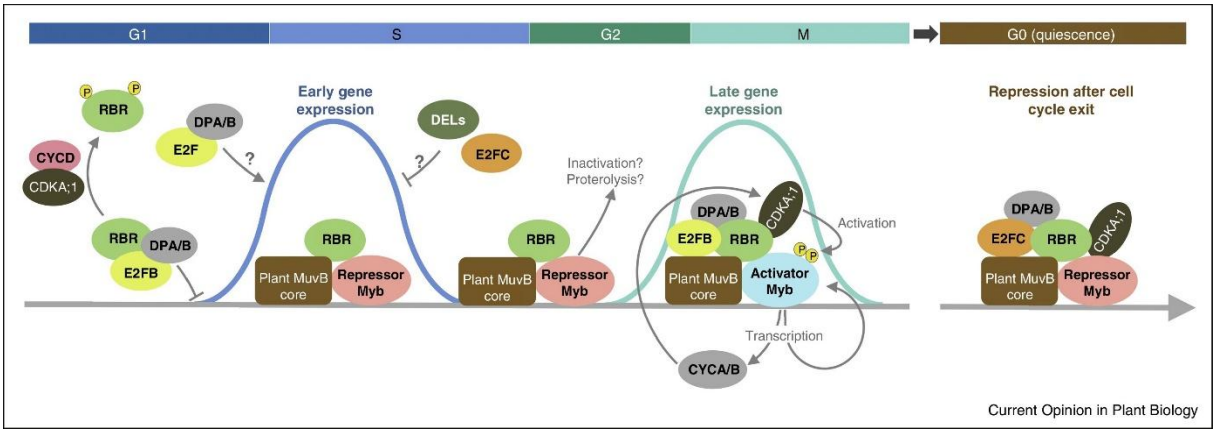

Figure 4. Regulation of cell cycle and quiescence by DREAM-like complexes in plants. In proliferating cells, early cell cycle genes are repressed by the E2FB-DPA/B-RBR complex during G1. The phosphorylation of RBR by CYCD-CDKA;1 kinase induced the release of active E2F-DPA/B heterodimers to initiate the transcription of early cell cycle genes. E2FC may also have played a role in repressing transcription of the early cell cycle genes. This repression may have been accompanied by the action of DEL transcription factors, known as atypical E2Fs, which functioned as monomers in an RBR and DP-independent manner (Vlieghe et al., 2005). During G1, S and early G2, the late cell cycle genes are transcriptionally suppressed by the protein complex containing repressor-type MYB3R, RBR and possibly MuvB-like core complex. During late G2, this repressive complex on the target promoters was replaced by the MYB3R-E2F activator complex (containing activator-type MYB3R, E2FB, RBR, and MuvB-like core complex), triggering its auto-activation through the positive feedback loops and enabling transcription of the late cell cycle genes. In post-mitotic cells, the late cell cycle genes were maintained in a silenced state by a separate MYB3R-E2F complex with a repressive function (containing repressor-type MYB3R, E2FC, RBR and MuvB-like complex (Magyar, Z., Bögre, L., & Ito, M., 2016).

Contrary to mitotic cyclins, the expression of D-type cyclins does not fluctuate during the cell cycle but rather depends on the presence of mitogens, suggesting that they act as sensors of both internal and environmental signals to the cell cycle control system (Fig. 3 and Shimotohno *et al.*, 2021). For instance, the expression of *CYCD3;1*, one of the most studied D-type cyclins in Arabidopsis, is induced by sucrose and plant growth hormone cytokinin (Riou-Kamlichi et al.,

1999). Similarly, the phosphorylation level of RBR is dependent on sucrose levels, which are elevated in the presence and reduced in the absence of sucrose (Magyar et al., 2012). CYCDs are crucial for linking environmental conditions to the cell cycle; however, ectopic over-expression of *CYCD3;1* stimulates the phosphorylation of RBR irrespective of sucrose levels (Magyar et al., 2012). RBR, however, is not solely an inhibitor of the cell cycle but is also required for quiescence and appropriate differentiation of the cells exiting the meristem (Fig. 5 and Borghi et al., 2010; Perilli et al., 2013; Harashima and Sugimoto, 2016; Gombos et al., 2023). Recent research indicates that RBR primarily regulates cell cycle genes through E2Fs, and the disruption of its binding to E2Fs in a triple E2F mutant (*e2fabc*) led to the cessation of quiescence in both stem and differentiated cells (Gombos et al., 2023). Consequently, cell proliferation was not suppressed in this *e2fabc* triple mutant; rather, it was activated. In contrast to the growth-arrested *rbr* mutants, the tripe *e2fabc* develop larger organs composed of a greater number of cells, and exhibit significantly greater height than the WT. It was discovered that E2Fs, in conjunction with RBR, target both G1-to-S and G2-to-M regulatory genes. Furthermore, the activator and DREAM component MYB3R4 was identified as a direct E2F-RBR target, supporting the notion that RBR regulates both cell cycle transitions primarily through E2Fs (Fig. 5 and Gombos et al., 2023).

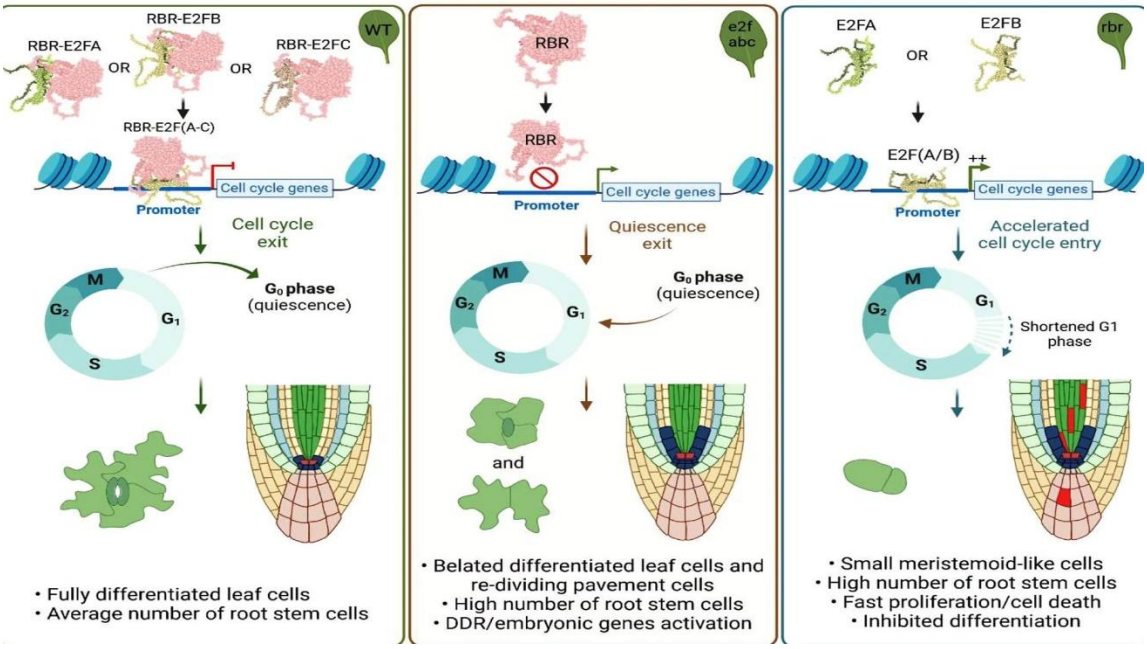

Figure 5. Canonical E2Fs function as co-repressors of cell cycle genes with RBR in quiescent cells. Left: in the wild-type, E2Fs form complexes with RBR to repress cell cycle genes and allow cell division arrest in quiescent and differentiated cells. Middle: in the *e2fabc* mutant, lack of RBR-E2F complexes results in de-repression of cell cycle genes leading to a delay in cell differentiation as well as division reactivation in quiescent cells. Right: in RBR-deficient lines, E2F/RBR complexes are also lacking, but E2Fs are fully active, leading to a more pronounced hyperactivation of cell cycle genes and thus completely preventing cell differentiation, and inducing cell death (Gombos et al., 2023).

In conclusion, the RBR, in conjunction with E2Fs and MYB3Rs, serves a regulatory function in both the initiation of the cell cycle and the transition from the G2 to M phase by modulating the expression of key cell cycle regulatory genes. Its activity is believed to be regulated by phosphorylation, with CYCDs playing a significant role under the impact of developmental and environmental signals. However, the mechanisms by which these signals regulate RBR and its distinct complexes remain less understood.

1.2 Cell size controls cell cycle entry

In multicellular organisms, it is essential to establish an appropriate cell size for tissue and organ development with characteristic functions, suitable dimensions and structure (Miettinen, T.P. et al., 2017). Cell proliferation is tightly regulated during organ growth and development. Cell number and cell size are significantly affected during cell cycle progression. Determined by the developmental programs (Roeder, A. H. et al., 2010, Polyn, S, et al. 2015, Andriankaja, M. et al., 2012) and influenced by active responses to the environmental conditions (Komaki, S. & Sugimoto, K 2012, Qi, F. & Zhang, F. 2020) in plants, the cell number produced during organ development and growth is governed by the rate of the cell cycle during proliferation and the point of exit when cells enter the cellular differentiation stage. Meristematic cells, where the mitotic cycle occurs, comprise four different phases: Gap1 (G1), DNA synthesis (S), Gap2 (G2), and mitosis (M). After leaving the meristem and exiting cell proliferation, various plant species including Arabidopsis thaliana, enter a specialized cell cycle mode knows as endoreduplication, where in cells repetitively synthesize DNA without cytokinesis and mitosis, leading to a subsequent increase in DNA content and consequently cell enlargement (Joubes J, & Chevalier 2000; Lang L., & Schnittger A., 2020). A controlled cell proliferation necessitates balanced and coordinated gene expression during and at the time of exit from the cell cycle. During the cell cycle there are generally two main sets of genes that exhibit waves of transcription, namely G1/S-specific and G2/M-specific genes (Berckmans, B. & De Veylder, L., 2009). Genes specific to G1-S phase that facilitate the initiation and progression of DNA replication are strictly regulated by the activity of E2F transcription factors (Őszi, E. et al., 2020; Gombos et al., 2023).

1.2.1 Cell cycle inhibitors as sensors of cell size: The dilution model of a cell cycle repressor

Recent research highlights a molecular mechanism by which cell size and growth influence cell cycle transitions through the dilution of specific inhibitors. Cell size control helps maintain narrow size distributions within cell populations by correcting size deviations. In proliferating cells, this regulation often involves coupling cell division and growth to cell size (Fig. 6). While our understanding of how growth rate regulation influences size is still developing, the connection between cell division and size has been extensively studied, with several mathematical models proposed. These models are usually categorized as sizers, adders, or timers. Sizers aim for cells to reach a specific size before dividing, resulting in smaller cells growing more and larger cells growing less to achieve uniform sizes at division. Adders, on the other hand, involve adding a fixed volume or mass each cycle, regardless of initial size. Timers, particularly for specific cell cycle phases, may be combined with sizers, as they maintain size homeostasis by timing the division process, even though they cannot correct size deviations in exponentially growing cells (see Figure 6A and B). In budding yeast, during the G1 phase, cell growth dilutes the concentration of the cell cycle inhibitor Whiskey 5 (Whi5), a functional analogue of the animal tumour suppressor and cell cycle inhibitor RB. This dilution occurs at birth and throughout G1, facilitating cell cycle progression (Swaffer et al., 2021; Schmoller et al., 2015) and serving as a cell size indicator (Fig. 6). Whi5 inhibits the SBF transcription factor, which is analogous to E2F (Medina et al., 2016). SBF activates genes that promote the G1-S transition (Costanzo et al., 2004; De Bruin et al., 2004). However, the precise mechanism by which reduced Whi5 concentration enhances SBF activity remains unclear. This process establishes a size-dependent probability of transitioning to S-phase, with larger cells more likely to enter this phase (Schmoller et al., 2015). Notably, all cells possess the same Whi5 concentration at birth, resulting in smaller cells having higher Whi5 levels, which

prolongs their G1 phase and allows for additional growth. In mammals, the functional orthologs of Whi5 are the Retinoblastoma (RB) family proteins: RB, p107, and p130 (Medina et al., 2016). These pocket proteins inhibit E2F transcription factors, regulating the G1/S transition (F.A. Dick et al., 2013). In a manner similar to *Whi5* deletion in yeast, which results in smaller cells, the absence of RB family proteins also decreases the cell size of mouse embryonic fibroblasts (Sage et al., 2000, Fig. 6). A recent study has described a mechanism in the shoot apical meristem (SAM) of Arabidopsis thaliana that uses chromatin content as a cell size-independent gauge for assessing cell size. While both the G1-to-S and G2-to-M transitions are size dependent in the SAM, cell size regulation mainly occurs at G1-to-S transition (D'Ario et al., 2021). This mechanism involves on the dilution of the KIP-related protein 4 (KRP4), a CYCD/CDKA inhibitor (Sablowski R, Gutierrez 2022, and Fig. 4), which directly inhibits G1/S transition and associates itself with mitotic chromosomes. The F BOX-LIKE 17 (FBL17) protein helps removes excess KRP4 proteins. In this process KRP4 is distributed equally in the daughter cells and cells that are born smaller during asymmetric cell division have to grow more to dilute the KRP4 to reach a minimum threshold to proceed through G1/S transition (D'Ario et al. 2021, Fig.6).

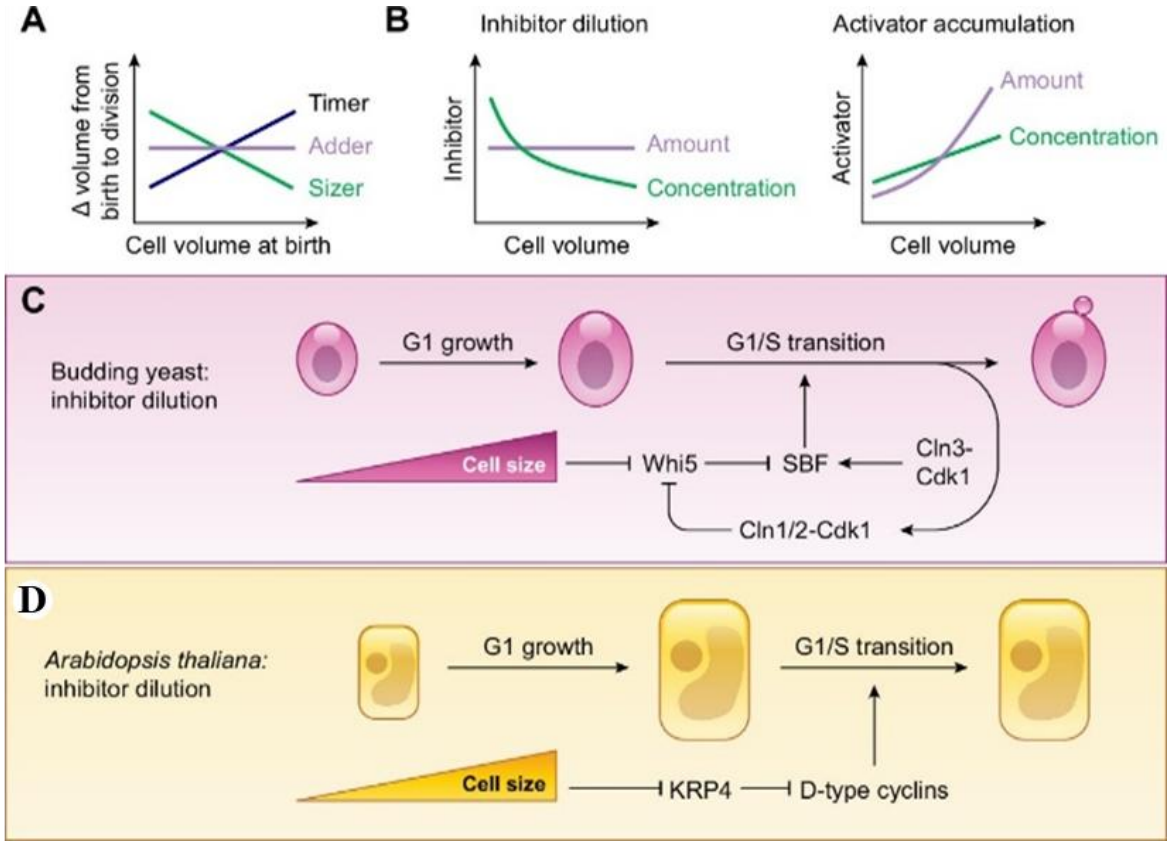

Figure 6. Cell size control of proliferating cells requires that cell cycle progression is coordinated with cell growth. A: Different types of strategies include sizers, adders, and timers. **B**: on a molecular level, cell size sensing can be implemented through subscaling cell cycle inhibitors or superscaling activators. **C-D**: specific cell size reporters have been identified in yeast, and plants. Chadha, Y., Khurana, A., & Schmoller, K. M. (2024). Eukaryotic cell size regulation and its implications for cellular function and dysfunction. *Physiological Reviews*, *104*(4), 1679-1717.

Previous studies have demonstrated that reducing the rate of cell cycle progression is sufficient to increase the size of the proliferating cells, as observed in mammals and yeast cells (Larson-Rabin et al., 2009, Adachi, S et al., 2011), emphasizing the role of negative regulators of the cell cycle in cell size control. Two CDK-kinase inhibitor (CKI) families have been identified in plants as negative regulators of the cell cycle in cell size control: KIP-RELATED PROTEINS (KRPs) and the SIAMESE (SIM) as well as the SIAMESE-RELATED PROTEINS (SMRs). Both families play

an essential role in interacting with growth and environmental signals and directing critical developmental processes (De Veylder et al., 2001, Peres S., et al., 2007). Recently emerged molecular mechanisms utilize chromatin content as a cell-size-independent measure to assess cell size (Fig. 6 and D'Ario M. et al., 2021). KRP proteins are central to this mechanism, which regulates G1-S phase progression of the cell cycle. In Arabidopsis, ectopic expression of KRPs results in reduced leaf size, decreased cell number, and increased cell size (De Veylder et al., 2001). Overexpression of KRPs inhibits both G1/S and G2/M transitions in leaves, resulting in plants with large cells and reduced endoreduplication, which is characterized by repetitive DNA replication without intervening mitosis and cytokinesis, thus producing cells with higher levels of ploidy (Kumar, N et al., 2018). SMR proteins are plant specific CKIs (Kumar, N et al., 2015), and when overexpressed, SMR genes promote endoreduplication, resulting in cells with elevated levels of ploidy (Churchman et al., 2006; Yi, D et al., 2014). Reduction and over-accumulation of SMRs in roots lead to smaller and larger meristematic cells, respectively, providing insight into the significant role of SMRs in cell cycle-dependent regulation of cell size (Fig.7 and Dubois et al., 2018, Nomoto, Y et al., 2022). Conversely, the MYB3R family positively or negatively regulates the majority of genes, such as *CYCLIN B1;1* (*CYCB1;1*), *CYCLIN-DEPENDENT KINASE B2* (*CDKB2*), and *KNOLLE* (*KN*), which are involved in G2/M transition in plants (Haga, N. et al., 2011, Kobayashi, K. et al., 2015). Five MYB3R genes have been identified in the Arabidopsis genome, which are subdivided into two main subcategories based on their functions: such as transcriptional activators MYB3R1 and MYB3R4 (Haga N. et al., 2007) and transcriptional repressors MYB3R3 and MYB3R5 (Kobayashi, K. et al., 2015). A direct target of MYB3Rs, a mitosis-specific GRAS family transcription factor, SCARECROW-LIKE28 (SCL28) was recently identified (Nomoto, Y et al., 2022). Despite being induced directly by MYB3R4, whose main

function is the acceleration of G2/M transition, SCL28 affects the progression, exhibiting shorter and larger cell cycles in *scl28* knockout mutants and SCL28-overexpressing lines, respectively (Nomoto, Y et al., 2022). SCL28 was demonstrated to form a dimer with the AP2-type transcription factor AtSMOS1. This, in turn, enhances the expression of SMR genes, delays G2/M progression, and promotes the transition from mitosis to the endocycle (Nomoto, Y et al., 2022).

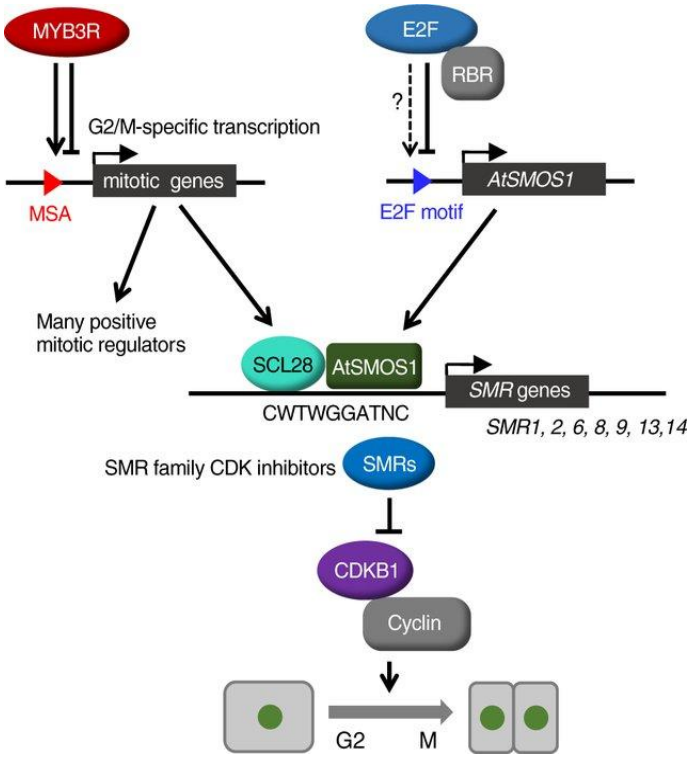

Figure 7. A hierarchical transcriptional network that regulates G2 phase to control cell size. MYB3R transcription factors are responsible for regulating a set of G2/M-specific genes, which include several positive regulators of mitosis. In contrast, SCL28, also regulated by MYB3Rs, acts as a negative regulator of the cell cycle in collaboration with AtSMOS1, potentially under the influence of the E2F-RBR pathway. The SCL28-AtSMOS1 heterodimer formation results in specific binding sequences, facilitating the direct transcriptional activation of SMR family genes. The accumulation of SMR proteins subsequently inhibits CDK activity, thereby exerting a negative effect on cell cycle progression during the G2 phase. By modulating the activity of the SCL28-AtSMOS1 heterodimer, the duration of the G2 phase in the cell cycle can be precisely controlled to maintain an appropriate balance between cell size and cell number in developing plant organs (Nomoto et al., 2022).

1.2.2 Regulation of the division of stomatal lineage cells – a nuclear factor with cell size regulatory function

Asymmetric cell divisions during stomatal lineage development serves as an exemplary model for investigating regulatory mechanisms that govern these divisions. However, the rationale for selecting the stomatal lineage development as a focal point for this remains to be elucidated. Stomata are microscopic pores flanked by paired guard cells on the aerial part of the plant leaf surface, which function as essential mediators of gas exchange and transpiration. The mechanism of stomatal development has been extensively studied in detail in Arabidopsis thaliana. The complex progression of the stomatal lineage necessitates stringent transcriptional regulation to govern cell identity. Research in Arabidopsis has demonstrated that the regulation of stomatal differentiation is achieved through a series of stereotypical cell divisions orchestrated by three master-regulatory basic-helix-loop-helix transcription factors: SPEECHLESS (SPCH), MUTE and FAMA (Lau and Bergmann, 2012, Han and Torii, 2016). SPCH initiates and maintains asymmetric cell divisions (ACD) of stem cell like precursors termed meristemoids (MacAlister et al., 2007, Pillitteri et al., 2007). MUTE, which is a direct target of SPCH after several rounds of ACD, is activated and triggers the differentiation of guard mother cells (GMCs, MacAlister et al., 2007, Pillitteri et al., 2007). FAMA plays a crucial role in regulating and facilitating the terminal differentiation of guard cells, while simultaneously restricting SCD (Lai et al., 2005). The mechanism by which stomatal-lineage bHLH proteins interact with the cell cycle machinery to transition between different cell cycle modes remains a significant area of research, with previous studies having identified several critical connections (Fig.8, Han and Torri 2019). For instance, the expression of the G1-specific D-Type cyclin CYCD3;1 is induced by *SPCH* during the initiation of ACDs (Lau et al., 2014). CYCD3;1 is hypothesized to form complex with CDKA to initiate the

cell cycle and induce mitotic divisions (Dewitte et al., 2007). Subsequently, MUTE terminates SPCH-mediated ACDs through direct upregulation of *SMR4*, a plant-specific cyclin-dependent kinase inhibitor. Furthermore, MUTE inhibits the expression of *CYCD3*s while simultaneously inducing the expression of the G1 cyclin CYCD5;1 to facilitate progression to a terminal SCD (Han et al., 2022). An additional G1 cyclin, CYCD7;1, may also contribute to the coordination of terminal SCD (Weimer et al., 2018). Finally, MUTE directly induces the expression of Myb protein FOUR LIPS (FLP), which inhibits the expression of core cell cycle genes, including *CDKB1;1*, thereby ensuring that terminal SCD occurs only once (Xie et al. 2010, Hachez et al. 2011).

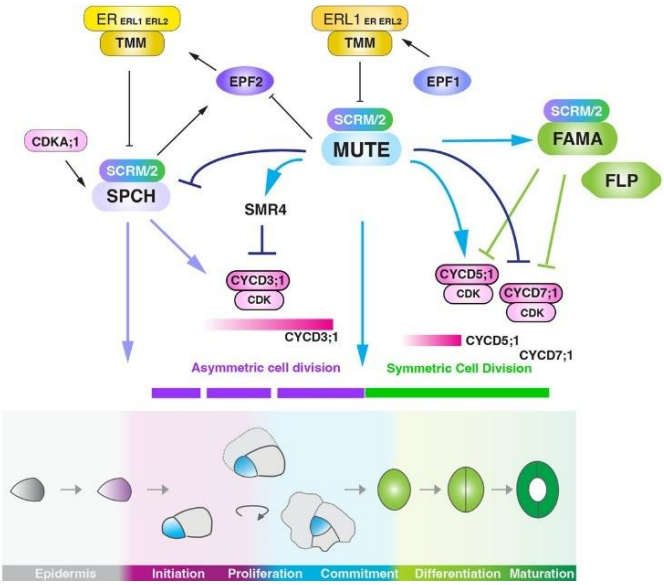

Figure 8. A current model for post-embryogenic stomatal development in Arabidopsis. The stomatal lineage's progression is finely orchestrated by a sequence of stage-specific transcription factors. Initially, SPCH and SCRM govern lineage specification and proliferation. MUTE and SCRM take over for proliferation and fate commitment, followed by FAMA and SCRM, directing differentiation and maturation. Within the ERECTA (ER) pathway, EPIDERMAL PATTERNING FACTORs (EPF1) and (EPF2) bind to ER-TOO MANY MOUTHS (TMM), regulated by SPCH and SCRM. EPF1, perceived by ERECTA-LIKE1 (ERL1), enforces stomatal spacing during the

meristemoid-to-GMC transition, a process initiated by MUTE-induced ERL1. The SPCH-SCRM module activates asymmetric divisions via the E-box in the *SPCH* promoter. The coloured arrows indicate positive regulation by transcription factors, while the coloured, inverted Ts denote negative regulation. The coloured bars represent the duration of each gene's expression or the length of each cell division.

A recent study by Gong et al., 2023 demonstrated that the commitment to stomatal fate is triggered by overcoming a critical cell size threshold. Until this critical cell size threshold is reached the stomatal meristemoids repeatedly undergo asymmetric divisions. Modelling stem cell behaviour indicates that setting a cell size threshold for differentiation is sufficient to predict the number of asymmetric divisions stem cells undergo before transitioning. This finding suggests a mechanism by which cell size can integrate environmental factors to regulate the number of meristemoid divisions, also referred to as amplifying divisions, in developing leaves. In this study they suggested in the stomatal lineage, size is sensed in the nucleus via a mechanism that is sensitive to DNA content. While the identity of this nuclear factor remains unknown, the *crwn1* mutant and tetraploid analyses from Gong et al., 2023 revealed that size is sensed through a nuclear factor that is sensitive but not primarily bound to chromatin.

2. AIMS AND OBJECTIVES

During my thesis work I focused on two main topics:

1, Previous research on Arabidopsis thaliana has underscored the influence of warm ambient temperatures on overall growth and accelerated development, primarily attributing these effects to cell elongation. This study investigates how warm temperatures affect meristematic activity in *Arabidopsis thaliana* during thermomorphogenesis, focusing on the role of RBR, a cell cycle inhibitor. By modulating RBR levels, we aim to assess any morphological, cellular and molecular changes its impact on phosphorylation, cell cycle dynamics, and key thermo-morphogenic genes in shoot and root meristems.

2, In our investigation of thermomorphogenesis, RBR has been identified as a regulator of post-mitotic cell size in a temperature-dependent context. Given that RBR functions as a cell cycle inhibitor, predominantly localized within the nucleus, and influences both the G1/S and G2/M transitions, it emerges as a viable candidate for investigating cell size regulation in mitotically active cells. Our primary hypothesis posted that the dosage of RBR in Arabidopsis plants affects cell size *in vivo*. To test this hypothesis, we examined transgenic Arabidopsis plants with either elevated or reduced levels of RBR, observing corresponding changes in cell size from embryogenesis through to organ development. We utilized transgenic Arabidopsis lines in which an additional copy of RBR genomic clone fused with GFP was introduced under the control of its native promoter (RBR-GFP), as well as an RBR mutant (*rbr1-2*) with reduced RBR levels compared to the wild-type control WT. Significantly, the reduction in RBR levels resulted in the formation of clusters of small stomatal meristemoids, thereby confirming its influence on their cell size. The primary objective was to elucidate the molecular mechanism underlying this

phenomenon by analysing key regulatory genes involved in the proliferation-differentiation balance during stomatal development.

3. MATERIAL AND METHODS

3.1 Plant material and growth conditions

Arabidopsis thaliana Col-0 ecotype was used as WT control, and was the background of the other transgenic lines utilized in this study. Most of the transgenic lines have been previously published: RBR-GFP (Magyar et al., 2012), CYCB1;2-YFP (Iwata et al., 2011), *rbr1-2* mutant (Nowack et al., 2006), *e2fa-1* and *e2fb-2* mutant (Leviczky et al., 2019), triple *cycd3;1-3* mutant (Dewitte et al., 2007). We generated an *e2fa-1*/RBR-GFP, *e2fb-2*/RBR-GFP double transgenic line by crossing *e2fa-1* and *e2fb-2* mutant line with the RBR-GFP expressing line.

Seeds were surface sterilized, rinsed with sterile water and subsequently stratified for 72 hours in the dark (4ºC). After sowing, seeds were germinated and cultivated on half-strength germination medium supplemented with 1% (w/v) sucrose either on vertically or horizontally oriented plates in climate-controlled growth cabinets (MLR-350, Sanyo, Gallenkamp, UK) at constant temperatures of 22 ºC or 28 ºC under long day conditions (16 h light/8 h dark) and with 100 µmol m^{-2} s^{-1} photosynthetically active radiation (PAR) from white fluorescent lamps. For temperature shift experiments, plants were grown for 4 days after germination (DAG) at 22 ºC and then half of them were kept on the same temperature while the other half were transferred to 28 ºC and grown for few more days afterward. For cell size analysis the plants were grown under continuous light conditions at constant temperature of 22 ºC and then analysed at different time points 3DAG, 7DAG.

3.2 Microscopy

For analysing roots under confocal laser microscopy (SP5, Leica) seedlings were grown on vertically oriented plates, and roots were stained with propidium iodide (PI – 20 µg/mL) and photographed afterwards. Cell length was measured by using Image J software.

3.2.1 Microscopic observation of the first leaf

Young seedlings were fixed in a 9:1 of ethanol and acetic acid solution and cleared with Hoyer's solution (a mixture of 100 g chloral hydrate, 10 g glycerol, 15 g gum arabic, and 25 mL water), we performed microscopic observations using the 1st leaf. After whole leaf images were captured, palisade cells were observed with differential interference contrast (DIC) microscope (Leica). The captured images were analysed using Image J software (ver.2.1.0; rsb.info.nih.gov/ij) and the average size of palisade cell, the number of cells in the uppermost layer of palisade tissue per leaf, were calculated according to methods described previously (Nomoto et al., 2022).

3.2.2 Scanning electron microscopy observation of leaf primordium and hypocotyls

Young seedlings were vacuum infiltrated and fixed with 100% methanol for 20 min, dehydrated in 100% ethanol for 30 min and then in fresh 100% ethanol overnight. Next day samples were critical point dried, mounted on SEM stubs and observed in a JEOL JSM-7100F/LV scanning electron microscope in low-vacuum mode. High contrast cell outlines in the uncoated plants were imaged according to Talbot and White (2013) by detecting backscattered electrons at 15 kV

accelerating voltage and 40 Pa pressure in the specimen chamber. Cell length was measured by using Image J software.

3.2.2 EdU staining of root meristem

For the 5′ - ethynyl - 2′ - deoxyuridine (EdU) incorporation assay WT and transgenic seedlings were grown at 22 ºC for 4 DAG, and half of the seedlings were transferred to 28 ºC or 22 ºC for 8, 24, 48 hours when they were placed into half strength liquid MS containing 5 µM EdU (Click-iT Alexa Fluor 647 Imaging Kit; Invitrogene) and incubated for 30 minutes at the same temperatures. EdU detection was carried out according to Kazda et al., 2016. The root samples were also stained with HCS NuclearMask Blue stain provided in the kit (Invitrogene), and the observations were carried out under the confocal laser microscope.

3.3 Dissecting the mature embryos

Mature dried seeds of WT and transgenic lines (RBR-GFP and *rbr1-2*) were imbibed for 1 h and dissected under the stereo-microscope. Isolated embryos were stained with PI and photographed under confocal laser microscope (Leica). Embryonic leaf and epidermal cell sizes were measured using Image J software (Schneider et al., 2012).

3.4 RT-qPCR

RNA was extracted from young seedlings in the thermomorphogenesis experiment while young cotyledons and Ist leaf pair was used to extract RNA for the cell size experiment. This was done by using a CTAB-LiCl method described as Jaakola et al., 2001. RNA samples were treated with

DNase1 (ThermoScientific #EN0521) according to the manufacturer's protocol. cDNA was synthesised using 1 µg of RNA using the ThermoScientific Reverse Transcription Kit (#K1691) with random hexamers based on the manufacturer's prescription. Mock reaction without RevertAid enzyme was also prepared to ensure that there is no contaminating genomic DNA in the samples. RT-qPCR in the presence of SYBR Green (TaKaRa TB Green Primer Ex TaqII, #RR820Q) was carried out according to the manufacturer's instructions in a BioRAD CFX 384 Thermal Cycler (BioRAD) with the following setup: 50 °C 2 min, 95 °C 10 min, 95 °C 15 s, 60 °C 1 min, 40 cycles followed by melting point analysis. Each reaction was carried out in tree technical replicates and reaction specificity was confirmed by the presence of a single peak in the melting curve. All the data were normalised to the average Ct value of two housekeeping genes (ACTIN and UBIQUITIN) unless otherwise mentioned and the calculated efficiency was added to the analysis. Amplification efficiencies were derived from the slope of amplification curves at the exponential phase. Primer sequences are summarised in Supplementary Table 1.

3.5 Immunoblotting and Antibody production

For immunoblotting assay, we used whole seedlings, and proteins were extracted in extraction buffer (25mM Tris-HCl, pH 7.5, 75mM NaCl, 15 mM $MgCl_2$, 15 mM EGTA, 15 mM p-nitrophenylphosphate, 60 mM β-glycerophosphate, 1mM dithiothreitol, 0.1% (v/v), IGEPAL CA-630, 0.5mM NaF, 1 mM phenylmethylsulfonyl fluoride, and protease inhibitor cocktail for plant tissue (P9599, Sigma). 40 µg extracted proteins were loaded on SDS-PAGE gel (8%), and after the gel electrophoresis proteins were transferred onto polyvinylidene difluoride membrane (PVDF, Milipore). Primary antibodies used in the immunoblotting experiments were chicken anti-RBR antibody (1:2000 dilution; Agrisera), and anti-phospho-specific Rb (Ser-807/811) rabbit

polyclonal antibody (1:500 dilution; cell Signalling Tech). Membrane was blocked in 5% (w/v) milk powder with 0.05% (v/v) Tween 20 in Tris-buffered saline (TBS; 25 mM tris-HCl, pH 8.0, and 150 mM NaCl; TBS plus Tween 20 TBST). Membrane was incubated with primary antibody for overnight on a shaker at 4°C, an after washing with TBST, next the membrane was incubated with the appropriate secondary antibody conjugated with horseradish peroxidase at room temperature. Chemiluminescence substrates were applied either purchased from Thermo Fisher Scientific (SuperSignal West Pico Plus) or from Milipore (Immobilon western horseradish peroxidase).

For RBR antibody production, the N - terminal domain of RBR (encoding the first 374 amino acids) was cloned into the expression vector pET28a to BamHI - SalI sites which provides an N - terminal 6 × histidine tag. For cloning the RBR N - terminal coding region we used cDNA synthetised with M - MLV Reverse Transcriptase (ThermoScientific #28025013) and oligo(dT)25 as priming from 5 µg total RNA of 7DAG old A. thaliana Col. seedlings grown under normal conditions. Than RBR N - terminal region (1122nd) was amplified with Takara PrimeSTAR Max Polimerase with the following primers: > AT - RBR - alpha - 5′ - BamHI: 5′ - cgcggatccATGGAAGAA GTTCAGCCTCCAG - 3′ and > AT - RBR - alpha - 3′ - SalI: 5′ - acgcgtcg acGCTCAAAGCATCAATTTTCCTCT - 3′ according to the manufacturer's manual (https://www.takarabio.com/documents/User%20Manual/R045A/R045A_e.v1510Da.pdf). Protein expression construct was transformed into Escherichia coli ArcticExpress cells. Induction and purification were done under native conditions as described in the AGILENT handbook (https://www.agilent.com/cs/library/usermanuals/Public/230191.pdf). For polyclonal antibody production, mice (6–8 week old Balb/c) were immunised

biweekly (three times) with 100 µg of the native protein extract/immunisation supplemented with Freud's Adjuvant in 1:1 ratio [Complet Freud's Adjuvant (Sigma, Cat. no.: F5881) for the first immunisation and Incomplete Freud's Adjuvant (Sigma, Cat. no.: F5506) for the second and third immunisation]. One week after the third immunisation total serum was harvested and supplemented with sodium - azide (0.01%–0.04%) than stored at 4°C.

3.6 Flow cytometry analysis of hypocotyls

For flow cytometry measurement, the hypocotyls were collected and chopped by razor blades in nuclei extraction buffer and stained with DAPI with the CyStain UV Precise Kit (Partec, Magyar et al., 2005). Nuclear DNA content was determined by using Partec PAS2 Particle Analysing system (Partec, Germany).

3.7 Statistical analyses

Quantitative data are presented as the mean ± SD and the statistical analysis between different groups was analysed by one-way analysis of variance (ANOVA) following Tukey's HSD post hoc test to determine, which group are significantly different from each other; p-values of less than 0.05 were considered significant.

4. RESULTS

4.1 Cell proliferation is activated by warm temperatures in the meristems of young Arabidopsis seedlings

Rising ambient temperatures accelerate plant growth and development, but the underlying mechanisms are not completely elucidated. Plant growth heavily relies on apical meristems, which are the main sites of cell proliferation in plants. Therefore, it is astonishing that the impact of elevated temperatures on cell proliferation in shoot and root apices remains largely unexplored. To understand the early events triggered by warm temperatures in Arabidopsis plants, young seedlings grown under long-day conditions were examined after being transferred from 22 ºC to 28 ºC four days after germination (4 DAG). Two days later, we investigated the effect of the temperature increase on the activity of apical meristems. Examining the leaf primordia in the shoot apex using a scanning electron microscope (SEM), the size of the primordia was enlarged at 28 ºC compared to those developed at 22 ºC (Fig. 9A). This showed that warm temperatures quickly accelerated primordium development. Measurements of epidermal cell size in the 3rd leaf primordium of seedlings grown at either 22 ºC or 28 ºC revealed no apparent differences, falling within the range of 20-60 µm characteristic of meristemoid and protodermal cells (Fig. 9B, Dong et al., 2009). These data support the idea that warm temperatures accelerate primordium growth by activating cell proliferation rather than cell elongation. The faster development of seedlings was even more evident five days after being transferred to the warmer temperature. At this time, the seedlings that were developed at 28 ºC had four visible-sized leaves, while those grown at 22 ºC only had two (Fig. 9C). In addition, the first leaf pair (L1-2) was significantly larger at 28 ºC than at 22 ºC (Fig. 9D, E). To investigate the reason for their enlargement, we measured the area of palisade leaf cells

and found that they were nearly 1.5 times larger at 28ºC than at 22ºC (Fig. 9F). By calculating the number of constituent cells in these leaves, we discovered that it was doubled at 28ºC compared to 22ºC (Fig. 9G). These data indicate that both cell proliferation and cell enlargement were activated by warm temperatures during early leaf development, resulting in an enlarged leaf area.

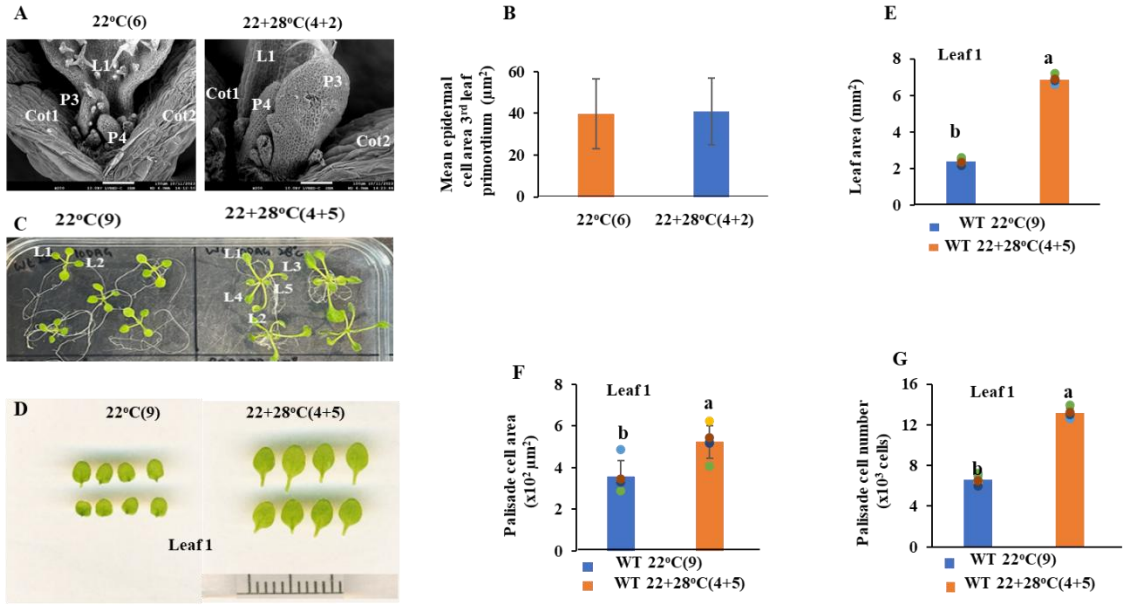

Figure 9. Warm temperature increases proliferation activity in the shoot meristems of Arabidopsis Col-WT. **A**) Leaf primordium of WT-Col seedlings grow at continuous 22ºC for six days after germination (DAG) or 2 days after transfer (DAT) of 4 DAG old seedlings from 22ºC to 28ºC in the shoot apex was pictured under scanning electron microscope (SEM). Position and order of cotyledons (Cot), leaf (L), and primordium (P) are indicated by number. Scale bar is 100 µm. **B**) Epidermal cell size of the 3rd leaf primordium was determined by using Image J software. **C**) Seedlings were grown either at continuous 22ºC for 9 DAG or for 4 DAG and then transferred to 28ºC for 5 more days. Order of cotyledons (C) and leaves (L) were marked with numbers. **D**) Representative picture of the first leaf pair of seedlings at 9DAG at 22ºC or 4 DAG and then 5 DAT from 22ºC to 28ºC. **E-G**) Leaf area (**E**), palisade cell area (**F**), was measured, and palisade cell number (**G**) was calculated of the first leaf derived from seedlings grown at both temperatures.

4.2 Cortex cell number in roots was stimulated by warm ambient temperatures by enhancing cell cycle genes

It is well-known that warm temperatures stimulate root growth resulting in much longer roots at 28ºC than at 22ºC (Quint et al., 2005; Quint et al., 2009; Hanzawa et al., 2013; Wang et al., 2016; Feraru et al., 2019; Galliochet et al., 2020, Ai et al., 2023). When the seedlings were continuously grown at 28ºC, their roots were the longest (Fig. 10A, and Suppl. Fig. S1A). Warm temperatures also resulted in significantly longer roots when the seedlings were transferred from 22ºC to 28ºC at 4 DAG for a period of five more days (Fig. 10A and Suppl. Fig. S1A). To investigate why roots at 28ºC grow longer than at 22ºC, the root tips of seven-day-old seedlings either grown at 22ºC continuously or transferred from 22ºC to 28ºC at 4DAG for 3 more days were stained with propidium iodide (PI). The samples were then analysed under confocal microscopy (Fig. 10B). The length of cortex cells was determined and plotted based on their distance from the quiescent centre. The results showed that warm temperatures increased the size of the cells (Suppl. Fig. S1B) and elevated the number of small, non-elongated cells in the cortical cell file, indicating that the size of the root meristem enlarged at the higher temperature (Fig. 10B, C, D). To further support this assumption, we grew Arabidopsis seedlings expressing the mitotic marker CYCB1;2 under the control of its own promoter and fused with YFP containing a nuclear localization signal (Iwata et al., 2013). We then compared the fluorescence signal in the roots grown either at 22ºC or after being transferred from 22ºC to 28ºC for 1 or 2 days (Suppl. Fig. S1C and Fig. 10E). We detected an expanded CYCB1;2-YFP signal in the roots due to their growth at 28ºC, confirming that more root cells were in mitosis in the root meristem after the temperature was switched from 22ºC to 28ºC.

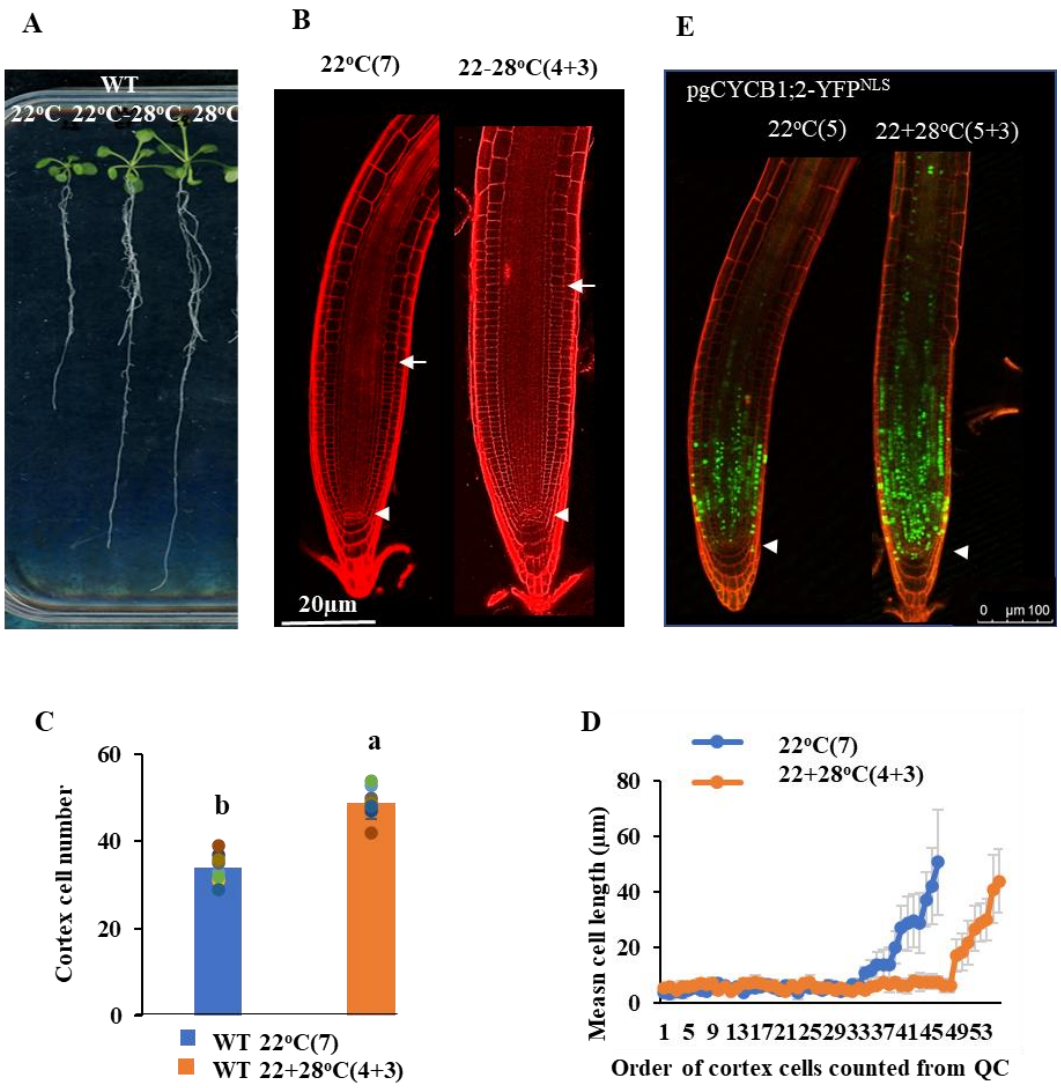

Figure 10. Warm temperature stimulates root growth by enhancing cell number in the root meristem. A) Seedlings were grown for 11 DAG at continuous 22ºC or 28ºC (left and right seedlings, respectively) or 7 DAT of the 4 DAG seedlings to 28ºC (middle seedling). **B**) Representative pictures of propidium iodide-stained roots of seedlings grown for 7 DAG at continuous 22ºC or 3 DAT of 4 DAG old seedlings from 22ºC to 28ºC were analysed under confocal laser microscope. Scale bar is: x um. **C**) Cortex cell number was also counted in the root meristem of seedlings grown either at 22ºC or 3 DAT from 22ºC to 28ºC (n=y). **D**) Spatial distribution of cell length across root meristems in WT grown either for 7 DAG at 22ºC or 3 DAT of 4 DAG old seedlings from 22ºC to 28ºC. Mean cell length was calculated at each position along the cortical cell file, which is defined by counts of cortical cells from the quiescent centre. Values are averages from the data analysed in x roots from different plants (±SD), in each of which

more than 30 cells were analysed. **E**) Root tip of transgenic seedlings expressing CYCB1;2-YFP^{NLS} G2 and M-phase marker under the control of its own promoter was grown for 5 DAG at 22ºC or for 3 DAG at 22ºC and 2 days after transfer to 28ºC were pictured after propidium iodide staining under confocal laser microscope. Arrowhead indicate quiescent centre. Scale bar is: 100um.

Finally, we analysed the expression of two cell cycle regulatory genes: The S-phase specific *ORIGIN RECOGNITION COMPLEX 2* (*ORC2*), and the G2-M-phase specific *CYCLIN-DEPENDENT KINASE B1;1* (*CDKB1;1*) in seedlings 8, 24 and 48 hours after transferring them from 22ºC to 28ºC (Fig. 11A-B). We compared these expression data with those obtained from seedlings continuously grown at 22ºC. Both cell cycle regulatory genes were up-regulated in the first sample, only 8 hours after the seedlings were transferred from 22ºC to 28ºC. The expression of the genes remained at a higher level throughout the 28ºC treatment compared to the continuous growth at 22ºC, further supporting that warm temperatures activate cell proliferation. All together, these data show that raising the ambient temperature from 22ºC to 28ºC rapidly activates cell proliferation in both the shoot and root meristems.

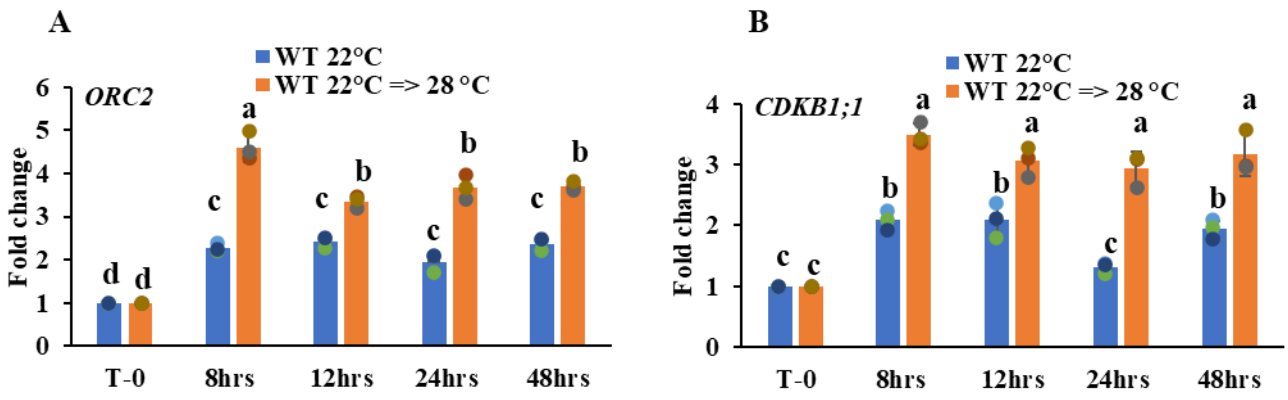

Figure 11. The expression of cell cycle genes shows a temperature dependent upregulation. A-B) The expression levels of the S- and the G2-M-phase regulatory gene *ORC2* (**A**) and *CDKB1;1* (**B**) are increased in seedlings transferred at 4 DAG from 22ºC to 28ºC, in comparison to seedlings continuously grown at 22ºC. gene expression was analysed at 8, 12, -24, and 48 hours (hrs) after transfer and compared to the non-transferred controls. Values represent fold change normalized to the value of the relevant transcript of the seedlings at T0 (4 DAG), which was set arbitrarily at 1. Data are means +/- sd. N=3 biological replicates.

4.3 RBR levels can influence cell proliferation and cell lengths in root meristem

It is well established that cell proliferation in plants is regulated by the RETINOBLASTOMA-RELATED protein coded by a single gene in Arabidopsis (Desvoyes & Gutierrez, 2020). We assumed that warm temperatures might regulate cell proliferation by controlling the function of RBR. We were curious about whether RBR is indeed involved in this regulation and if yes, how. Previously, we have generated a transgenic Arabidopsis line expressing RBR under the control of its own promoter (Magyar et al., 2012). The protein was fused to a GFP-tag providing an opportunity to follow RBR level in seedlings growing at different temperatures. Confirming previous findings, RBR is expressed at a ubiquitously high level in the root tip of young seedlings at 22ºC (Fig. 12A). When seedlings were grown at a continuous temperature of 22ºC or 28ºC for

5 days after germination or transferred to 28ºC 4DAG for 8 or 24 hours, respectively, the GFP signal was present both in the root tip and the hypocotyl (Fig. 12A-C). Beside the root meristem, strong RBR-GFP signal was detected in non-dividing post-mitotic cells in the transient zone of the root as well as in the hypocotyl epidermis both at 22ºC and at 28ºC (Fig. 12A-C). These data indicated that the RBR protein accumulates in the root and hypocotyl at both 22ºC and 28ºC. Therefore, it may be involved in regulating both cell proliferation and cell enlargement in response to warm temperatures. Previously, the RBR-GFP fusion under the control of its own promoter was reported to be functional resulting in a slightly smaller root meristem when expressed in wild-type seedlings (Magyar et al., 2012). Using a western blot assay, we confirmed an increased RBR level in this transgenic line compared to the WT (Fig. 12D). In contrast, slightly less RBR protein was detected in the *rbr1-2* mutant seedlings than in the WT confirming previous observations (Chen et al, 2011). The modest reduction in RBR levels resulted in an over-proliferation of meristemoid-like cells in the cotyledon epidermis and spontaneous cell death in the root meristem similar to what has been reported in another RBR-reduced line (Fig. 12E, and Nowack et al., 2012; Borghi et al., 2010). These data support the previous observations that even slight modifications in its level influence RBR's growth regulatory role.

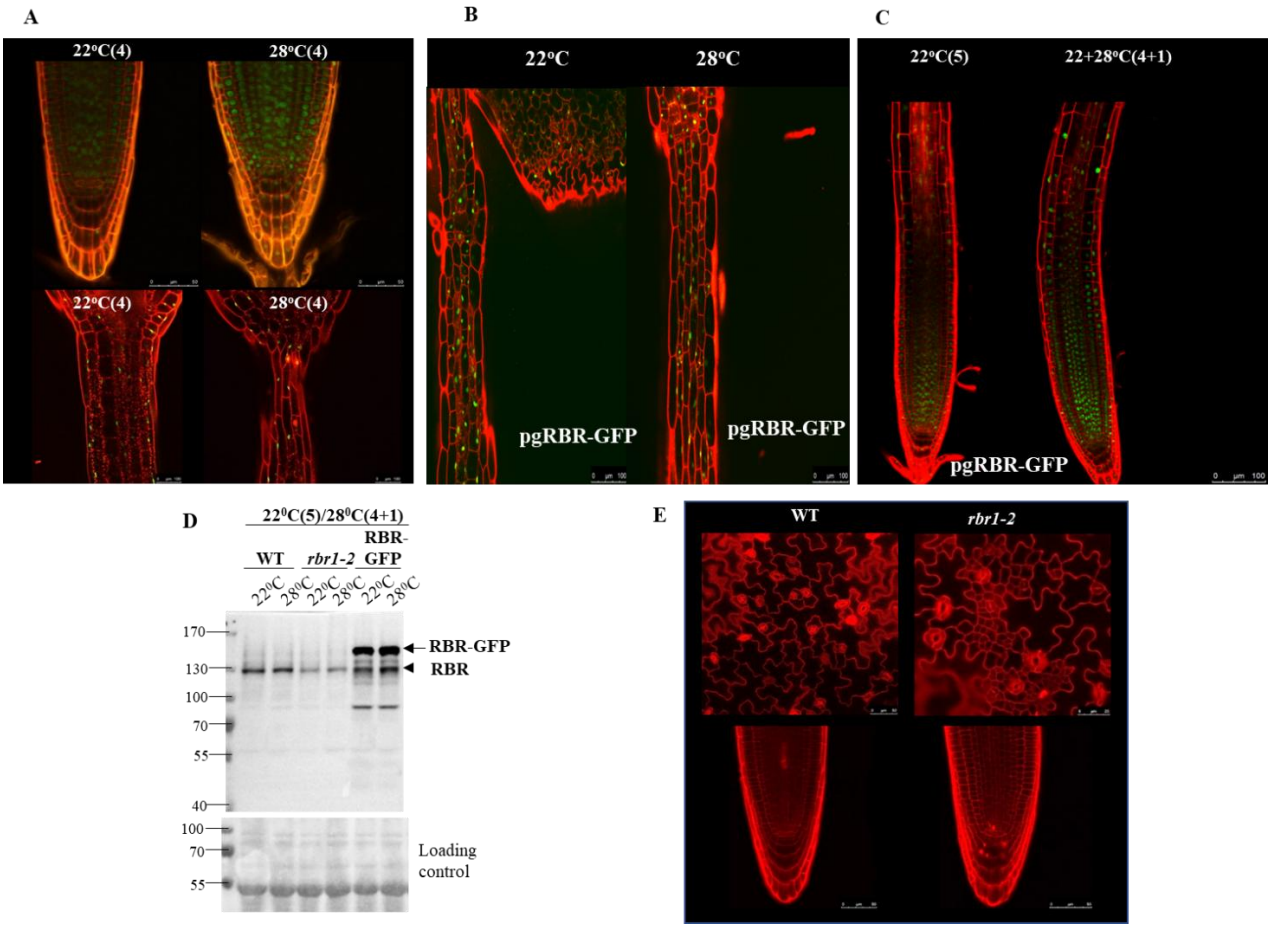

Figure 12. Characterization of transgenic lines expressing various levels of RBR. **A**) RBR-GFP seedlings were grown either at continuous 22ºC or 28ºC for 4DAG and both the root tip (upper pictures) and the hypocotyl (bottom images) were analysed under confocal laser microscopy after propidium iodide staining. **B,** RBR-GFP signal was comparable in the hypocotyl epidermal cells of seedlings grow at continuous 22ºC for 4 DAG, or 8 hours after transfer of 4 DAG seedlings to 28ºC. **C**) RBR-GFP signal was increased at warm temperature 1 DAT of seedlings to 28ºC in comparison to 22ºC. **D**) Western blot of RBR levels in WT, RBR-GFP and *rbr1-2* seedlings grow long day condition (16/8 hours light-dark cycle). Open arrow shows RBR-GFP, black arrow marks endogen RBR protein. Ponceau-S-stained membrane was used as loading control. Molecular weight is marked at the left side. **E**) Cell proliferation and cell death was induced in *rbr1-2* mutant cotyledon (upper pictures) and root (bottom images), respectively in comparison to the similar aged WT.

We tested the growth of seedlings of the above transgenic Arabidopsis lines having altered RBR levels and responses together with the WT control at a continuous temperature of 22ºC, and after transferring them to 28ºC 4DAG at 22ºC (Fig. 13A). The root length of the seedlings was measured daily during the period of three more days (Fig. 13B). Root length of the three lines was comparable at 22ºC. In comparison to the WT control roots, the *rbr1-2* line developed slightly shorter roots at 28ºC, while strong repression was observed in the ectopic RBR-GFP line (Fig. 13A-B).

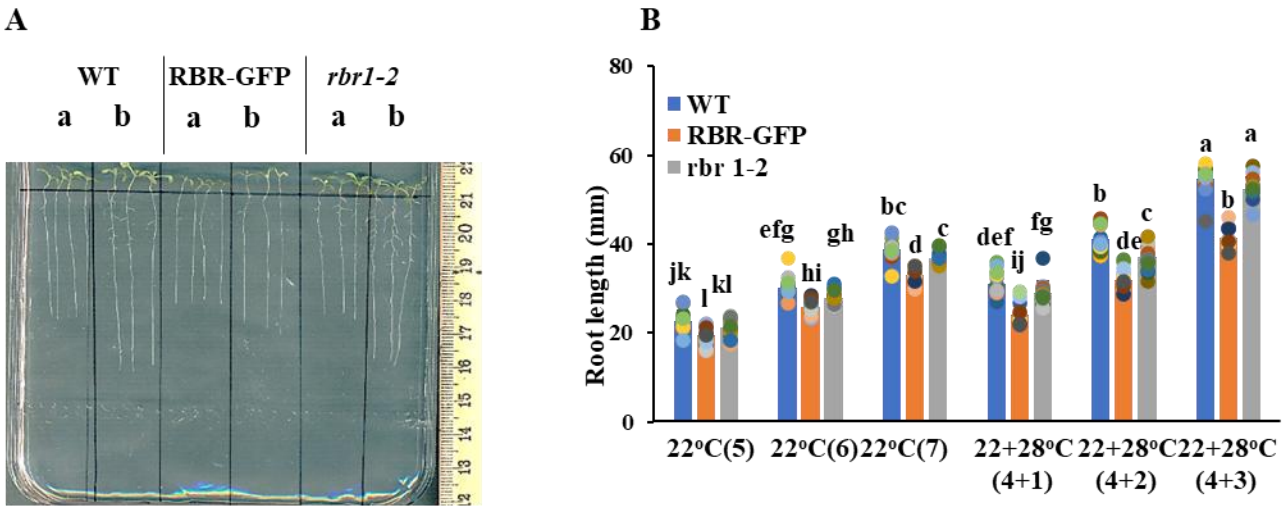

Figure 13. Ectopic RBR inhibits the warm temperature-induced root growth acceleration by repressing cell proliferation. Wilde type (WT), ectopic RBR-GFP expressing, and *rbr1-2* mutant seedlings were grown continuously at 22°C (control) or transferred from 22°C to 28°C (22+28°C) for the number of days indicated in the parentheses. **A**) Images of seedlings from the investigated lines grown on vertical plates at either 22°C (7) (a) or 22°C+28°C (4+3) (b). The scale bar is shown on the right side. **B**) Comparison of root length increase between the 5th and 7th days in WT, RBR GFP and *rbr1-2* seedlings grown continuously at 22°C or transferred on the fourth day to 28°C (n=15). Different letters mean statistically significant differences ($p < 0.05$) based on one-way ANOVA analyses with Tukey's HSD post-hoc test.

To investigate why these transgenic RBR lines produced shorter roots than the WT control when grown at a higher temperature, we studied root meristems (RMs) after staining them with propidium iodide and analysed them under confocal microscopy (Fig. 14A). The meristem size was calculated by counting the cortex cells from the quiescent centre (QC) to the transition zone, where they doubled in size (Fig. 14B). Three days after transferring the seedlings to 28ºC (7 days in total after germination) the number of cortex cells dramatically increased in the root meristem of all three lines but at different levels (Fig. 14B). In the *rbr1-2* line, the number of cortex cells was found to be higher than in the WT at both 22ºC and 28ºC. In contrast, a much smaller number of cortex cells were counted in the ectopic RBR-GFP expressing roots at both 22ºC and 28ºC compared to the control WT. However, warm temperatures were also able to increase the number of cortex cells in this line, indicating that the cell proliferation inhibitory function of RBR may be partially suppressed by 28ºC (Fig. 14B). We also determined the length of cortex cells in these genotypes at both temperatures. The cortex cells started to elongate in the RBR-GFP line much closer to the quiescent centre cells than in the WT, while the reduced RBR level in the *rbr1-2* mutant line had the opposite effect by delaying cell elongation in the root tip (Fig. 14C). We have observed a similar trend when growing these seedlings at a continuous temperature of 22ºC and 28ºC for either 7 or 14 days after germination (Suppl. Fig. S2). In all three lines, the root length increased over time, with the degree of increase dependent on both the temperature and the RBR level (Suppl. Fig. S2A-B). Accordingly, the warmer temperature likely activated cell proliferation in the RM of all investigated lines (Suppl. Fig. S2C). However, the RBR level was inversely correlated with the number of cells in the root meristem at both temperatures. The number of cortex cells increased the most at 28°C in the *rbr1-2* mutant roots, while the increase was the lowest in the RBR-GFP roots two weeks after germination (Suppl. Fig. S2D, E).

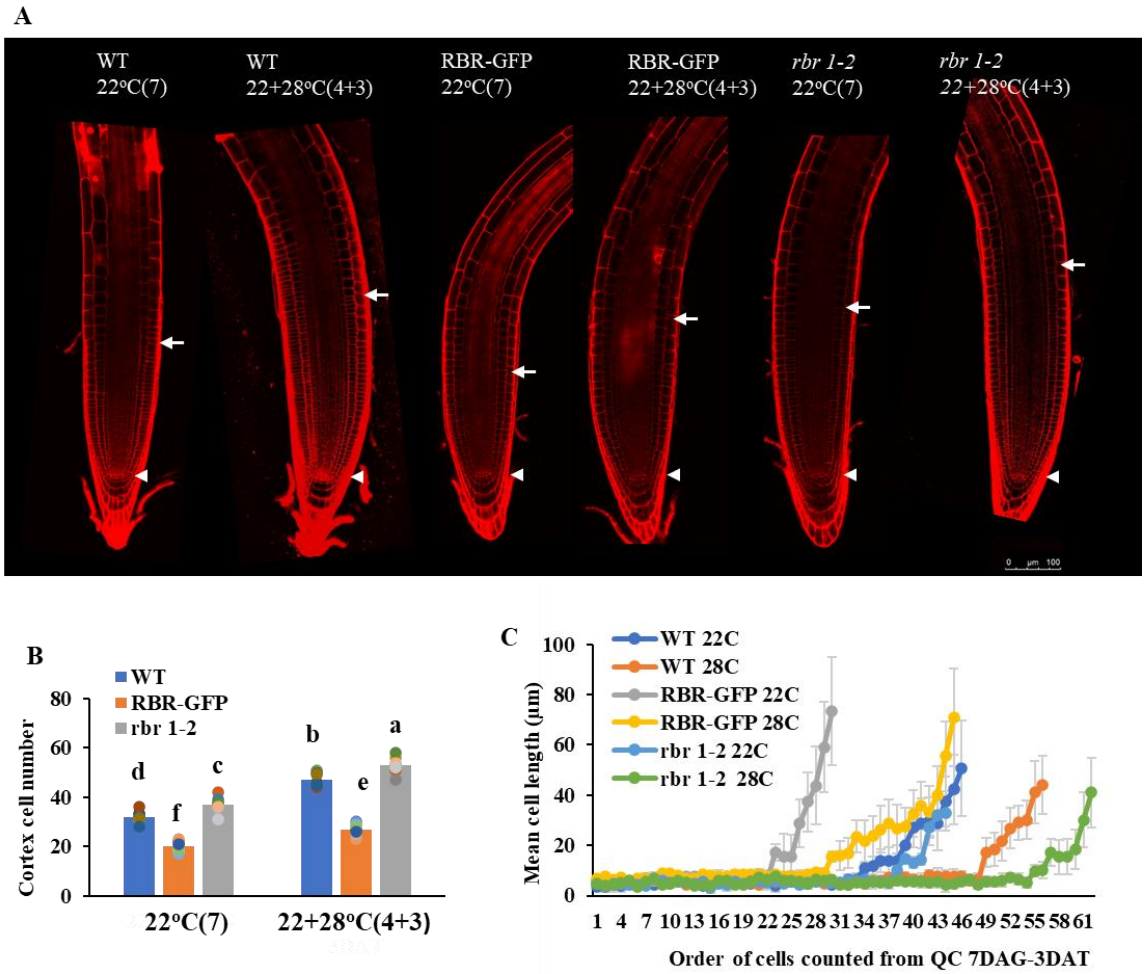

Figure 14. Root meristem size is oppositely affected by RBR levels. A) Representative images of root tips of WT, RBR-GFP and rbr1-2 seedlings grown at 22°C (7) for 22+28°C (4+3). The roots were stained with propidium iodide, and imaged under a confocal laser scanning microscope. Arrowheads indicate quiescent centres; arrows show the boundary of the root meristem in the cortex cell file. **B**) Cortex cell number in the root meristem of 7-day-old WT, RBR-GFP and rbr1-2 seedlings grown at 22°C (7) or 22+28°C (4+3) (n=8 roots). Different letters mean statistically significant differences ($p < 0.05$) based on one-way ANOVA analysis with Tukey's HSD post-hoc test. **C**) Spatial distribution of cell length across root meristems in WT, RBR-GFP and rbr1-2 seedlings grown either at 22°C (7) or 22+28°C (4+3). Mean cell length was calculated at each position along the cortical cell file, which is defined by counts of cortical cells from the quiescent centre. Values are averages from the data analysed in eight roots from different plants (±SD).

To further support that warm-temperatures, activate cell proliferation in the RM, we carried out a DNA replication-based assay. The seedlings were incubated with the thymidine analogue 5'-ethynyl-2'-deoxyuridine (5µM EdU) for 30 minutes to label the cells that are in the S-phase of the cell cycle. The roots of the three lines were labelled with EdU at 8, 24, or 48 hours after being transferred from 22ºC to 28ºC or remaining at 22ºC for the same period. Interestingly, most of the S-phase cells were detected 8 hours after the seedlings were transferred to 28ºC, indicating that entry into the cell cycle was quickly activated by the warm temperature in all three lines (Fig. 15A). However, as we have seen earlier in the case of the size of the root meristems, the EdU signal was negatively correlated with RBR levels, being strongest in the *rbr1-2* mutant and lowest in the RBR-GFP expressing line (Fig. 15B).

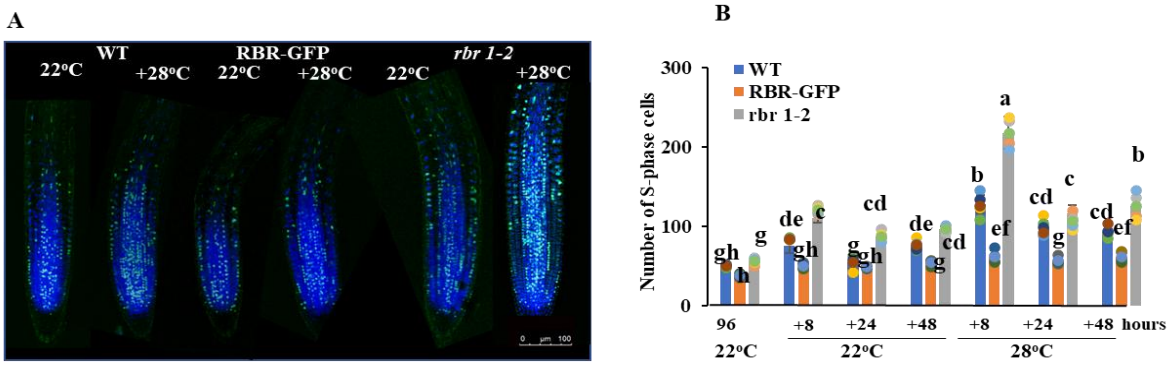

Figure 15. Elevated temperatures promote DNA synthesis initiation, though RBR levels modulate this advancement inversely. A) EdU (green) and Hoechst (blue) co-staining of nuclei in root tips of WT, RBR-GFP and *rbr1-2* lines grown at 22°C for 4 days and transferred to 28°C (+28°C) or left at 22°C for additional 8h before a 30 minuntes incubation with 5mM EdU labelling cells passing the S-phase of the cell cycle. Representative images of the roots were captured using a confocal laser microscope. Scale bar is (100µm). **B**) The number of EdU-positive root cells was counted at the indicated time points from eight roots for each genotype at each time point. Data are average ±standard deviation (n=3 biological replicates, N=8 samples in each). Different letters mean statistically significant differences ($p < 0.05$) based on one-way ANOVA analysis with Tukey's HSD post-hoc test.

4.4 Effect of RETINOBLASTOMA-RELATED protein (RBR) on leaf primordia development and temperature-dependent cell proliferation

We also analysed the shoot apex of young seedlings using scanning electron microscopy. As we have seen earlier in the case of WT seedlings, the leaf primordia of both RBR-GFP and *rbr1-2* lines were more developed just two days after being transferred from 22^{o}C to 28^{o}C (Suppl. Fig. S3A). However, we observed smaller and less developed leaf primordia in the shoot apex of RBR-GFP seedlings compared to the *rbr1-2* mutant and WT seedlings at both temperatures (Suppl. Fig. S3A). The average cell size in the 3rd leaf primordium epidermis was comparable among these lines at both temperatures, indicating that increasing the RBR level decreases proliferation activity (Suppl. Fig. S3B). In response to the temperature transfer, the first leaves of all three lines developed faster and grew larger (Fig. 16A). However, the *rbr1-2* mutant leaves reached a similar size as the wild-type ones, while the ectopic RBR-GFP leaves remained significantly smaller. By measuring the size of palisade cells (B), we could also estimate their numbers in these leaves (Fig.16 C, D, E). Warm temperatures increased both cell size and cell numbers in all three cases. However, while an elevated level of RBR had a negative effect on cell number, it had a positive effect on cell size. Conversely, the reduced level of RBR in the *rbr1-2* mutant leaf had a positive effect on cell number but negatively influenced cell size (Fig. 16 C-E). Altogether, these data indicate that warm temperatures activate cell proliferation in the shoot apex and in young leaves similarly to the root tip and RBR is likely involved in this regulation.

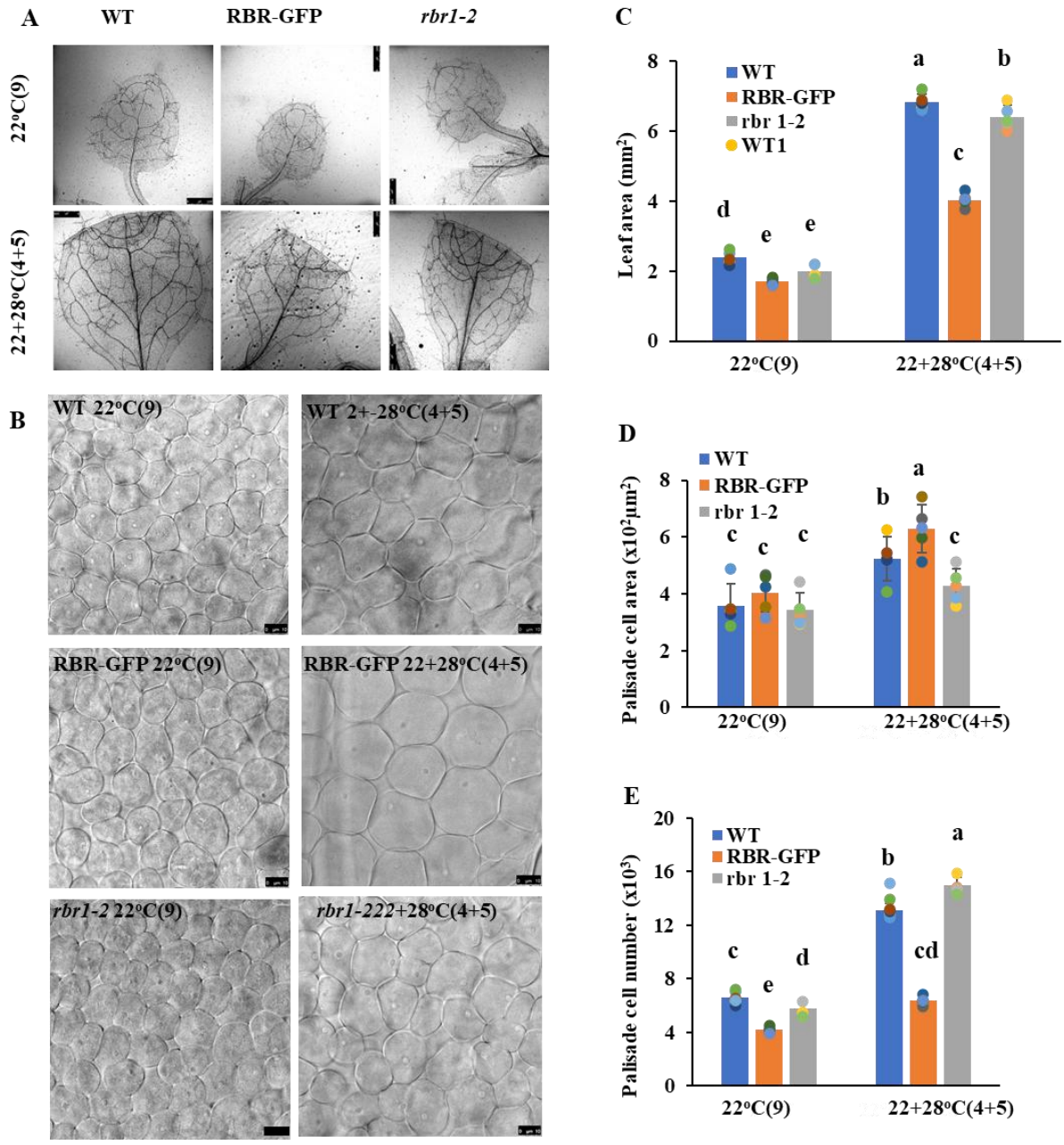

Figure 16. Elevated RBR levels positively regulate cell elongation. **A**) The 1st leaf of WT, RBR-GFP and *rbr1-2* lines were pictured under confocal laser microscope at both 22°C and 28°C as indicated. Scale bar is (500µm) **B)** Palisade cells of the first leaf of WT, RBR-GFP and *rbr1-2* seedlings grow at continuous 22°C for 9 DAG or for 4 DAG and 5 DAT to 28°C. Scale bar is 10 µm. **C-E**) Size of the first leaf (**C**), the palisade cell area (**D**) were measured of each genotype at both temperatures, and cell number was calculated (**E**).

To further support this hypothesis, we analysed the expression of the cell cycle regulatory and E2F-RBR target genes, ORC2 and CDKB1;1 (Őszi et al., 2020; Gombos et al., 2023), in RBR-GFP and *rbr1-2* seedlings, as well as in the WT control soon after transferring them from 22°C to 28°C (Fig. 17A).

Both the S-phase (*ORC2*) and the G2-M phase specific (*CDKB1;1*) regulatory genes were up-regulated in all three lines eight hours after the transfer. Afterwards, they both remained expressed at a higher level than at 22°C. The ectopic and reduced RBR-expressing lines showed opposite effects on the expression levels of these cell cycle genes increasing and decreasing them, respectively, in relation to the expression in the WT (Fig. 17B).

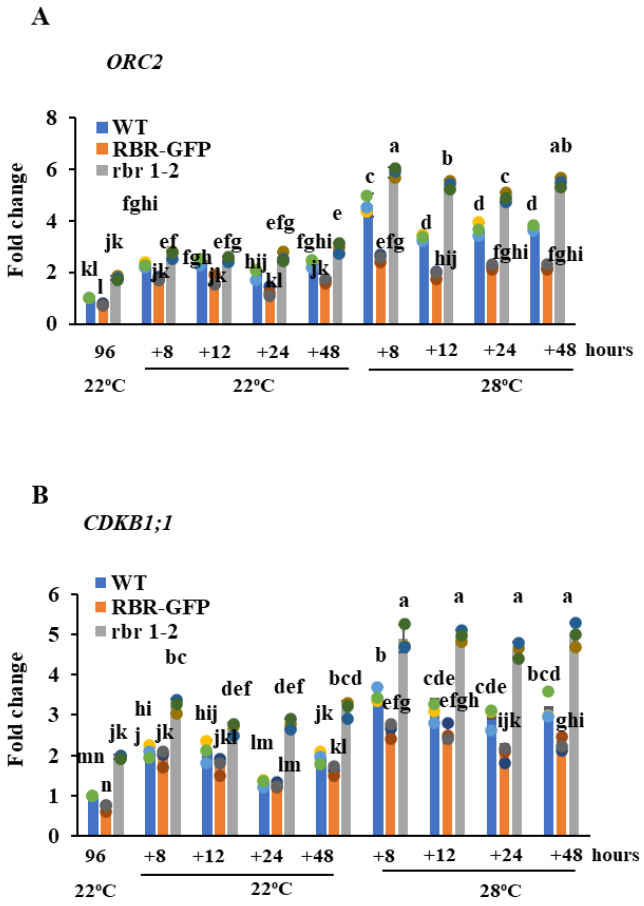

Figure 17. Cell cycle regulatory genes are activated by warm temperatures in a manner dependent of RBR. A-B) The expression of S- and the G2-M-phase-specific genes *ORC2* (**A**) and *CDKB1;1* (**B**) was induced by warm temperatures, depending on RBR. The expression levels of both genes (**A-B**) was assessed using qRT-PCR. Seedlings of WT, RBR-GFP and *rbr1-2* lines were grown for 96 hours at 22°C post-germination, and samples were collected at the indicated time points at either 22°C or 28°C, respectively. Values represent fold change normalized to the value of the relevant transcript of the seedlings at T0 (96h), which was set arbitrarily at 1. Data are means±SD. N=3 biological replicates. Different letters mean statistically significant differences ($p < 0.05$) based on one-way ANOVA analyses with Tukey's HSD post-hoc test.

4.5 The function of the RETINOBLASTOMA-RELATED (RBR) cell cycle inhibitor is suppressed by warm temperatures, in correlation with its phosphorylation status

RBR is known to be regulated by phosphorylation and we suggest that warm temperatures may repress RBR's cell cycle inhibitory function by stimulating and increasing its phosphorylation. To investigate this hypothesis, we first studied the expression of two G1 CYCLIN genes: *CYCLIN D3;1* (*CYCD3;1*) and *CYCLIN A3;1* (*CYCA3;1*) (Fig. 18A-B). These genes are known to be the regulatory subunits of the plant RBR-kinase CYCLIN-DEPENDENT KINASE A;1 (CDKA;1 – Van Leene et al., 2011; Takahashi et al., 2010). They both exhibited a similar expression pattern under our experimental conditions, similar to that of the cell cycle regulatory genes (Fig. 17 A-B: and Fig. 18 A-B). They showed an early up-regulation at 8 hours of 28ºC and afterwards maintained a generally and significantly higher expression level at 28oC compared to 22ºC. Additionally, their expression levels were oppositely regulated by RBR; they were low in the ectopic RBR line, while high in the *rbr1-2* mutant indicating that they are E2F-RBR target genes (Bouyer et al., 2018; Őszi et al., 2020; Gombos et al., 2023; Fig. 18 A-B). These data support the idea that RBR-kinase(s) could be activated by warm temperatures. To investigate this hypothesis, we monitored the phosphorylation of RBR through a western blot assay using a phosphosite-

specific anti-RETINOBLASTOMA protein antibody. This antibody has been shown to label the Arabidopsis RBR protein in a serine 911 (911S) phosphorylation-dependent manner (Magyar et al., 2012; Wang et al., 2014). Previously, it was demonstrated that the RBR protein, phosphorylated on 911S, could not form a complex with E2Fs (Magyar et al., 2012). As shown in Fig. 18C, RBR became increasingly phosphorylated over time in WT seedlings at 22°C, indicating its developmental control. However, the level of the phosphorylated RBR form was much higher at 28°C, already 8 hours after the transfer, and continued to elevate afterwards. All of this data supports the view that warm temperatures activate cell proliferation in young seedlings by suppressing the cell cycle inhibitor RBR through stimulating its phosphorylation

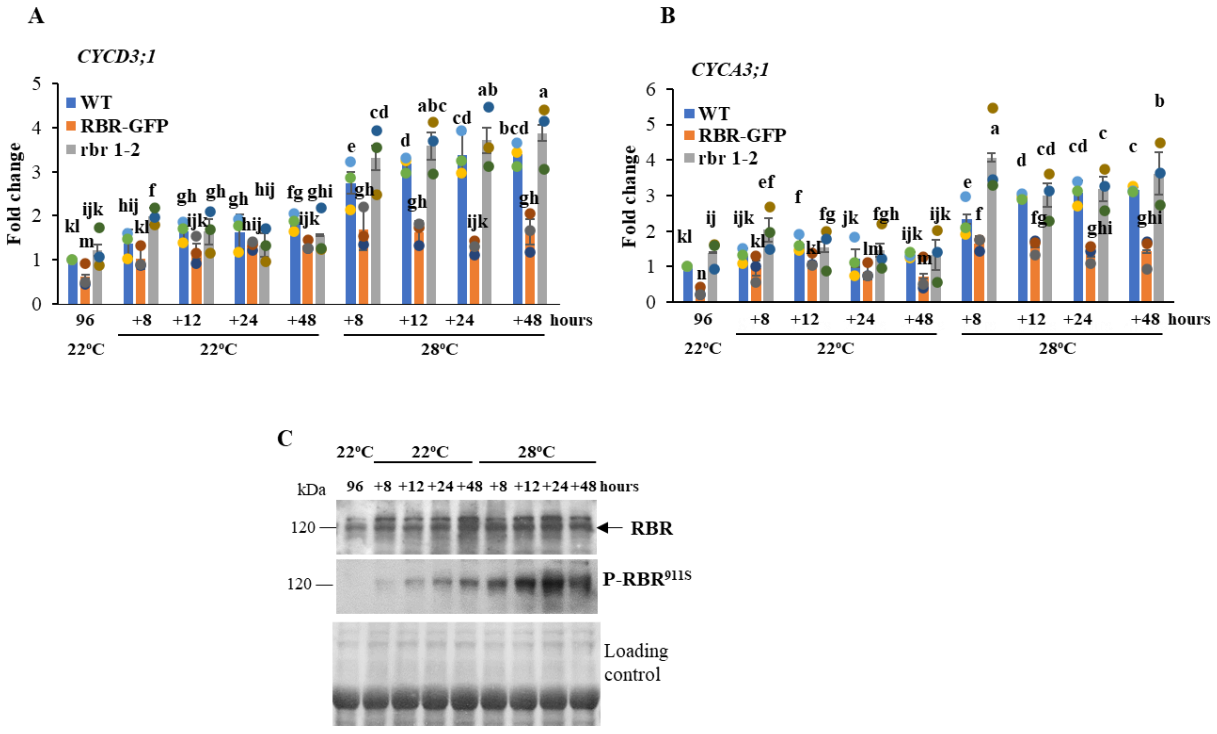

Figure 18. Temperature-Dependent regulation of RBR phosphorylation. A-B) Transcript levels of the G1 cyclins, *CYCLIN D3;1* (*CYCD3;1*- **A**) and *CYCLIN A3;1* (*CYCA3;1* - **B**), were found to be elevated in response to increased temperatures and exhibited differential regulation in the RBR-GFP and *rbr1-2* lines. The expression of these genes

(**A**–**B**) was monitored using qRT-PCR. Seedlings of WT, RBR-GFP and *rbr1-2* lines were grown for 96 hours at 22°C post-germination, with samples were collected at the indicated time points at either 22°C or 28°C. The values represent fold change normalized to the value of the relevant transcript of the seedlings at T0 (96h), which was set arbitrarily at 1. Data are means ± SD. N=3 biological replicates. Distinct letters mean statistically significant differences ($p < 0.05$) based on one-way ANOVA analyses with Tukey's HSD post-hoc test. **C)** The Western blot analysis shows the levels of RBR and phospho-RBR (P-RBR at the 911 serine site) in WT seedlings cultivated as indicated. Sampling was made as in (**A-B**). The membrane was stained with Coomassie brilliant blue to indicate equal loading. Molecular weight marker (kDa) is shown at the left side. Arrow marks the position of the RBR protein.

4.6 RBR positively regulates hypocotyl elongation induced by warm temperatures

Contrary to the apical meristem, the hypocotyl consists of mostly non-dividing post-mitotic cells. In the hypocotyl epidermis, there are only a few dividing cells, and they are all concentrated in the non-protruding longitudinal cell files belonging to the stomatal lineage in the upper half of the hypocotyl (Kono et al., 2007). Interestingly, the number of cells was previously found to be slightly elevated in the hypocotyl epidermis when the temperature was increased to 28ºC, but cell elongation was considered to be the dominant process driving hypocotyl elongation at the higher temperature (Bellstaedt et al., 2019). Increasing the amount of RBR slowed down the acceleration of growth in both the shoot and root meristems under warm temperature (Figs 9 and 10). However, surprisingly, the hypocotyl of RBR-GFP expressing seedlings grew significantly longer after transfer from 22ºC to 28ºC compared to that of the WT (Fig. 19 A, B). Contrary to the RBR-GFP expressing seedlings, the hypocotyl length of the rbr1- 2 mutant seedlings was shorter compared to the WT at 28ºC (Fig. 19A-C).

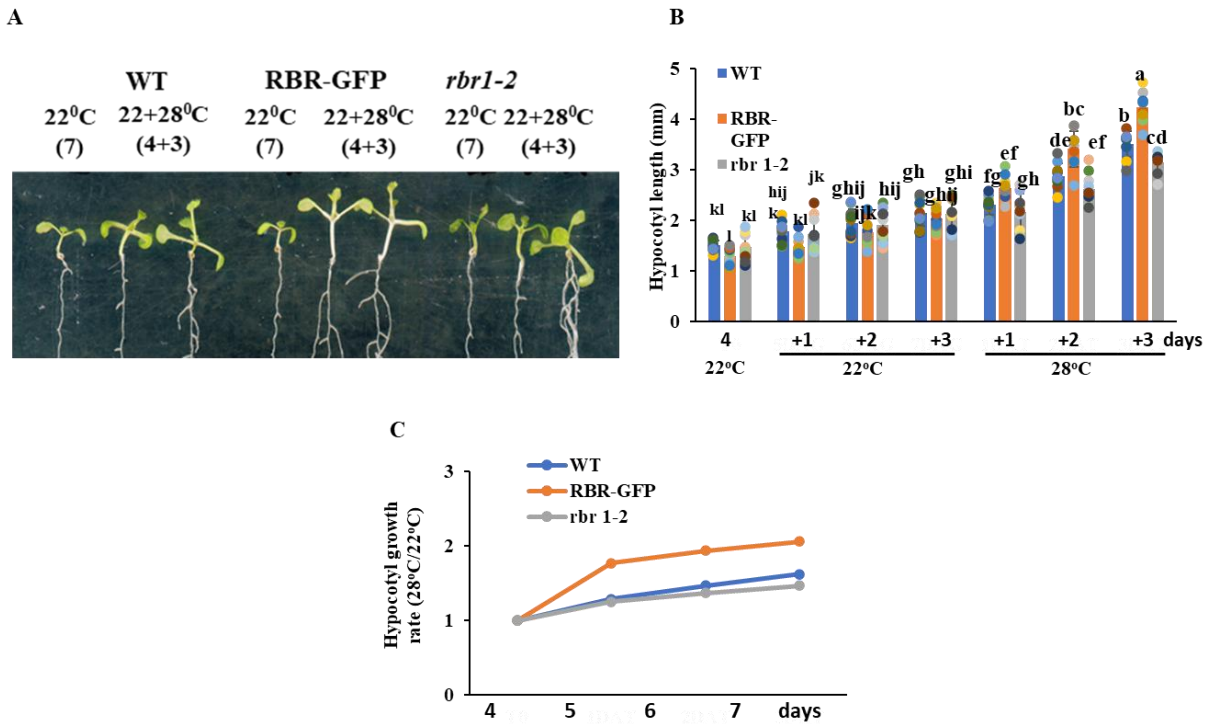

Figure 19. RBR induces hypocotyl elongation at elevated temperatures in a concentration-dependent manner. Wild type (WT) control, ectopic RBR-GFP expressing, and *rbr1-2* mutant seedlings were either grown continuously at 22°C or transferred from 22°C to 28°C (22+28°C) for the number of days indicated in the parentheses. **A,** Ectopic RBR increases hypocotyl length following the transfer of seedlings to 28°C. (**B**) Hypocotyl length of the three genotypes with different RBR levels was measured both at continuous 22°C or after transfer to 28°C at the indicated time points. N=10; (**C**) Growth rate of hypocotyl was determined (28ºC/22ºC). Different letters mean statistically significant differences ($p < 0.05$) based on one-way ANOVA analyses with Tukey's HSD post-hoc test.

To understand the reasons for these phenotypic differences, we first measured the length of epidermal cells in the hypocotyl epidermis of WT, RBR-GFP and *rbr1-2* seedlings grown at either 22ºC or after being transferred from 22ºC to 28ºC at 4 DAG. The length of the epidermal cells was found to be comparable in all of these seedlings grown at 22°C, but it started to differ soon after the seedlings were transferred to 28°C (Fig. 20 A, B). Accordingly, epidermal cells elongated the most in the hypocotyl of the RBR-GFP seedlings, while they were less elongated in the *rbr1-2* mutant than in the WT (Fig. 20 A, B and Supplemental Fig. S4A-C). The difference in cell elongation might be explained by differential ploidy increase in the hypocotyl cells in response to the elevated temperature. Although the ploidy level was indeed increased in the hypocotyl of all the three lines at warm temperatures as more 16C nuclei were detected at 28ºC than at 22ºC, the increase was at a comparable level in all the three lines (Supplemental Fig. S4D).

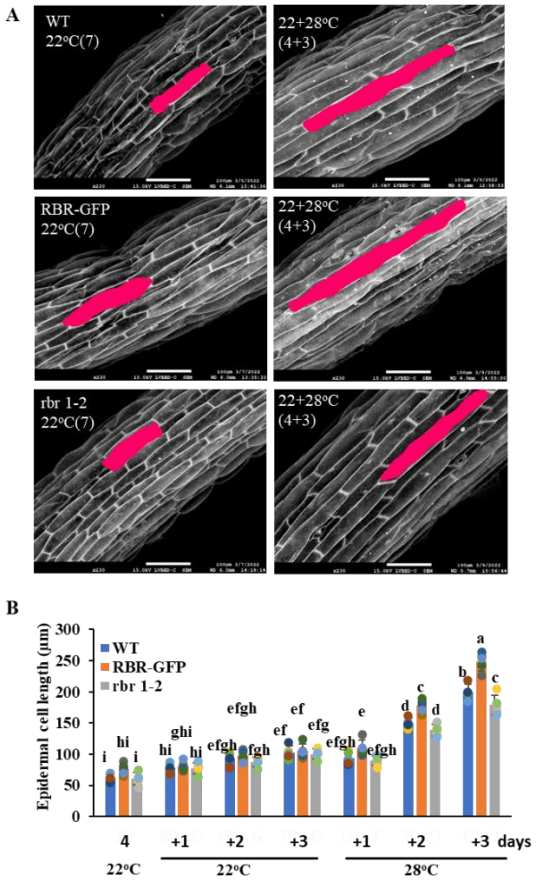

Figure 20. RBR induces hypocotyl elongation by enhancing cell elongation in a manner dependent on concentration. **A**) Hypocotyl epidermis was analysed under a scanning electron microscope at both temperature regimes at the indicated time points. Scale bar is 100 µm. (**B**) Cell length of hypocotyl epidermis in the three lines was measurred by using the Image J software (N= 5). Different letters mean statistically significant differences ($p < 0.05$) based on one-way ANOVA analyses with Tukey's HSD post-hoc test.

In the WT, the number of cells in the hypocotyl also increased in response to the elevated temperature, confirming previous observations (Bellstaedt et al., 2019 and Fig. 21 A-B). The *rbr1-2* mutant had more cells but showed a similar temperature response than the WT (Fig. 21A-B). The number of hypocotyl cells also increased in the RBR-GFP line, but the cell number and the increase were lower in comparison to the other two lines (Fig. 21A-B). Interestingly, small meristemoid-like cells belonging to the stomatal lineage were found to be the most proliferative in

the *rbr1-2* mutant, and warm temperatures further increased their number (Supplemental Fig. 5A-B). In contrast, ectopic RBR reduced the numbers of these cells at both temperatures compared to the WT (Supplemental Fig. S5A-B). These data indicate that the amount of RBR positively correlates with cell length but inversely with cell number in the hypocotyl.

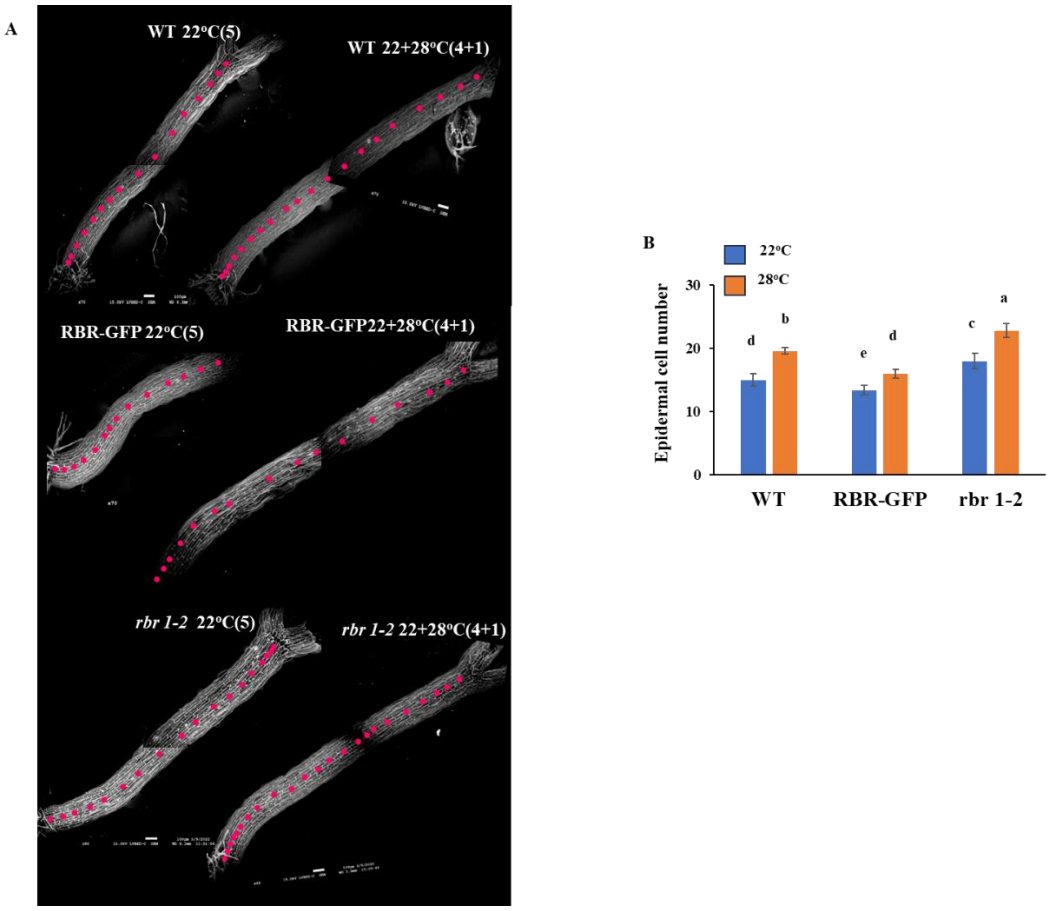

Figure 21. Warm temperatures result in an increased number of cells in the hypocotyl. **A**) Scanning electron microscopy (SEM) images depict the hypocotyl of WT, *rbr1-2* and RBR-GFP seedlings cultivated at a constant temperatures of 22ºC or subjected to 28ºC for one day after transfer (1DAT) of 4-day-old (4DAG) seedlings. Pink dots mark epidermal cells in the same longitudinal file. **B**) The number of epidermal cells was quantified and graphically represented. Different letters mean statistically significant differences ($p < 0.05$) based on one-way ANOVA analyses with Tukey's HSD post-hoc test.

4.7 RBR modulates *PIF4*/*PIF7* and *YUCCA* expression during temperature-induced hypocotyl elongation

Cell elongation is stimulated in the hypocotyl by warmth through the PIF4/PIF7-YUCCA auxin regulatory module (Casal & Balasubramanian, 2019). We were curious about whether RBR influences the expression of the main regulators of thermomorphogenesis. For this purpose, we grew seedlings for 4 days at 22ºC. Afterwards, we either continued their culture at 22ºC or transferred them to 28ºC. We conducted a q-RT-PCR experiment to determine the expression of *PIF4* and *PIF7*, at 8, 24, and 48 hours after transfer. As shown in Figure 22 A, B, both genes were expressed at comparable levels in all three lines at 22ºC. However, this picture dramatically changed when transferring the seedlings to 28°C. Both PIF genes were already upregulated in each line just 8 hours after warm treatment. The strongest activation was found in the ectopic RBR expressing line, while *rbr1-2* was less effective in the upregulation (Fig. 22 A, B). In addition, *PIF4/7* expression continuously increased in the RBR-GFP line at 28ºC, much more than their expressions change in the WT and in the rbr1-2 mutant line at 28ºC during the investigated period (Fig. 22 A, B)

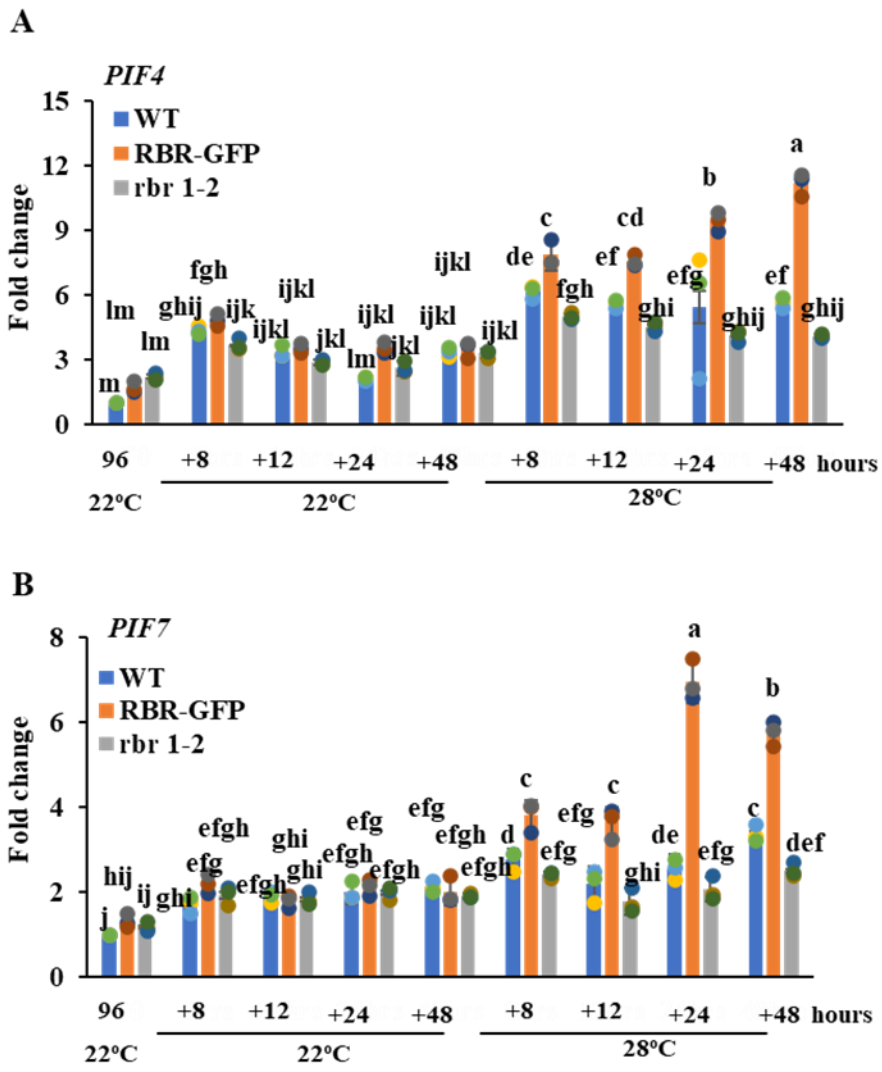

Figure 22. RBR positively regulates the expression of *PIF4* and *PIF7* in response to temperature. The expression levels of *PIF4* (**A**) and *PIF7* (**B**) were assessed in WT, RBR-GFP and *rbr1-2* seedlings at the indicated temperatures and time points. T0 denotes seedlings that are 96 hours old and have been cultivated at 22°C. These seedlings were either maintained at 22°C or transferred to 28°C, with samples collected at 8, 12, 24 and 48 hours post-transfer. Values represent fold change normalised to the value of the relevant transcript of the seedlings at T0 (96h), which was set arbitrarily at 1. Data are means ±SD. N=3biological replicates. Different letters mean statistically significant differences ($p < 0.05$) based on one-way ANOVA analyses with Tukey's HSD post-hoc test.

Emerging data support the view that PIFs activate the expression of auxin biosynthetic *YUCCA* genes under shade and warm temperatures, resulting in auxin-mediated elongation growth (Casal & Balasubramanian, 2019). To test whether ectopic RBR could also stimulate the expression of *YUCCA* genes, we analysed the expression of four *YUCCA* genes (*YUC1,2,8*, and *9*) including *YUC8* a rate-limiting auxin biosynthesis enzyme in temperature-dependent hypocotyl elongation in the same experiments described above (Fig. 23A-D). Interestingly, all these *YUCCA* genes showed similar expression patterns to the PIF4 and 7 genes, as they were all up-regulated by warm temperatures in all three lines 8 hours after the seedlings were transferred to 28ºC. Additionally, their expression levels correlated well with RBR levels, with the highest expression values in the ectopic RBR line and the lowest ones in the *rbr1-2* mutant line (Fig. 5). In addition, *TRANSPORT INHIBITOR RESPONSE 1* (*TIR1*), an auxin receptor F-box protein expressed similarly to *PIF4-7* in these lines at warm temperatures (Suppl. Fig. S6A). These data further support that RBR could accelerate hypocotyl elongation at 28ºC by positively regulating the PIF-YUCCA regulatory module and auxin signalling. In contrast to *PIF4-7*, the expression of (HY5), a key regulatory gene in photomorphogenesis, was similar to that of cell cycle genes under warm temperatures (Suppl. Fig. S6B and Fig. 17). Its level increased in the rbr1-2 mutant, while it decreased in the RBR-GFP line compared to the WT. Accordingly, RBR exerts opposite control over the expression of HY5 and PIF4-7, the regulators that play antagonistic roles in both light and temperature-induced developmental processes (Wang and Zhu, 2022).

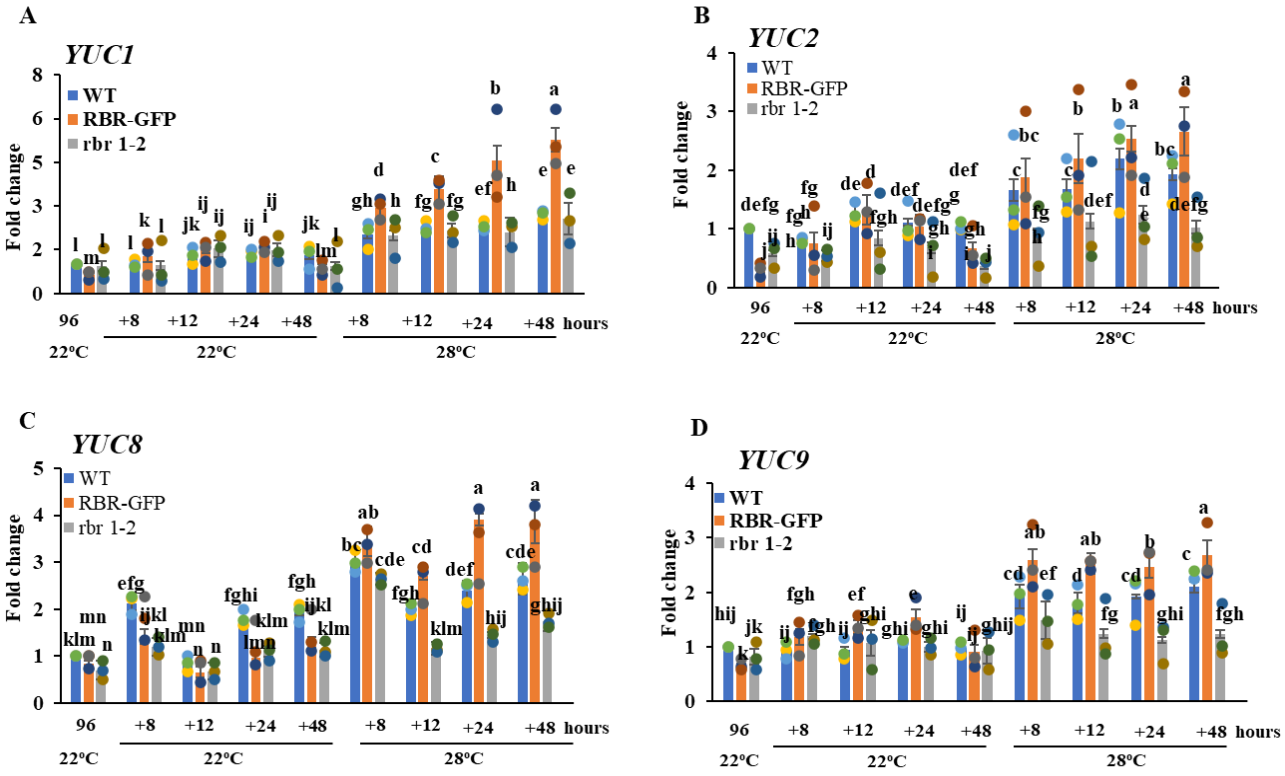

Figure 23. Under conditions of elevated temperature, RBR positively regulates the *YUCCA* genes involved in the regulation of auxin synthesis. (**A–D**) The expression of four *YUCCA* genes (*YUC1*, *YUC2*, *YUC8* and *YUC9*) were assessed using qRT-PCR as indicated. The initial time point (T0), corresponds to seedlings aged 96 hours. These seedlings were either maintained at a temperature of 22°C or transferred to 28°C, with samples were taken at 8, 12, 24 and 48 hours post-transfer. Values represent fold change normalised to the value of the relevant transcript of the seedlings at T0 (96h), which was set arbitrarily at 1. Data are means ±SD. N=3 biological replicates. Different letters mean statistically significant differences ($p < 0.05$) based on one-way ANOVA analyses with Tukey's HSD post-hoc test.

4.8 The thermo-responsive phenotype of ectopic RBR-GFP expressing seedlings is specifically complemented by the mutation of E2FB rather than E2FA

In previous research, we demonstrated that canonical E2Fs serve as the primary effectors of RBR in Arabidopsis, with the three E2Fs redundantly binding to a similar set of genes associated with the regulation of cell proliferation, in conjunction with RBR (Gombos et al., 2023). To investigate whether ectopic RBR promotes hypocotyl elongation at elevated temperatures via E2Fs, we crossed RBR-GFP expressing line with E2FA and E2FB mutant lines (*e2fa-1* and *e2fb-2*, respectively – Leviczky et al., 2019). Following the generation of double homozygous lines for both *e2fa-1*/RBR-GFP and *e2fb-2*/RBR-GFP, we assessed the impact of these E2F mutations on the thermo-response of RBR-GFP as previously described. The mutation of E2FA did not influence either the hypocotyl or the root length of the ectopic RBR-GFP expressing seedlings, suggesting that RBR regulate hypocotyl elongation independently of E2FA (Fig. 24A-B). In contrast, the double transgenic *e2fb-2*/RBR-GFP seedlings showed similar phenotype under warm temperature conditions as that of WT having longer roots and shorter hypocotyl than the ectopic RBR-GFP line. Accordingly, ectopic RBR regulates hypocotyl and root growth through E2FB under elevated temperature conditions. However, the underlying mechanism remains unidentified and requires further investigation (Fig. 24C-E).

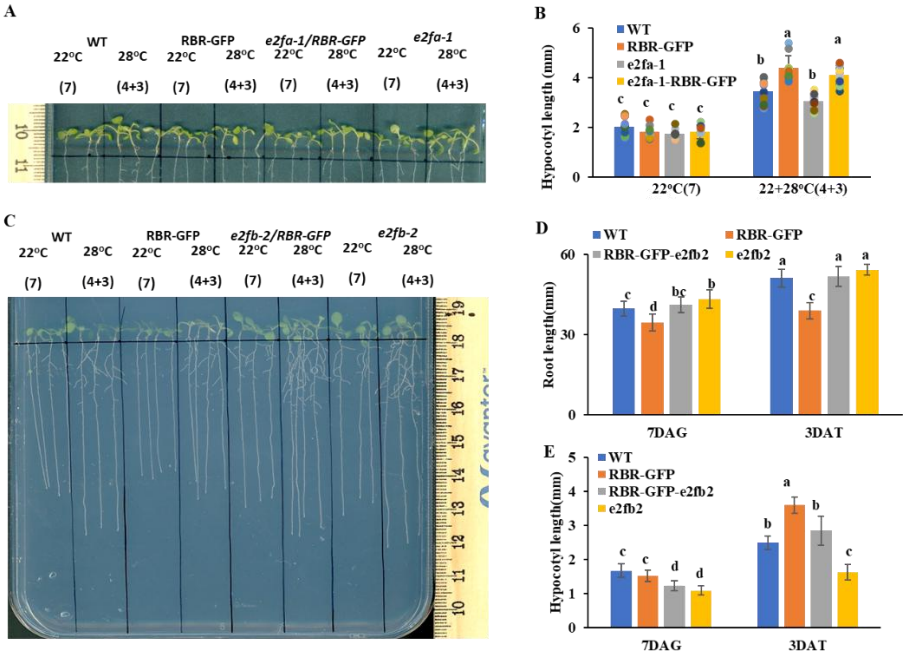

Figure 24. The thermo-responsive phenotype of RBR-GFP seedlings was unaffected by E2FA mutation but reverted to wild-type with E2FB mutation. A) The image depicts representative seven-day-old seedlings of the specified genotypes (WT, RBR-GFP, *e2fa-1*/RBR-GFP, *e2fa-1*), cultivated at either 22°C or 28°C as indicated. **B**) Hypocotyl length of was quantified (mm) and graphically represented. **C**) The image illustrates seedlings of the specified genotypes (WT, RBR-GFP, *e2fb-2*/RBR-GFP, and *e2fb-2*) grown under varying temperature conditions. **D-E**) Measurements of root (**D**) and hypocotyl (**E**) lengths were conducted and plotted. Seedlings were cultivated either for 7 days after germination (DAG) at a constant 22°C or for 4 DAG followed by 3 days at 28°C. Distinct letters indicate statistically significant differences ($p < 0.05$) as determined by one-way ANOVA with Tukey's HSD post-hoc test.

4.9 Mutation of *CYCD3;1-3* in Arabidopsis shows hypocotyl growth promotion similar to ectopic RBR under elevated temperatures.

Our previous analysis demonstrated that *CYCD3;1* expression rapidly increased under elevated temperature conditions, suggesting its role in accelerated seedling growth when exposed to warmer temperatures. Additionally, the phosphorylation of RBR was concurrently elevated at higher temperatures, indicating that CYCD3;1 activates an RBR-kinase, which subsequently inactivates RBR thereby facilitating accelerated development. Furthermore, the expression of *CYCD3;1* in the hypocotyl supports its involvement in elongation growth (Winter et al., 2007).

To evaluate these hypotheses, we initially assessed the root lengths of *cycd3;1-3* triple mutants (Dewitte et al., 2007), which lack all three D-type cyclins, at 22°C (7 days after germination, DAG) and 28°C (4 days at 22°C followed by 3 days at 28°C, DAT), comparing them to the RBR-GFP expressing line and the wild-type (WT) control. At 22°C, the root lengths of seedlings were comparable across all lines. However, at 28°C, both the ectopic RBR-GFP expressing and the *cycd3;1-3* mutant seedlings exhibited significantly shorter roots compared to the WT (Fig. 25 A-B). To further investigate the *cycd3;1-3* mutant phenotype, we stained the roots with propidium iodide (PI) and analysed cell numbers and lengths in the root tip at both 22°C (7 DAG) and 28°C (3 DAT, Suppl. Fig. S7A). Notably, the root meristem of *cycd3;1-3* mutant seedlings displayed a phenotype similar to the ectopic RBR-GFP at 22°C, with a smaller but comparable cell number to the WT control. However, at 28°C, the cell number in the *cycd3;1-3* mutant root meristem was significantly reduced compared to the WT, consistent with previous results observed in the ectopic RBR-GFP. Cell length was also measured in the root meristem, from the cells attached to the quiescent centre (QC) to the root transition zone where the meristem ends. We observed a

significant increase in cell size in the root meristem at 28°C compared to the WT, similar to the ectopic RBR-GFP line as described earlier in Suppl. Fig. S7 B-D. Additionally, we analysed the shoot apex of young seedlings using scanning electron microscopy (SEM). As previously observed in the case of WT and RBR-GFP seedlings, the leaf primordia of the *cycd3;1-3* triple mutant exhibited greater development merely one day after being transferred from 22°C to 28°C (Suppl. Fig. S8A). Nevertheless, the leaf primordia of the *cycd3;1-3* triple mutant remained smaller and less developed compared to the WT seedlings at both temperatures (Suppl. Fig. S8A). In response to the elevated temperature post-transfer, consistent with prior findings, the first leaf pair in *cycd3;1-3* developed more rapidly and attained a larger size at the higher temperature (Suppl. Fig. S8B). However, the *cycd3;1-3* leaves were still significantly smaller than those of the WT (Suppl. Fig. S8C). By measuring the size of the palisade cells (Suppl. Fig. S8D), we estimated their numbers in these leaves (Suppl. Fig. S8E). Warm temperatures led to an increase in both cell size and cell numbers in both lines; however, they exhibited opposite patterns: leaf cells were fewer in number but enlarged in the *cycd3;1-3* triple mutant compared to the WT control. Consequently, the CYCD3 subclass mediates temperature signals to suppress RBR function in both the shoot and root apex, thereby accelerating plant growth under elevated temperature conditions.

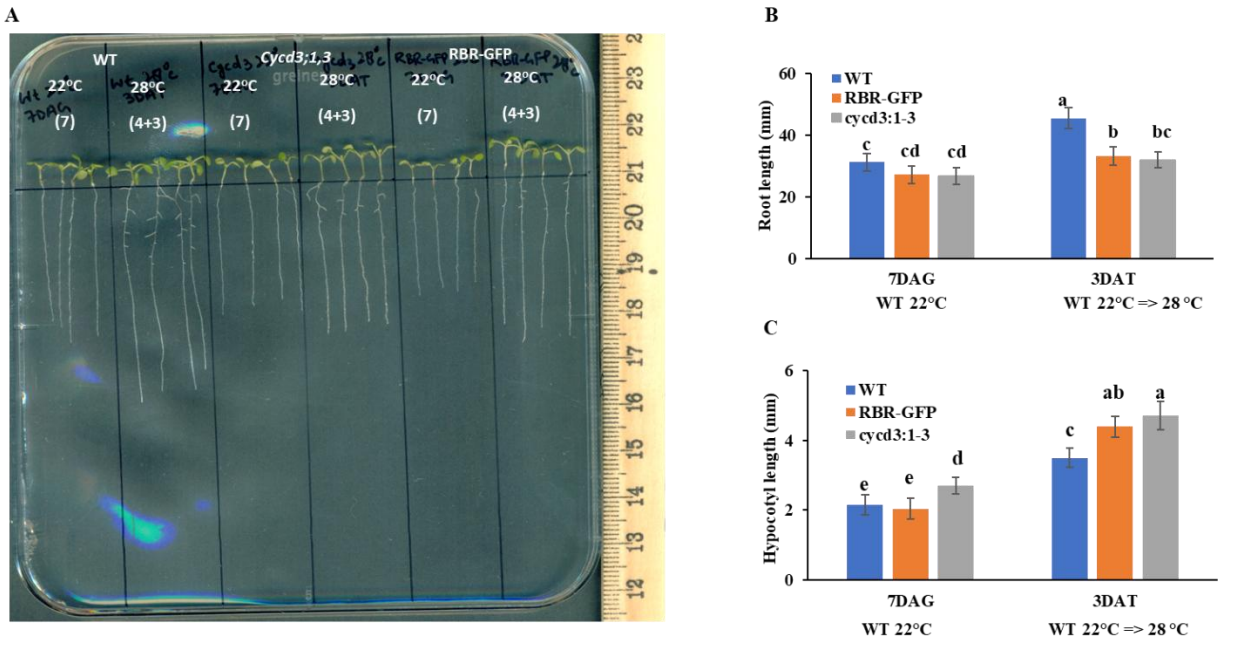

Figure 25. The triple mutant *cycd3;1-3* exhibits a thermo-response comparable to that of the ectopic RBR-GFP expressing line. A) Representative picture of the seedlings with distinct genotypes (WT, cycd3;1-3, RBR-GFP) maintained at various temperatures as indicated. **B-C**) Measurements of root length (**B**) and hypocotyl length (**C**) were conducted and plotted. Seedlings were grown either for 7 DAG at continuous 22ºC or for 4 DAG and 3 DAT at 28ºC. Different letters mean statistically significant differences ($p < 0.05$) based on one-way ANOVA analyses with Tukey's HSD post-hoc test.

Subsequently, we assessed the hypocotyl length of the triple *cycd3;1-3* mutant seedlings cultivated at 22°C (7 days after germination, DAG) and 28°C (3 days after transfer, DAT). Notably, the hypocotyl length in *cycd3;1-3* triple mutant seedlings was already increased at 22°C compared to the RBR-GFP and wild-type (WT) lines, indicating that these lines inhibit hypocotyl elongation under standard growth conditions. Furthermore, at the elevated temperature, the hypocotyl length of the *cycd3;1-3* mutant was significantly greater than that of the WT, yet comparable to the ectopic RBR-GFP line. We also conducted scanning electron microscopy (SEM) analysis of the hypocotyl epidermis at 22°C (7 DAG) and 28°C (3 DAT) to measure epidermal cell lengths. The

results demonstrated that *cycd3;1-3* mutants exhibited significantly longer epidermal cells but a markedly reduced number of epidermal cells at 28°C compared to the WT (Fig. 26B, C).

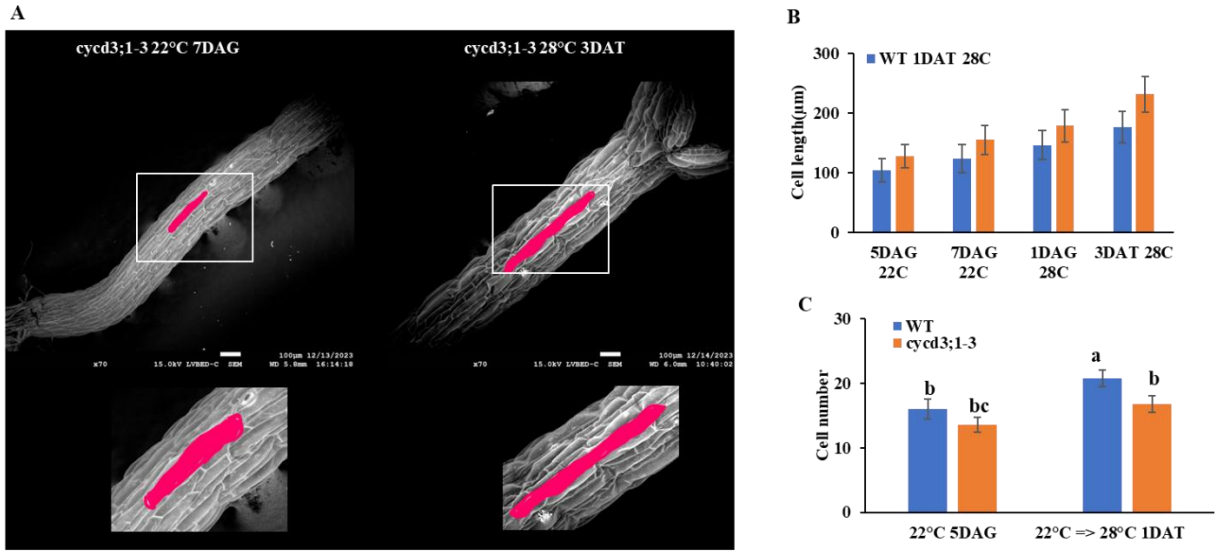

Figure 26. Mutation of the three D3-type cyclins (*cycd3;1-3)* induces cell elongation in the hypocotyl at 28°C. A) The hypocotyl epidermis was analysed under a scanning electron microscope (SEM) under both temperature conditions at the indicated time points. Scale bar is 100 µm. (B) The cell length of hypocotyl epidermal cells was measured utilizing Image J software (N= 5). C) The number of epidermal cells was counted and plotted at the time point indicated in the figure. Different letters mean statistically significant differences ($p < 0.05$) based on one-way ANOVA analyses with Tukey's HSD post-hoc test.

Phenotypic data from the *cycd3;1-3* triple mutant seedlings under elevated temperature conditions reveal effects on growth and development analogous to those observed in seedlings expressing the RBR-GFP line. Subsequently, we examined the expression of both cell cycle-related genes (*ORC2* and *CDKB1;1*) and key thermomorphogenic genes (*PIF4*, *PIF7*, *YUC2*, and *YUC8*) under increased temperature conditions. Expression levels were assessed using the Q-RT-PCR method in both WT and *cycd3;1-3* seedlings at 24- and 48-hours post-transfer from 22°C to 28°C (Fig. 27A-B). In the WT, both cell cycle regulatory genes were upregulated, whereas in the *cycd3;1-3*

mutants, their expression was less upregulated by elevated temperature, consistent with observations in the ectopic RBR line. Conversely, all key thermomorphogenic genes were upregulated in the *cycd3;1-3* triple mutant seedlings at 28°C compared to the control WT, as observed in the ectopic RBR-GFP line (Fig. 27C-E). These findings suggest that the absence of D-type cyclins inhibits cell proliferation while promoting cell elongation through a mechanism similar to that of the ectopic RBR, supporting the notion that *CYCD3* functions via RBR.

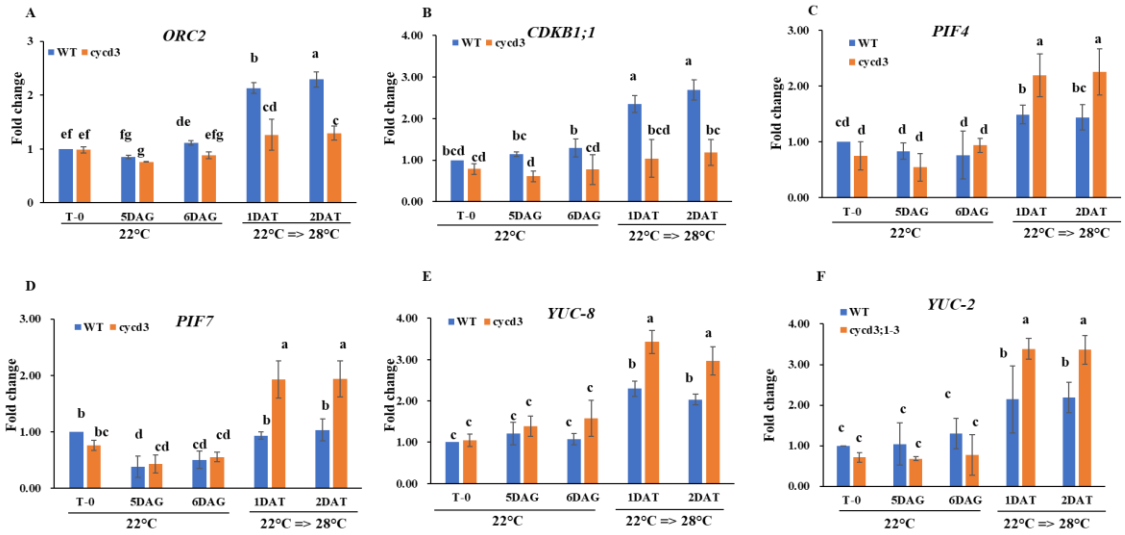

Figure 27. The expression of cell cycle and thermo-regulatory genes showed similar thermal response in *cycd3;1-3* triple mutant seedlings and RBR-GFP lines at elevated temperatures. (**A, B**) S- and G-M-phase specific *ORC2* (**A**) and *CDKB1;1* (**B**) were upregulated at warm temperatures. (**C-F**) Thermo-morphogenic genes *PIF4* (**C**), *PIF7* (**D**), *YUC8* (**E**) and *YUC2* (**F**) were induced by *cycd3;1-3* mutation. Gene expression (**A-E**) was assessed using qRT-PCR. WT and *cycd3;1-3* seedlings were grown for 96 hours at 22°C after germination, with samples collected at the indicated time points at 22°C or 28°C. Values represent fold change normalized to the value of the relevant transcript of the seedlings at T0 (96h), which was set arbitrarily at 1. Data are means ± SD. N=3 biological replicates. Different letters mean statistically significant differences ($p < 0.05$) based on one-way ANOVA analyses with Tukey's HSD post-hoc test.

4.10 Cell size of dividing cells depends on RBR level in developing Arabidopsis seedlings

4.11 Cortex cells in the root meristem divide with different cell size depending on the level of RBR

In the previous chapter we demonstrated that RBR influences post-mitotic cell size under warm ambient temperatures in a manner dependent on its concentration. The data suggest that RBR acts as a cell sizer in post-mitotic cells within both the hypocotyl and the leaf in a concentration-dependent manner. Additionally, we are interested in examining its impact on cell size in actively dividing tissues, such as plant meristems and young developing organs.

To investigate the possibility of RBR being a potential cell size regulator in dividing cells, we examined its concentration-dependent effect on cell size in the previously described two lines where RBR level was either elevated (ectopic RBR-GFP line) or decreased (*rbr1-2* mutant line), and compare them to the WT control. To eliminate any circadian clock effect, the seedlings were grown in continuous light conditions at normal growth temperature.

The root is a continuously growing organ with an indeterminate size, as its meristem consisting of renewable stem cells, which are maintained in a specific environment called stem cell niche (SCN). Stem cells are attached to the quiescent cells (QC), and they divide asymmetrically to produce the initials for all the cell layers consisting of the root tissues. Their daughter progenitor cells divide symmetrically in the proximal root meristem (RM), and cells further away from the QC cease proliferating as they reach the transition zone. Stem cells in the RM are rarely divide, while the progenitor cells proliferate multiple times providing an opportunity to observe their size in the growing root meristem. Confirming previous findings, the GFP signal from the RBR-GFP

expressing line exhibits a ubiquitous pattern throughout the root tip and in all cells of the root meristem as well as in the non-dividing elongation and differentiation zones (Fig. 28 A, and Magyar et al., 2012; Őszi et al., 2020). In all observed locations, it was predominantly localized in the nuclei. The nuclear RBR-GFP signal was absent only from dividing cells presumably those in M-phase as previously demonstrated (Fig. 28 B, and Miguel-Hernández et al., 2024). Arabidopsis roots of WT, RBR-GFP and *rbr1-2* lines were grown together on vertical plates, and their root tip consisting of the root meristems was visualized under confocal laser microscopy following propidium iodide (PI) staining (Fig. 28C). Cortex cell length was measured and plotted using Image J software from the distance of QC until the transition zone. In the root meristem, cell length of cortex cells from the QC remained small in all the three lines and they started to elongate as they reach the transition zone (Fig. 28D). In comparison to the WT, the length of these dividing cortex cells was changed according to the RBR levels; it was found to be increased in the ectopic RBR-GFP, while decreased in the *rbr1-2* mutant (Fig. 28E). In agreement, the number of cortex cells in the RM was inversely correlated with RBR level resulted in different root meristem size (Fig. 28F). That further confirms the cell cycle repressor function of RBR. These data indicate that cell size of symmetrically dividing progenitor root cells is regulated by RBR level; they undergo division with larger or smaller cell size when RBR level is elevated or reduced, respectively.

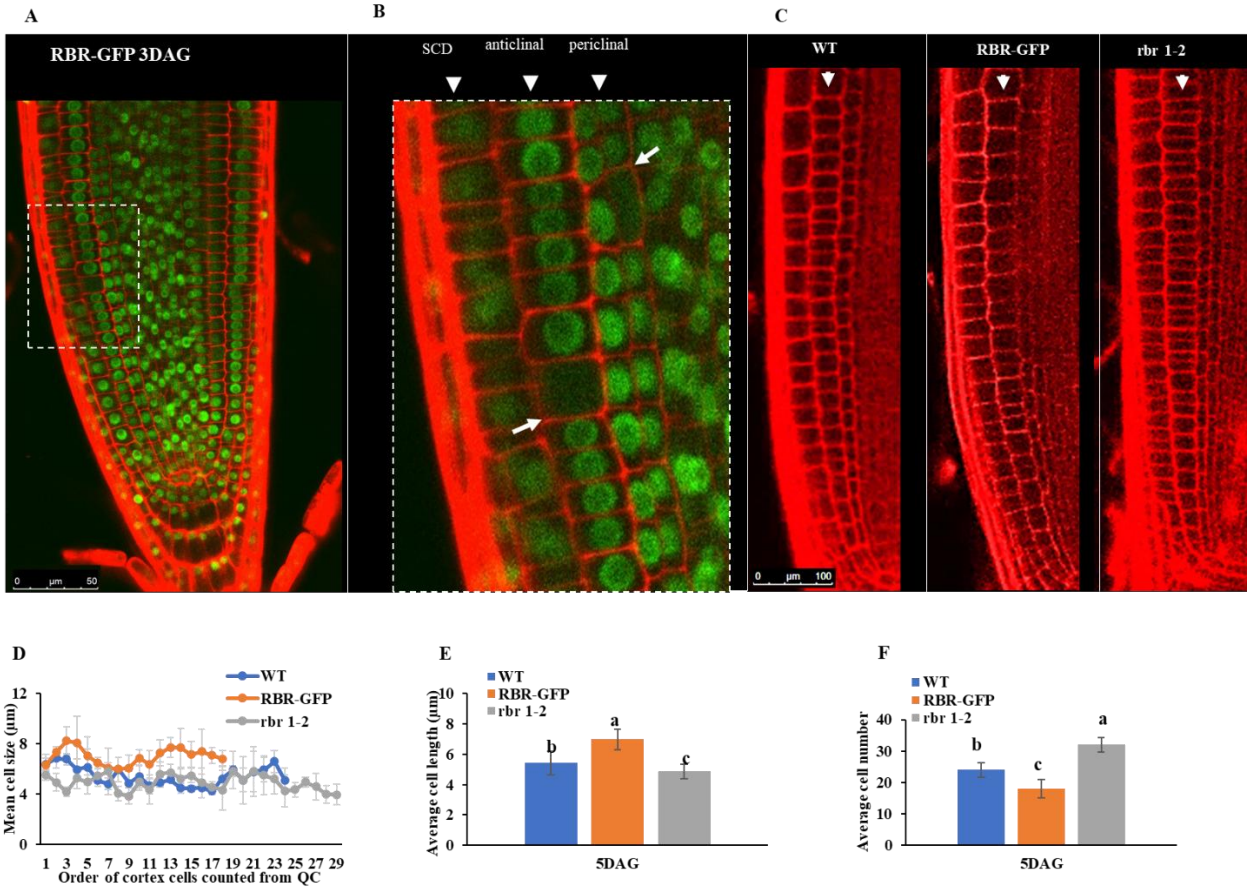

Figure 28. The RBR protein, primarily found in the nucleus, is widely distributed throughout the root meristem and influences cell length based on its concentration. **A**) The GFP signal from RBR-GFP line displays a ubiquitous pattern throughout the root tip, including all cells of the root meristem and non-dividing zones. **B**) Arrowheads indicate cell files, while arrows point to cells in M-phase lacking nuclear RBR-GFP signal. **C**) Images of propidium iodide-stained roots of seedlings, grown for 5 DAG at 22°C, were analysed using confocal microscopy. The scale bar represents 100 µm. **D**) The spatial distribution of cell length across root meristems is shown for all lines. **E**) Mean cell length was calculated along the cortical cell file from the quiescent centre. Values are averages from different plants (n=10±SD). **F**) Cortex cells in the root meristem were counted and plotted. Different letters indicate significant differences ($p < 0.05$) based on ANOVA with Tukey's HSD test.

4.12 Stomatal meristemoids divide smaller or larger cell size depending on RBR level

In contrast to the root, the mature embryo exhibits a determinate size, comprising a relatively fixed number of cells (Leviczky et al., 2019). However, in this final embryonic stage most of the cells are arrested in a transient quiescent state, and they re-initiate the division cycle during germination. In the embryonic cotyledons, for instance, cells in the epidermis are all meristemoid-like and protodermal cells, as neither puzzle-shaped differentiated pavement nor fully developed stomatal guard cells are observable (Fig. 29). Initially, we investigated whether varying RBR levels could influence cell number and cell size in the embryonic cotyledon epidermis. To this end, embryos from dry seeds of WT, RBR-GFP and *rbr1-2* lines were dissected and analysed under a confocal laser microscope after PI-staining (Fig. 29A). Notably, numerous asymmetric cell divisions characteristic for stomatal meristemoid cells could be observed in the *rbr1-2* mutant embryonic cotyledon epidermis, resulting in clusters of small cells spreading throughout the entire epidermis. By measuring epidermal cell size, the distribution of cells with various sizes was determined; a new, smallest category of cell size was detected in the *rbr1-2* line, suggesting that these cells undergo more divisions than in the WT (Fig. 29B). It was hypothesized that the smaller sized and triangular shaped cells belong to the stomatal meristemoids therefore we measure the size of these cells (Fig. 29C). In contrast to the *rbr1-2* line, cell size exhibited a shift towards the more enlarged category in the ectopic RBR line in compared to the WT indicating that these cells underwent fewer divisions, resulting in larger cell size relative to the control. Indeed, embryonic cotyledon of the *rbr1-2* line consists of the most cells in comparison to the control WT, while fewer cells were observed in the ectopic RBR line than in the WT (Fig. 29D). It is established that proliferation is more characteristic of the initial morphogenic development phase of the embryo, and it completely ceases during the maturation developmental stage, when the seed nutrient reserves accumulate in

the embryo (Leviczky et al., 2019). This observation suggests cellular phenotype observed in the *rbr1-2* mutant may be embryo-specific, as cells might undergo division for a longer period compared to the WT embryo.

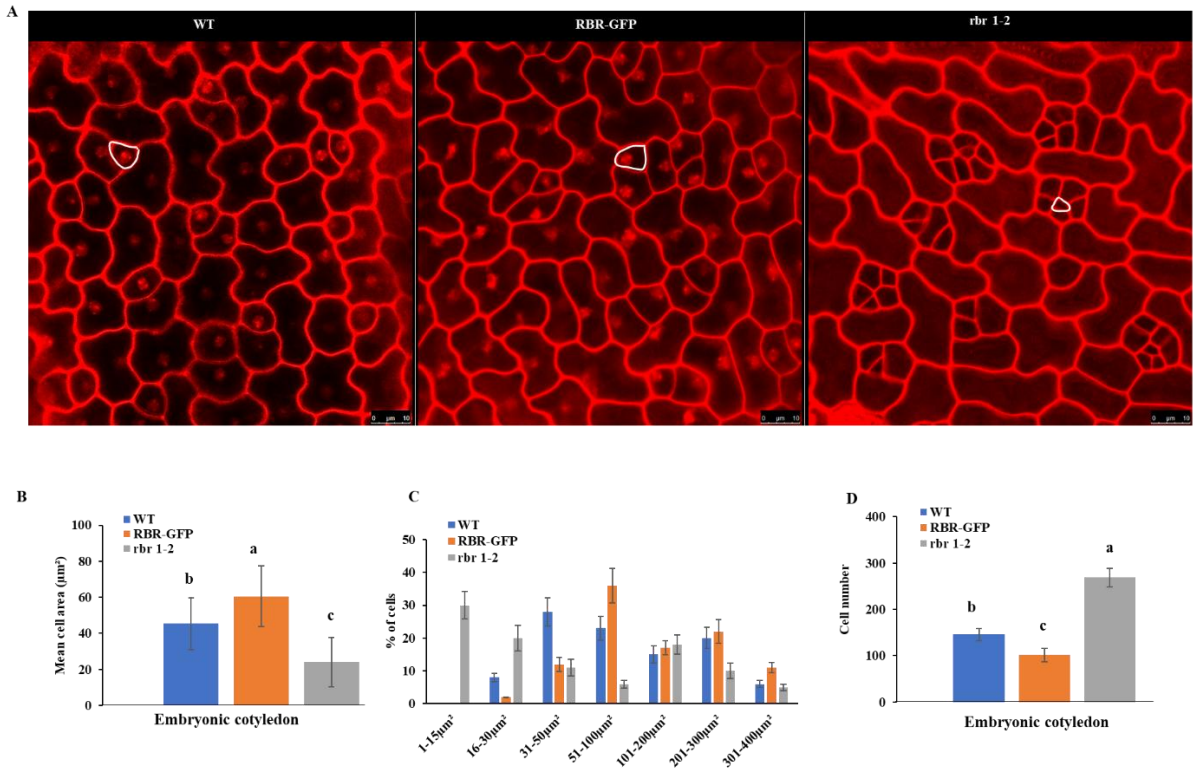

Figure 29. RBR plays a crucial role in regulating the size and number of meristemoid cells in embryonic cotyledons. **A**) The confocal microscope images presented are representative of the propidium iodide-stained epidermis of embryonic cotyledon. The cells marked in white indicate the meristemoid-like cells in the lines indicated. Scale bar is 10 µm. **B**) The mean area of the triangular-shaped stomatal meristemoids was calculated and plotted. Values are averages from the data analysed (n=10). **C**) Spatial distribution of cell area across the whole embryonic cotyledon in all the three lines. **D**) The number of meristemoid cells was also quantified and plotted for all the three lines (n=10). Different letters mean statistically significant differences ($p < 0.05$) based on one-way ANOVA analyses with Tukey's HSD post-hoc test.

During post-embryonic development stomatal meristemoid cells in the cotyledon epidermis typically undergo asymmetric division one to three times before reaching a critical cell size at which point they transition to symmetric cell division as they develop into guard mother cells (Gong et al., 2023). Using the RBR-GFP line as a reporter the presence of RBR-GFP in every cell of the cotyledon and the first leaf epidermis was confirmed and RBR was found to be a predominant nuclear factor (Fig. 30 A-B, and Őszi et. al., 2020). It is noteworthy that the fluorescence intensity of RBR-GFP increases in correlation with nuclear size; however, its signal remains consistent in asymmetrically dividing meristemoid cells (Fig. 30B).

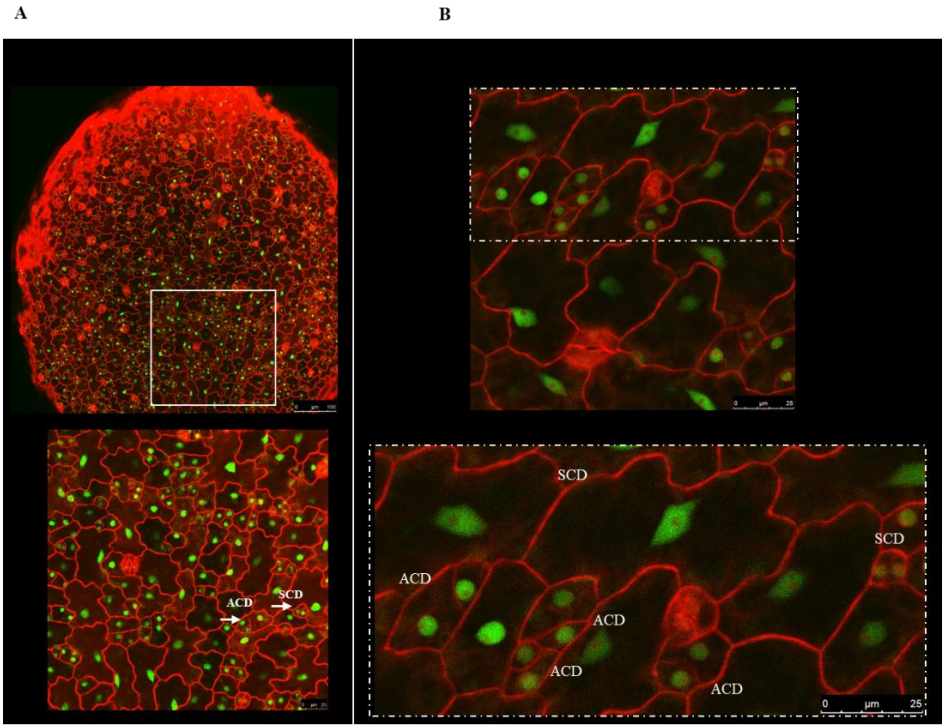

Figure 30. RBR-GFP exhibits widespread nuclear localization, with its fluorescence intensity increasing in correlation with nuclear size. A) Green fluorescence signal (GFP) from the RBR-GFP expressing line exhibits a ubiquitous distribution throughout the cotyledon 3DAG, observable in both dividing and non-dividing differentiated cells under a confocal laser microscope. The area within the white-lined box in the upper image of panel A is magnified and presented below. Arrows show asymmetric and symmetric divisions (ACD and SCD). The scale bars represent

100 µm and 25 µm, respectively. **B**) RBR-GFP signal follows the nuclear volume across both ACDs and SCDs in RBR-GFP expressing lines. The region delineated by the white-lined box in the upper image of panel B is enlarged and displayed below. Green and red signals indicate fluorescence of GFP and propidium iodide (PI), respectively. Scale bar: 25 µm.

To investigate the progression of these mersitemoid-like cells during post-embryonic development, we analysed cotyledon epidermis of all the lines under confocal microscopy following PI staining 3 days and 7 days after germination (Fig. 31 A-C and Suppl. Fig. 9A-D). In all the three lines, differentiated pavement cells and stomatal guard cells could be observed in varying sizes and quantities; however, notable differences were evident among these lines regarding the stomatal meristemoid cells: a reduced number was observed in the ectopic RBR line, while they were found to proliferate excessively in the *rbr1-2* line in compared to the WT (Fig. 31D-F). In comparison to the embryonic cotyledon epidermis, the area of the small cells clusters further increased in the *rbr1-2* line suggesting that these meristemoid cells continue to divide after germination. Moreover, the cluster size was observed to be larger at 7-day post germination in comparison to the 3-days-old cotyledon suggesting extended proliferation within the stomatal lineage. In *rbr1-2* line, these meristemoid cells were significantly smaller and more numerous than in the WT, whereas they were conversely larger in the ectopic RBR line with significantly lower number (Fig. 31 D, E). Notably, many dead small meristemoid-like cells could also be visualized specifically in the *rbr1-2* mutant epidermis (Fig. 31C). It can be hypothesized that the smallest meristemoid cells may experience a higher frequency of cell death; however, no definitive correlation between the occurrence of cell death and cell size was observed. Fig. 31C (data not shown).

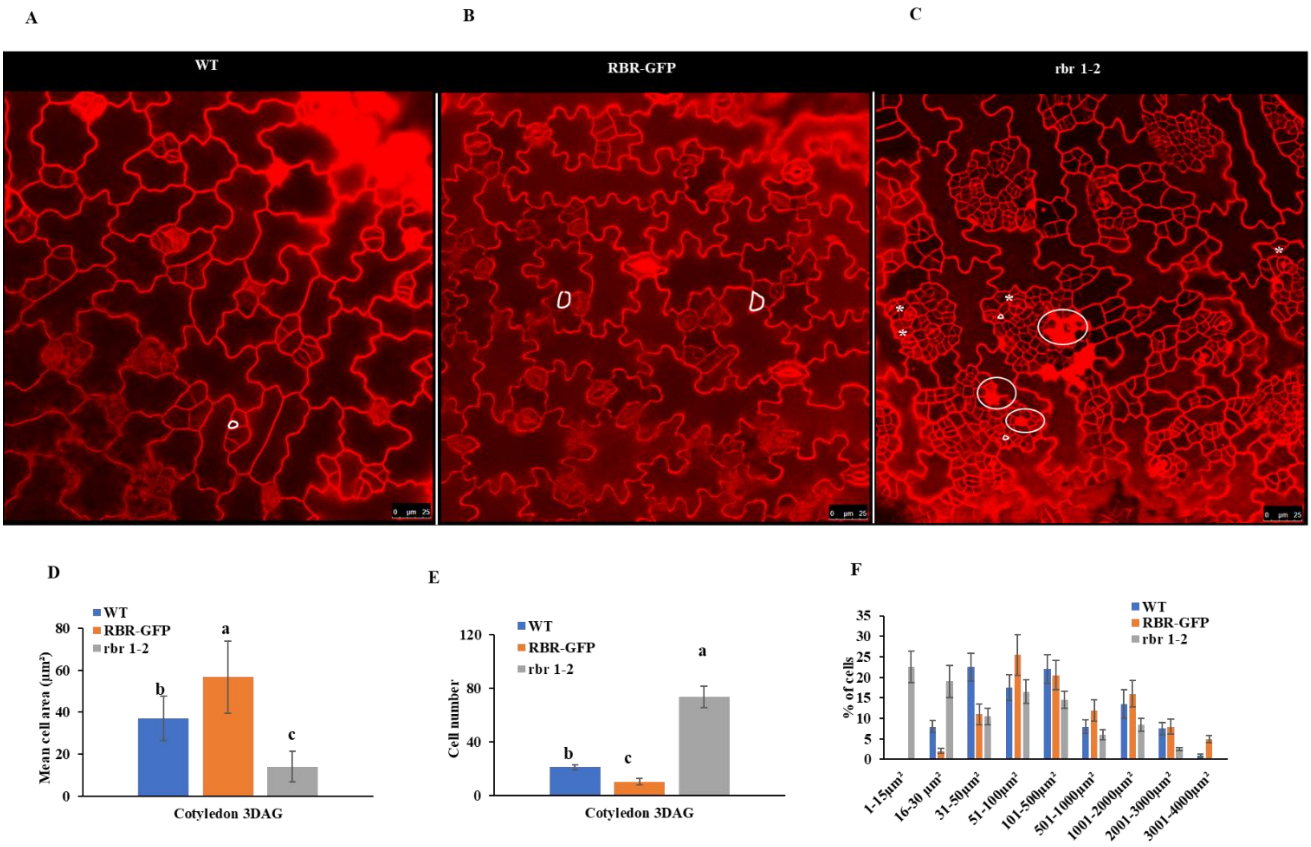

Figure 31. RBR regulates the proliferation of meristemoid cells and the patterning of stomata in post-embryonic cotyledons. A-C) Representative images of post-embryonic cotyledon stained with propidium iodide 3 days after germination. Triangular cells outlined by white lines represents meristemoid-like cells, asterisks indicate stomata with more than two guard cells, and circular shapes signify cell death in the specified lines. Scale bar is 25 µm. **D**) The mean cell area of the stomatal meristemoids 3 days after germination was calculated and plotted. Values are averages from the data analysed (n=10). **E**) Meristemoid cell number was also counted and plotted in all the three lines (n=10). **F**) Spatial distribution of cell area across the whole embryonic cotyledon in all the three lines. Different letters mean statistically significant differences ($p < 0.05$) based on one-way ANOVA analyses with Tukey's HSD post-hoc test.

We also examined the first true leaf of these lines under the confocal laser microscopy following PI staining at both a relatively young dividing developmental stage at 7 days after germination (DAG) and a later developmental stage at 14 DAG when cell elongation was predominated over proliferation (Fig. 32A-C and Suppl. Fig. 10 A-D). Similar to the cotyledon epidermis, clusters of small cells belonging to the stomatal lineage were observed in the *rbr1-2* mutant leaf, whereas these cells were less numerous in the leaf epidermis of ectopic RBR line in comparison to the control WT leaf (Fig. 32 E, F). By measuring epidermal cell size in the first leaf of these lines, we were able to compare their distribution according to size; notably, the smallest epidermal leaf cells were characteristic to the *rbr1-2* line, while cell size was markedly shifted from smaller cells towards larger cells in the ectopic RBR line in comparison to the other two lines (Fig. 32D). According to our observation, the smallest cells in the *rbr1-2* line were found to be the stomatal meristemoids, while these types of cells were enlarged in the RBR-GFP line in comparison to the WT. These cells were significantly smaller and increased in number in the *rbr1-2* line in comparison to the WT control. Similar to cotyledon epidermis, dead meristemoid-like cells appeared only in the *rbr1-2* line further supporting that RBR regulates cell survival. In the epidermis of *rbr1-2* leaf, differentiated guard cells comprising three or four cells, rather than the typical two, were observed (Fig. 32C). This finding supports the role of RBR in establishing and maintaining permanent quiescence in these normally differentiated cells (Fig. 32C; Gombos et al., 2023).

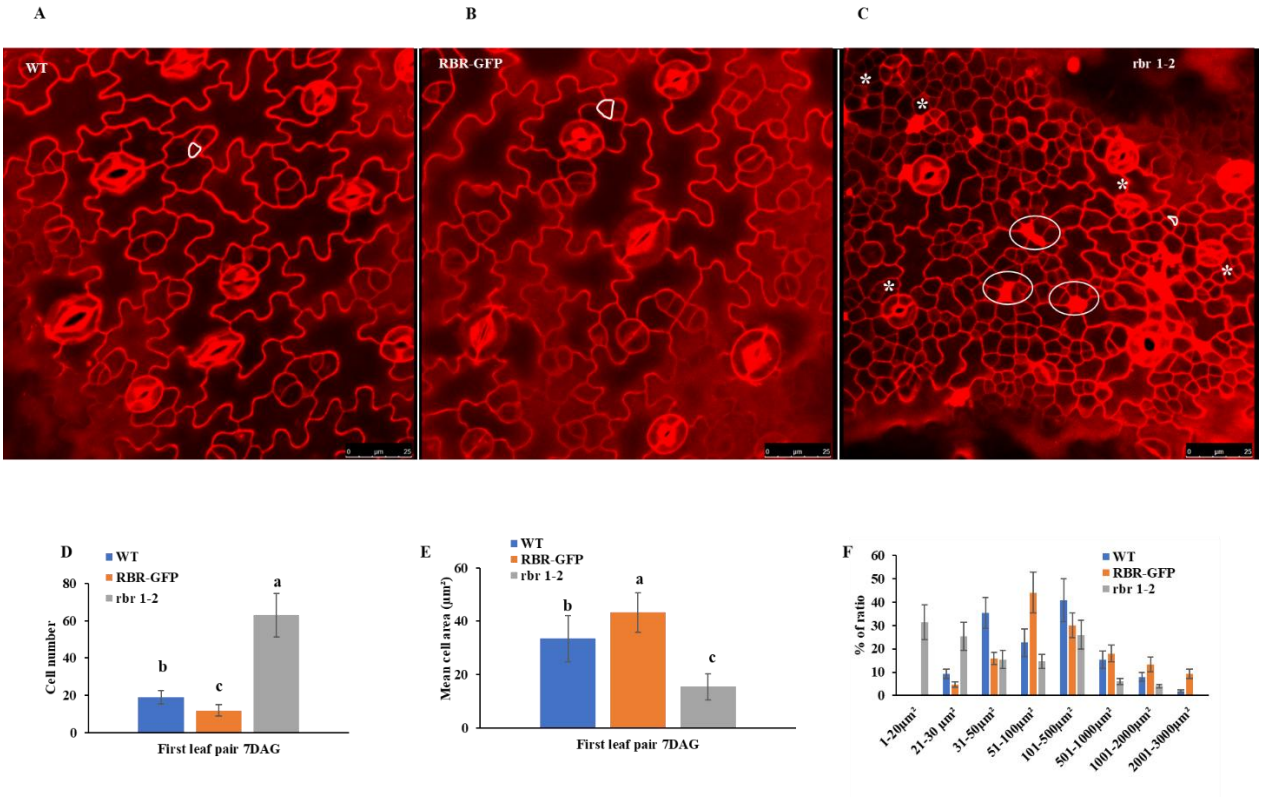

Figure 32. RBR dependent control of cell size and number in developing leaves. A-C) Representative confocal laser microscopy images of propidium iodide-stained first leaf pairs at 7 days after germination (DAG) are presented. The marked triangular cells indicate meristemoid-like cells, while asterisks denote stomata with more than two guard cells, and circular shapes signify cell death in the specified lines. The scale bar represents 25 µm. **D**) Mean cell area of the stomatal meristemoids 7 DAG was calculated and plotted. Values are averages from the data analysed (n=10). **E**) Spatial distribution of cell area across the whole leaf (150 cells counted per image) in all the three lines. **F**) Meristemoid cell number was also counted and plotted in all the three lines (n=10). Different letters mean statistically significant differences ($p < 0.05$) based on one-way ANOVA analyses with Tukey's HSD post-hoc test.

4.13 RBR levels could determine *SPEECHLESS* and *MUTE* expression and their CYCLIN D targets driving asymmetric or symmetric divisions in the stomatal lineage

The cellular analysis revealed that cell proliferation was oppositely regulated in the *rbr1-2* mutant and in the RBR ectopic lines in comparison to the WT; it was activated in the former and inhibited in the latter. Consistent with the excessive proliferation in the *rbr1-2* line, the expression level of the S-phase related *ORIGIN RECOGNITION COMPLEX 2* (*ORC2*) and the mitotic *CYCLIN-DEPENDENT KINASE B1;1* (*CDKB1;1*) increased in the first real leaf pairs at their young developmental stage at 9DAG in comparison to the similar aged WT, while their expressions decreased in the RBR-GFP line (Fig. 33A, B). At later leaf developmental stage at 12 days after germination, the expression differences were attenuated in both of these lines and were more similar to the WT control (Fig. 33A, B).

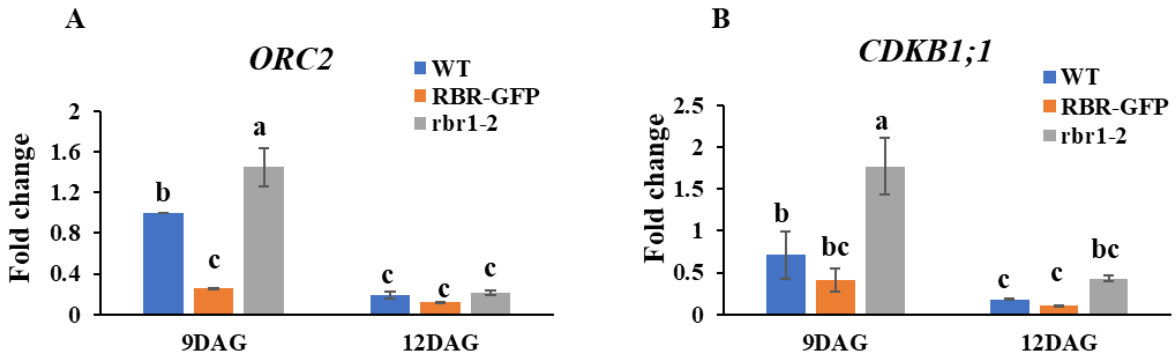

Figure 33. RBR-dependent regulation of cell cycle genes in leaves. A-B) The regulation of *ORC2,* specific to the S-phase (**A**) and the *CDKB1;1* pertinent to the G2-M-phase (**B**), was influenced by the concentration levels of RBR. Values represent fold change normalized to the value of the relevant transcript of the seedlings at 9DAG), which was set arbitrarily at 1. Data are means ± SD. N=3 biological replicates. Different letters mean statistically significant differences ($p < 0.05$) based on one-way ANOVA analyses with Tukey's HSD post-hoc test.

The progression of stomatal lineage is regulated by basic helix-loop-helix (bHLH) transcription factors, SPEECHLESS (SPCH), MUTE, and FAMA and their other dimeric partners (MacAlister et al., 2007; Kim & Torii, 2023). SPCH initiates asymmetric divisions within protodermal cells, leading to the formation of meristemoids that act as self-renewing stomatal precursor. Subsequently MUTE terminates this self-renewing activity and commits the cell to differentiation. We examined the expression of *SPCH* and *MUTE* in the first leaf pair of 9- and 12-days old seedlings. The expression of *SPCH* was upregulated in the young leaf at 9DAG in an RBR concentration-dependent manner; higher expression was observed in the *rbr1-2* mutant as compared to WT and the ectopic RBR-GFP expressing line (Fig. 34A). In contrast to *SPCH*, the expression of *MUTE* increased the most in the leaf of RBR-GFP line at 9DAG, while it was repressed in the *rbr1-2* in comparison to the WT (Fig. 34B). Recent research was demonstrated that SPCH and MUTE target different G1-type *CYCLIN D* genes; SPCH activates *CYCLIN D3;1* (*CYCD3;1*), which is involved in the activation of asymmetric divisions, while MUTE stimulates the expression of *CYCD5;1* and *CYCD7;1*. Both of these CYCLINs regulate the transition of meristemoid cells to guard mother cells by activating symmetric divisions. These three D-type CYCLINs exhibited differential regulation in the *rbr1-2* and in the ectopic RBR-GFP lines; *CYCD3;1* demonstrated elevated expression in the *rbr1-2* line, while *CYCD5;1* and *CYCD7;1* displayed the most significant increase in the RBR-GFP line in compared to the WT control (Fig. 34 C, D, E).

These data indicate that RBR levels may play role in determining cell fate within the stomatal lineage. Specifically, elevated RBR levels promote the final symmetric division by stimulating the expression of *MUTE*, whereas reduced RBR levels maintain asymmetric divisions by sustaining high levels of *SPCH* expression.

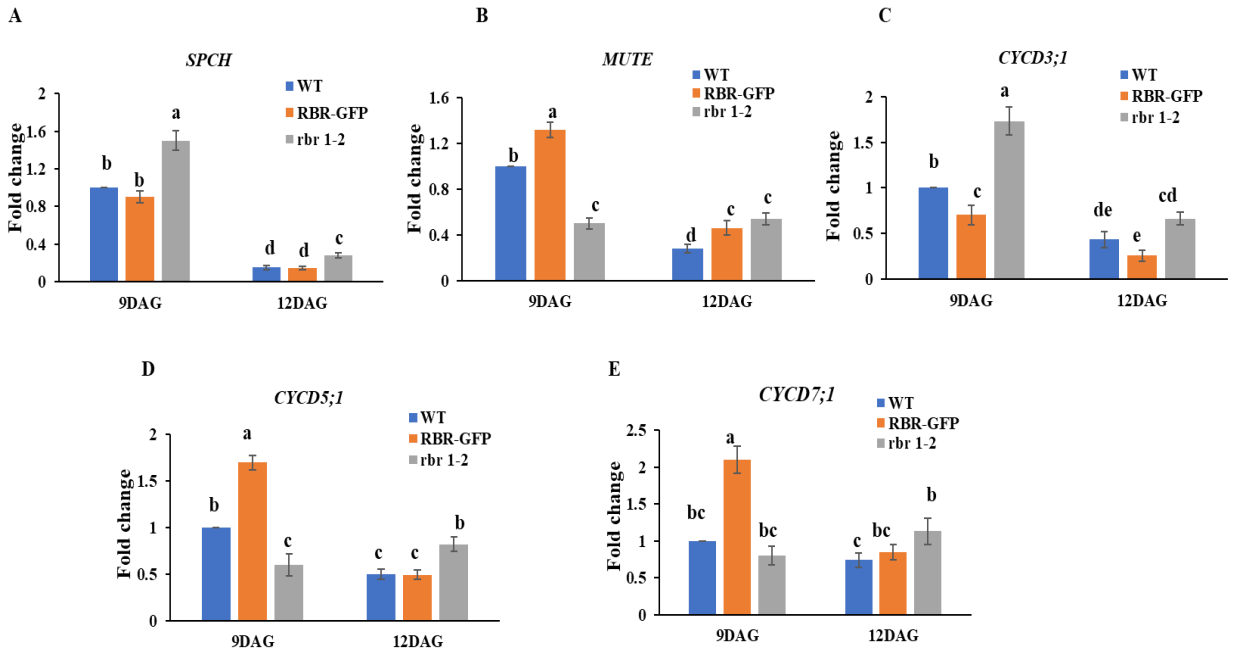

Figure 34. RBR modulates the expression of the transcription factors SPCH and MUTE instomatal meristemoid development, in a concentration-dependent manner. A-B) *SPCH* and *MUTE* regulation inversely relates to RBR concentration after 9 days of germination in the first leaf pair. **C**) SPCH activates *CYCD3;1* for asymmetric cell divisions, influenced by RBR concentration**. D-E**) MUTE induces *CYCD5;1* (**D**) and *CYCD7;1* (**E**), which promote symmetric divisions for meristemoid to guard mother cell transition. In contrast to *SPCH*, the expression of *MUTE* was induced in the ectopic RBR-expressing line. Values represent fold change normalized to the value of the relevant transcript of the seedlings at 9DAG, which was set arbitrarily at 1. Data are means ± SD. N=3 biological replicates. Different letters mean statistically significant differences ($p < 0.05$) based on one-way ANOVA analyses with Tukey's HSD post-hoc test.

5. DISCUSSION

5.1 Thermomorphogenesis: How do plants respond to warm ambient temperatures?

Plants exposed to non-stressful warm temperatures change their growth rate and accelerate their development. It is suggested that plant thermo-responses could either be passive or active and growth acceleration was speculated to be a general response caused by thermodynamic effects on metabolic rates and enzyme activities (Casal and Balasubramanian, 2019). In favour of this theory, recently ten Arabidopsis accessions were analysed at different temperatures and all showed similar robust growth accelerations throughout the vegetative phase under warm temperatures indicating that genotype has just limited effect on this temperature induced growth-related phenotype (Ibanez et al., 2017). All of these accessions, however, might have intact and conserved signalling elements responsible for robust temperature-induced growth responses. Here we show that warm temperature activates cell proliferation in the meristems both in the shoot and in the root apices where cell division in plants is concentrated. We demonstrate that cell proliferation in Arabidopsis seedlings is rapidly activated soon after temperature was raised. A recent study has already pointed to cell proliferation as a major process to accelerate root growth (Ai et al., 2023). Here, we not only confirm their findings, but also show that leaf primordia in the shoot apex and the developing young leaves grow faster under warm temperatures. This is because they produce more cells than at normal growth temperatures. We suggest that warm temperatures accelerate meristem functions through the conserved CYCD-RBR-E2F molecular pathway. This is supported by the following evidence: (i) the expression of G1 cyclins such as *CYCD3;1* and *CYCA3;1* rapidly increased at elevated temperatures (Fig. 18A, B), (ii) at the same time, the phosphorylation of the cell cycle inhibitor RBR at a conserved CDK site was augmented (Fig. 18C), and (iii) the expressions of E2F-target cell cycle regulatory genes *ORC2* and *CDKB1;1* were also up-regulated with warm

temperatures (Fig. 1 A, B; Fig. 17A, B). How warm temperatures could activate the canonical cell cycle regulatory CYCD-RBR-E2F pathway? Plant cyclin Ds have already been implicated to mediate both internal and environmental signals toward the cell cycle control system (DeVeylder, 2019; Dewitte et al., 2007). Interestingly, warm temperatures induce a similar growth acceleration phenotype in transgenic plants overexpressing *CYCD2;1* without affecting the final organ size and plant stature (Cockroft et al., 2000). In the case of ectopic *CYCD2;1*, it was shown that cells enter the cell cycle faster by shortening the G1 phase (Cockcroft et al., 2000). It is also very possible that warm temperatures similarly affect the length of the cell cycle. The increased number of S-phase cells in the root meristem, just eight hours after the temperature was shifted, supports the idea that cells are entering the cell cycle at a faster rate. Expression of Arabidopsis *CYCD2;1* and *CYCD3;1* both quickly respond to the sucrose level (within 30 minutes and 4 hours, respectively) in the nutrient medium (Riou-Khamlichi et al., 2000). Overexpression of *CYCD3;1* activates mitosis and stimulates the phosphorylation of RBR even in nutrient limited condition (Magyar et al., 2012). We show here that warm temperature also rapidly activates the expression of *CYCD3;1* indicating that CYCDs might be targeted soon after temperature was sensed. It is tempting to speculate that warm temperatures activate *CYCD3;1* (and/or *CYCD2*) by changing nutrient and sucrose levels, due to increased metabolic rates in the plants. Recently it was noted that the expression of genes involved in sucrose transport and response in the root, and shoot, respectively, was quickly upregulated (within 4 hours) by warm temperature (Gaillochet et al., 2020). According to the classical plant cell cycle model, CYCDs activate the RBR-kinase *CDKA;1*, and hyperphosphorylation of RBR represses its cell cycle inhibitory function. RBR has numerous conserved CDK sites but only few has been experimentally verified in plants (Desvoyes and Gutierrez, 2020). Previously, it has been shown that phosphorylation of RBR at position 911, on

the serine residue of a conserved CDK site, represses its ability to bind to E2Fs (Magyar et al., 2012). In addition, phosphorylation of this site was observed in dividing cells and tissues, and its level increases when cells enter the cell cycle (Ábrahám et al., 2011; Magyar et al., 2012). Therefore, the phosphorylation of RBR at this site indicates a higher proliferation activity in seedlings growing at warmer temperatures (Fig. 18C). Our data support that warm temperatures act on meristems as a mitogenic factor, and its signal is mediated through the canonical CYCD-RBR-E2F pathway, resulting in faster growth and accelerated development (Fig. 5E). Unexpectedly, RBR not only functions as a cell cycle inhibitor, but also exerts a positive influence on the elongation growth of post-mitotic, quiescent cells under warm conditions. It is quite remarkable that the hypocotyl of the ectopic RBR-GFP expressing line grows significantly longer than that of the WT at warm temperatures (Fig. 19 A-C, 20A, B). The RBR protein could be detected in epidermal cells of the hypocotyl at both temperatures, regardless of whether they were proliferating or quiescent, supporting its regulatory role in both cell types (Fig. 12A, B, C). In the *rbr1-2* mutant, proliferation of meristemoid cells of the stomatal lineage were activated supporting the canonical cell cycle regulatory role of RBR in these cells, the division of which was further stimulated by warm temperatures indicating that elevated temperature has a positive effect on cell proliferation even in the hypocotyl confirming previous findings (Fig. 21A, B, Bellstaedt et al., 2019). The hypocotyl of the RBR-GFP expressing line grows longer at warm temperatures because cell elongation is stimulated by the ectopic RBR. This effect appears to be specific, as epidermal cells in the hypocotyl of the *rbr1-2* mutant line were less elongated compared to the WT control. This suggests that RBR regulates the cell size of post-mitotic hypocotyl cells under warm temperatures. How can the cell cycle inhibitor RBR stimulate elongation growth in post-mitotic hypocotyl cells? Surprisingly, thermo-morphogenic regulatory genes including the central *PIF4*

and *PIF7* together with their target auxin biosynthetic *YUCCA* genes (*YUC1-2* and *YUC8-9*) were all found to be positively regulated by RBR at the seedling level (Fig. 22A, B; Fig. 23A-D). This suggests that RBR mediates the effect of warm temperatures on hypocotyl elongation as a direct or indirect activator of gene expression. In dividing cells, elevated expression of CYCDs drives the RBR kinase, resulting in an activated cell cycle. However, we do not yet know what signal is present in elongated post-mitotic hypocotyl cells that leads to RBR activation. RBR may control the expression of thermo-regulatory genes, either directly or indirectly. RBR itself cannot bind to target gene sequences, but it regulates cell cycle control genes in complex with its primary effector, E2F transcription factors (Gombos et al., 2023). Neither *PIF4/7* nor *YUCCA* genes, however, contain conserved E2F-binding sequences in their regulatory promoter regions. In addition, RBR and E2Fs were not enriched in the promoter regions of these genes at normal growth temperature further supporting that they are regulated by RBR independently of E2Fs (Bouyer et al., 2018; Gombos et al., 2023). Additionally, hypocotyl elongation stimulated by ectopic RBR at warm temperature was not affected by mutating E2FA, one of the three canonical E2Fs (Fig. 24A, B). However, E2FB mutation reversed the ectopic RBR phenotype at elevated temperatures, suggesting a specific functional relationship between RBR and E2FB. According to the plant cell cycle model, CYCD3;1 activates CDKA;1, an RBR-kinase, leading to the inactivation of RBR through phosphorylation (Fig. 3). Interestingly, CYCDs, such as *CYCD3;1*, are expressed at the highest levels in the hypocotyl, indicating that CYCD3;1 may also function in non-dividing cells similarly to RBR. Our investigation into the thermomorphogenic response of a triple *cycd3;1-3* mutant has revealed a thermo-response similar to that of the ectopic RBR-GFP expressing line, characterized by shorter root with fewer dividing cells and slower leaf development under warm temperatures compared to the WT control (Fig. 25, and Suppl. Fig. 8A-D). This observation further

supports the notion that warm temperatures suppress the cell cycle inhibitory function of RBR in the SAM and RAM via phosphorylation by the CYCD3-CDKA kinase. Interestingly, the triple *cycd3;1-3* mutant develops significantly longer hypocotyls under both standard and elevated temperature conditions compared to the WT, with warm temperature further enhancing hypocotyl elongation in the mutant. This elongation attributed to increase cell enlargement in the epidermis, akin to the ectopic RBR expressing line. This suggests that CYCD3s suppress the function of RBR in both proliferating and post-mitotic tissues. Additionally, thermomorphogenic regulatory genes, including *PIF4* and *YUC8*, were found to be up-regulated in the *cycd3;1-3* mutant seedlings, suggesting a potential increase in auxin levels in the hypocotyl of this mutant. Consequently, the non-phosphorylated, active RBR in association with E2Fs may enhance auxin signalling and biosynthetic processes. Interestingly, E2FB is identified as the primary partner of RBR at standard temperatures, with several phosphorylated forms of RBR specifically associated with E2FB (Lang et al., 2021 and unpublished results). This observation implies that not all phosphorylation of RBR disrupt its association with E2FB (our unpublished data). In animals, it has been shown that monophosphorylated forms of RB are present in various protein complexes and they function beyond the regulation of the cell cycle (Sanidas et al., 2019). Further research is necessary to ascertain whether these phosphorylation sites on plant RBR are also modified under warm temperature conditions and to identify the kinase responsible for phosphorylating RBR. Altogether, our data indicated that warm temperatures have a dual effect on RBR activity. It suppresses its canonical cell cycle inhibitor function in both shoot and root meristems, driving faster growth and development. Additionally, it activates its non-canonical cell elongation regulatory function in the hypocotyl by increasing, among others, the expression of auxin

biosynthetic *YUCCA* genes. In both pathways, Cyclin Ds might mediate the temperature control on RBR function, however, this hypothesis needs further experimental verification.

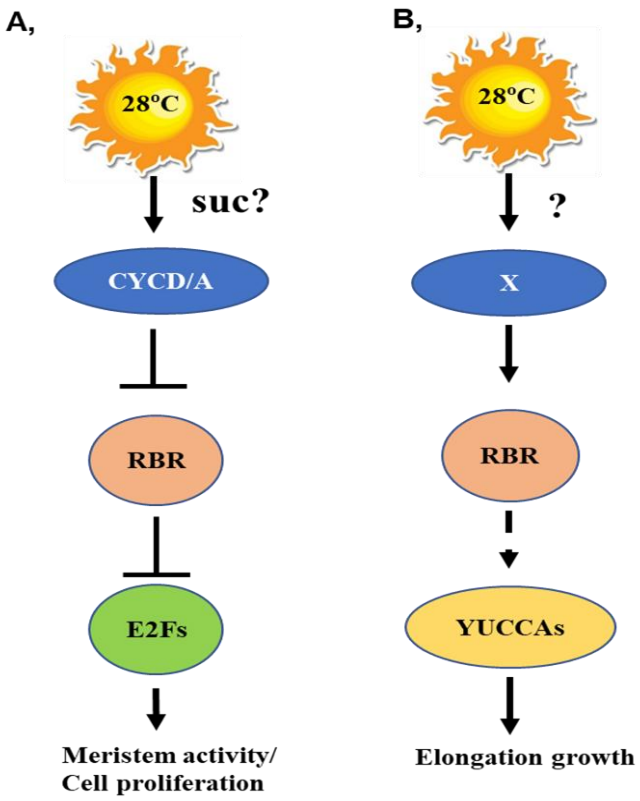

Figure 35. The model elucidates the role of RBR in both mitotic and post-mitotic tissues under conditions of elevated temperature. Warm temperatures activate G1 cyclins like CYCD3;1 and CYCA3;1. This might be mediated by the increased sucrose (suc) level due to the temperature-enhanced metabolic activity. The cell cycle inhibitor RBR is phosphorylated and repressed by an RBR-kinase complex, such as CDKA;1-CYCD/A. This results in RBR-free E2Fs, which drive cell cycle entry and accelerate meristematic function in both the root and shoot apices. Warm temperatures might cause post-translational modifications on RBR, such as phosphorylation at unknown site(s) in post-mitotic cells. This could result in the stimulation, either directly or indirectly, of the expression of non-canonical targets, like YUCCAs.

5.2 RBR as a potential cell size regulator

In our thermo-morphogenic study, RBR has been identified as a regulator of post-mitotic cell size in a temperature-dependent manner, suggesting its potential role in controlling cell size generally and during cell proliferation under standard conditions. In animals, the RB protein regulates cell size, and its functional homolog, Whi5, in budding yeast, has similar implications. The concentration of cell cycle inhibitors RB and Whi5 becomes diluted during cellular growth, reaching a size where they no longer inhibit cell cycle initiation. Thus, cell size promotes entry into cell cycle by diluting the inhibitory RB and Whi5 (Zatulovskiy et al., 2020; Schmoller et al., 2015 and Fig. 6).

In plants, the regulatory role of RBR as cell size controller has not been investigated yet, but two CDK inhibitory proteins (CKI), KRPs and SMRs, were found implicated in cell size control in proliferating meristematic regions of Arabidopsis plants (D'Ario et al., 2021; Nomoto et al., 2022). These CKIs regulate cell size in a concentration-dependent manner, suggesting operation according to the inhibitor dilution model. They function in distinct cell cycle phases: KRP4 in G1-to-S transition, SMRs in G2-to-M transition. A recent study indicates that cell size regulation in plants occurs at both transitions indicating the existence of a coordinating molecular mechanism functioning during the cell cycle (Jones et al., 2017). It has been noted that modifying the duration of one of the gap phases (G1 or G2) leads to a corresponding inverse change in the duration of the other gap phase. Our research suggests RBR can regulate both CKIs, potentially involved in cell size control. *FBL17*, encoding an F-Box protein for KRP degradation, was shown to be repressed by RBR through E2F complexes (Zhao et al., 2012; Gombos M., unpublished data). We've shown that mitotic activator MYB3R4 is regulated by E2F-RBR complexes, which regulates SCL28,

activating SMR expression (Fig. 7 and Nomoto et a., 2022). These findings indicate CKIs as either direct or indirect downstream RBR targets. Consequently, RBR can regulate cell size in dividing cells by modulating CKI levels. We hypothesized that cell size in developing Arabidopsis plants could be influenced by altering RBR protein concentrations. Our finding indicates that the size of dividing cells within the root meristem, embryo, and proliferating post-embryonic cotyledon and true leaves is indeed affected by the concentration of RBR (Fig. 31, and Fig. 32). Increased RBR in ectopic RBR expressing seedlings results in enlargement of dividing cell size, whereas reduced RBR in *rbr1-2* mutant plants leads to decreased cell size during proliferations (Fig. 31E and, Fig. 32D). In plant meristems and young developing organs, symmetric and asymmetric mitotic cell divisions (SCD and ACD) occur in a spatially regulated manner. In the root meristem (RM), cortex cells arise from asymmetric divisions of the cortex endodermis initial cell (CEI), situated adjacent to quiescent centre cells. Subsequently, established cortical cells undergo numerous symmetric and anticlinal divisions until reaching the transition zone, where they cease dividing and begin to increase in size. In the RM, the cell size of symmetrically dividing cortical cells was influenced by RBR quantity; these cells were significantly larger or smaller than in the control WT, contingent upon RBR level (Fig. 28C-E). Moreover, the cortex file comprised a significantly greater number of smaller cells in the *rbr1-2* mutant compared to the control WT. Conversely, cortical cells were fewer and larger in ectopic RBR-expressing RM than in the WT. The data substantiate that the cell cycle inhibitor RBR regulates cell cycle entry in a concentration-dependent manner, with cell size serving as an indicator of RBR concentration. These findings suggest an increased concentration of RBR may extend the G1 or G2 phase or both, leading to an enlarged cell size until RBR is diluted to a level insufficient to impede cell cycle progression. Conversely, a reduced RBR concentration is diluted more rapidly, resulting in premature cell cycle entry with a smaller cell

size. Previous research indicates that RBR modulates the duration of both G1 and G2 phases, reinforcing its role in governing cell cycle progression at G1-to-S and G2-to-M transitions and consequently affecting cell size (Borghi et al., 2010).

In the context of asymmetric divisions within the shoot meristem, daughter cell size inversely correlates with time required for cell cycle entry, as larger cells divide more rapidly than smaller ones (D'Ario et al., 2021; Jones et al., 2017). However, this pattern is not universal for all asymmetrically dividing plant cells. In cotyledon and true leaf epidermis, stomatal meristemoid cells undergo multiple asymmetric divisions before transitioning to symmetric division and differentiating into guard cells. These small meristemoids progressively decrease in size until reaching a critical threshold for symmetric division. We observed over-proliferation of stomatal meristemoids in *rbr1-2* mutant cotyledons and true leaves, resulting in clusters of small cells compared to the WT control (Fig. 31C, and Fig. 32C). These meristemoid cells were significantly smaller than in WT, indicating more asymmetric divisions when RBR level is reduced. Conversely, ectopic RBR resulted in larger meristemoids than WT, indicating fewer asymmetric divisions. Indeed, both mersitemoid and guard cell numbers decreased in the ectopic RBR expressing line (Suppl. Fig. 11 A-E). Our data strongly support that RBR concentration is critical in determining the size at which meristemoids terminate asymmetric division and commence differentiation. This process begins with symmetric division, ultimately forming guard cells. Recent propositions suggest the stomatal lineage transition depends on a nuclear factor responsive to DNA content (Gong et al., 2023). Based on our data, it is plausible to hypothesize that RBR serves as this nuclear factor. We have confirmed previous findings that RBR is primarily localized within the nucleus throughout the stomata lineage (Fig. 30A, B). This hypothesis, however, raises a question: how does the cell cycle inhibitor RBR facilitate stomatal differentiation by promoting

symmetric division? By analysing the expression patterns of key regulatory genes, *SPCH* and *MUTE*, along with their downstream *CYCD* targets, *CYCD3;1* and *CYCD5;1*, respectively, in the first leaf pairs of lines with ectopic and reduced RBR expressions, we observed unexpected results. Specifically, we identified an antagonistic effect of both elevated and reduced RBR levels on the expression of regulatory genes involved in stomatal development. A reduced level of RBR was found to enhance the expression of *SPCH* and *CYCD3;1* thereby activating and sustaining asymmetric division. Concurrently, it downregulated *MUTE* and *CYCD5;1*, which are responsible for the transition from ACD to SCD (Fig, 34 A, C). Conversely, ectopic expression of RBR resulted in an increase in the transcript levels of *MUTE*, *CYCD5;1* and *CYCD7;1*, while it led to a decrease in the mRNA levels of *CYCD3;1* (Fig. 34). Accordingly, the upregulation of RBR enhances the differentiation of stomatal meristemoid cells by promoting the expression of genes associated with the transition from asymmetric to symmetric division. This dataset raises several unresolved questions: How does the cell cycle inhibitor RBR stimulate gene expression? Is RBR directly involved in this transcriptional regulation? RBR has been found to enhance the expression of auxin signalling and biosynthetic genes under elevated temperature conditions. Is RBR similarly involved in hormonal regulation during stomatal development?

Furthermore, CYCDs, which are implicated in the regulation of stomatal lineage, are potential regulators of RBR-kinase, where the catalytic component is a CDK, specifically CDKA or CDKB. The function of RBR during stomatal development may be influenced by specific phosphorylation events, leading RBR to form distinct complexes within stomatal meristemoids and guard mother cells. Consequently, RBR may target different gene sets depending on the transcription factor it complexes with. Recent unpublished data indicate that RBR can undergo phosphorylation at 13 distinct sites; however, these sites do not uniformly inhibit RBR's capacity to bind to E2F. For

example, various phosphorylated forms of RBR have been observed in complex with E2FB, suggesting that phosphorylation of RBR may lead to the formation of different complexes. Consequently, these distinct RBR containing complexes may regulate different set of genes leading to various outcomes.

In conclusion, this study consolidates evidence suggesting that RBR plays a crucial role in regulating the size of actively dividing plant cells through a concentration-dependent mechanism. These findings support the hypothesis that RBR could be the elusive nuclear factor responsible for regulating stomatal lineage development, balancing proliferation and differentiation by modulating key developmental transcription factors and their cyclin targets. This network highlights RBR's significance in determining cell fate, with implications for understanding plant development mechanisms.

6. Summary

In light of the effects of climate change on plant diversity and agriculture, it is imperative to comprehend the mechanisms by which plants adapt to increased temperatures, as this understanding is vital for ensuring food security. As sessile organisms, plants have developed strategies such as thermomorphogenesis, which involves altering growth and morphology in response to temperature fluctuations.

In plants, specific regions known as meristems are responsible for regulating growth and development. These regions are the primary sites of cell proliferation, which serves as the major driving force behind plant growth. While elevated temperatures accelerate growth and induce morphological changes like elongation of hypocotyl, petiole, and root, the role of meristems in these alterations remains less understood.

Through the analysis of meristematic function in young Arabidopsis seedlings shortly after an increase in temperature, we identified an activation of cell proliferation in both the shoot and root apices. This activation led to accelerated leaf development and enhanced root growth. The cell cycle regulatory genes, including G1-specific *CYCLIN D3;1* (*CYCD3;1*) and *CYCLIN A3;1* (*CYCA3;1*), were rapidly activated. These cyclins serve as the regulatory subunits of the RETINOBLASTOMA-RELATED (RBR)-kinase, CYCLIN-DEPENDENT-KINASE A;1 (CDKA;1). Notably, RBR was observed to undergo prompt phosphorylation following temperature shifts. RBR functions as a cell cycle inhibitor through E2F transcription factors. RBR phosphorylation activates E2Fs, which trigger S and G2 phase cell cycle genes under elevated temperatures. By modulating the RBR level in planta through the use of two transgenic lines that express either ectopic or reduced RBR (RBR-GFP and *rbr1-2* lines, respectively), we can either

enhance or mitigate the impact of elevated temperatures on meristematic function. In contrast to meristems, the hypocotyl predominantly consists of post-mitotic cells, and elevated temperatures promote their elongation growth. Notably, an increased level of ectopic RBR further enhances the elongation growth of these cells, whereas a reduced RBR level exerts the opposite effect, resulting in smaller epidermal cells compared to the WT control. Surprisingly, key thermomorphogenic regulatory genes, such as *PHYTOCHROME INTERACTING FACTOR 4* and *7* (*PIF4*, and *PIF7*), along with downstream targets, auxin biosynthetic *YUCCA* (such as *YUC8*) are induced by RBR. This indicates that RBR positively regulates their expression in a concentration-dependent manner under elevated temperature conditions. The ectopic RBR-mediated effect on hypocotyl elongation was significantly influenced by the E2FB mutation, while E2FA loss showed no effect under elevated temperature conditions. Therefore, we suggest that RBR controls hypocotyl elongation in conjunction with E2FB under conditions of elevated temperature. The mutation of the entire CYCD3 subclass demonstrates that the meristematic inhibitory and elongation-promoting functions of RBR are negatively regulated by CYCD3. Consequently, the *cycd3;1-3* triple mutant exhibits phenotypic similarities to the ectopic RBR-GFP expressing line, as evidenced by reduced root lengths and elongated hypocotyls at elevated temperatures compared to the wild-type (WT) control. Furthermore, the *cycd3;1-3* mutant exhibits diminished expression of cell cycle genes, such as *ORC2* and *CDKB1;1*, while demonstrating increased induction of thermomorphogenic genes, including *PIF4*, *PIF7*, *YUC2*, and *YUC8*, at elevated temperatures. This observation substantiates that CYCD3;1 and its closely related proteins promotes cell proliferation through RBR inactivation, whereas its absence redirects growth towards cell elongation, akin to the effects observed with RBR overexpression.

We also demonstrated that RBR serves as a regulator of cell size in developing Arabidopsis seedlings and embryos, operating in a concentration-dependent manner. Mitotic cells in plant tissues undergo proliferation either symmetrically or asymmetrically, contingent upon their positional context and developmental fate. In the root meristem, progenitor cells that divide symmetrically exhibit significant size variation influenced by the level of RBR. Specifically, an elevated RBR level in the ectopic RBR-GFP expressing line results in enlarged cells, whereas a reduced RBR level in the *rbr1-2* mutant leads to smaller cells compared to the WT control. We propose that RBR regulates the expression of cell cycle genes involved in the transitions from the G1 to S phase and from the G2 to M phase, thereby influencing the duration of the G1 and G2 phases, which have been identified as crucial for cell size control in plants.

In cotyledon and leaf epidermis, stomatal meristemoid cells undergo several rounds of asymmetric division before transitioning to symmetric division, ultimately resulting in the formation of guard cells. The reduction of RBR levels in the *rbr1-2* mutant led to an overproliferation of meristemoid cells, which notably became extremely small in size. Conversely, an increase in RBR levels resulted in decreased proliferation activity, accompanied by an enlargement in cell size. Our data indicate that RBR functions as the nuclear factor responsible for determining the cell size threshold in meristemoid cells. In support of this hypothesis, the RBR dosage modulates stomatal lineage progression by differentially regulating cell-cycle genes, such as *ORC2* and *CDKB1;1*, as well as bHLH transcription factors, primarily *SPCH* and *MUTE*. In *rbr1-2* mutants, elevated levels of SPCH and its downstream target CYCD3;1 led to excessive asymmetric divisions. Conversely, overexpression of RBR-GFP enhances the induction of MUTE and its cyclin-D targets, CYCD5;1 and CYCD7;1, thereby accelerating the formation of symmetric guard cells.

In summary, the cell cycle inhibitor RBR regulates cell size in both mitotically active cells within meristems and young developing organs, as well as in post-mitotic cells under conditions of elevated temperature. Our data suggest that RBR regulates both cell number and size through distinct mechanisms. A deeper understanding of these RBR-centred molecular pathways offers the potential to influence plant growth, which is beneficial for plant breeding programs. Further investigation is necessary to elucidate the precise molecular mechanisms underlying these RBR-mediated processes.

7. Összefoglaló

A növények növekedése és fejlődése nemcsak a genetikai programjuktól, hanem a környezeti tényezőktől is függ, mint amilyen a fény és a hőmérséklet. A növények már néhány fokos hőmérsékletemelkedésre növekedésük és fejlődésük megváltoztatásával válaszolnak; fejlődésük felgyorsul, megnyúlik a szár és a levélnyél valamint hosszabb gyökeret növesztenek. Mindezeket a hőmérséklet okozta fejlődési változásokat együttesen thermomorfogenezisnek hívjuk. A napjainkra jellemző felmelegedés ugyanakkor szárazságot és hőstresszt is okoz, érzékenyen érintve a mezőgazdasági termelést, aminek ilyen környezeti feltételek mellett is hatékonynak kellene maradnia. Éppen ezért fontos megérteni azokat a molekuláris szabályozási folyamatokat, amelyek a hőmérséklet okozta növekedési és fejlődési változások hátterében állnak.

A növények növekedése és fejlődése az osztódó, ún. merisztematikus régióiktól függ, itt találhatóak a megújulásra képes őssejtek, és itt keletkeznek a növények növekedéséhez szükséges új sejtek is. Meglepő módon, a merisztémák szerepét a hőmérséklet emelkedése okozta növekedési és fejlődési változásokban eddig kevésbé tanulmányozták.

Néhány napos Arabidopsis csíranövényen vizsgáltuk a magas, de még nem stressz hatású hőmérsékletet. Kimutattuk, hogy a felgyorsult levélfejlődés és a megnövekedett gyökérhossz hátterében a sejtosztódás aktiválódása áll. Megállapítottuk, hogy a hajtás- és gyökércsúcs merisztémák működése fokozódott. Néhány órával a hőmérséklet emelkedését követően *CIKLIN A* és *CIKLIN D* gének aktiválódását figyelhettük meg, amelyek a sejtciklus G1 fázisában lépnek működésbe. Ezek a ciklinek a RETINOBLASZTOMA-ROKON (RBR) kináz, a CIKLIN-FÜGGŐ PROTEIN KINÁZ A;1 (CDKA;1) szabályozó alegységei. Az RBR, a sejtosztódás inhibitora, az E2F transzkripciós faktorok gátlásán keresztül megakadályozza a sejtciklus gének

bekapcsolódását. Az RBR foszforiláció által szabályozódik, és röviddel a meleg kezelést követően fokozott RBR foszforilációt figyelhettünk meg. A foszforilált RBR szabadon engedi az E2F faktorokat, és a sejtek belépnek az osztódási ciklusba. Ennek a modellnek megfelelően meleg hőmérséklet hatására, mind az S- mind pedig a G2-fázisban működő sejtciklus gének aktiválódását tudtuk kimutatni (*ORC2* és *CDKB1;1*). Mindez arra engedett következtetni, hogy a meleg okozta felgyorsult fejlődés az RBR fehérjén keresztül szabályozódik. Valóban, az RBR mennyiségének a változtatásán keresztül, egy csökkent RBR fehérje szintű *rbr1-2* mutáns és egy túltermelő RBR-GFP vonal bevonásával, fokozni illetve csökkenteni tudtuk a hőmérsékletemelkedés okozta növekedési válaszokat. Érdekes módon a túltermelő RBR növelte a hipokotil hőmérsékletemelkedésre adott megnyúlási válaszát, míg a mutáns *rbr1-2* csíranövények szára kevésbé nyúlt meg a vad típusú növényhez képest. A sejtciklus génekkel szemben a thermo-morfogenezis szabályozásban kulcsszerepet játszó gének működését az RBR pozitívan szabályozza: magas hőmérséklet mellett a *PHYTOCHROME INTERACTING FACTOR 4* és *7* (*PIF4* és *7*) a túltermeltetett RBR vonalban indukálódott, míg az *rbr1-2* mutánsban gátolódott. A PIF4 az auxin bioszintézisben szerepet játszó *YUCCA* (*YUC*) gének aktiválódásán keresztül stimulálja a sejtmegnyúlást, és az RBR-GFP túltermelő vonalban számos *YUC* gén fokozott működését figyelhettük meg (pl. *YUC8*, és *YUC9*). Ennek megfelelően a hipokotil bőrszöveti sejtjei hosszabbra nyúltak az RBR túltermelő vonalban a kontrol vad típusú növényekhez képest, míg rövidebbek lettek az *rbr1-2* mutánsban. Az RBR hipokotil megnyúlást stimulaló hatását kompenzálni tudtuk az E2FB mutációjával, míg az E2FA szerepe ebben a hőmérséklet indukálta folyamat szabályozásban nélkülözhetőnek tűnt. Mindez az RBR-E2FB kapcsolat kitüntetett szerepére utal a hőmérséklet indukálta növekedési és morfológiai változásokban. Az E2FB-RBR komplex kialakulását a CYCD fehérjék szabályozzák. Megvizsgáltuk, mi történik az Arabidopsis

csíranövények hőmérsékletemelkedésre adott válaszával, ha a teljes CYCD3 alcsalád hiányzik (*cycd3;1-3*). Ezek a tripla *cycd3;1-3* mutáns növények a túltermelő RBR vonalra emlékeztető fenotípust mutatták: magasabb hőmérsékleten a vad típusú növényekhez képest lelassult a fejlődésük, és meghosszabbodott a hipokotiljuk. Hasonlóképpen, a meleg hőmérséklet a sejtciklus gének működését csak kevésbé tudta stimulálni a *cycd3;1-3* mutánsban, míg a *PIF4* és *YUC8* gének az RBR-GFP expresszáló vonalhoz hasonlóan idukálódtak. Ezek az eredmények arra engednek következtetni, hogy a hőmérséklet az RBR funkción keresztül szabályozza a sejtosztódást és a sejtmegnyúlást: a merisztémákban indukálja az RBR foszforilációját, és ezen keresztül aktiválja a sejtciklus gének működését. A hipokotil poszt-mitotikus sejtjeiben az RBR fokozni képes a sejtmegnyúlást, mégpedig feltehetően az auxin bioszintézis növelésén keresztül. Pontosan hogyan aktiválja ezt a folyamatot az RBR még nem teljesen ismert, de az E2FB funkciójára ebben a szabályozásban szükség van: az RBR túltermelő vonalban az E2FB funkció hiányában a vad típushoz hasonló hipokotil növekedési választ figyelhettünk meg, amikor megemeltük a hőmérsékletet.

Kimutattuk, hogy az RBR a sejtméretet nemcsak a magasabb, hanem normál növekedési hőmérsékleten is szabályozza, mégpedig az aktívan osztódó sejtekben. A fejlődő Arabidopsis csíranövényben a mitotikus sejtosztódás a sejtek típusától és helyzetétől függően lehet szimmetrikus vagy aszimmetrikus, aminek köszönhetően a keletkező új sejtek mérete lényegesen eltérhet egymástól. A gyökérmerisztéma progenitor sejtjei döntően szimmetrikusan osztódnak, és ezeknek az osztódó sejteknek a méretét az RBR koncentrációjának a megváltoztatásán keresztül befolyásolni tudtuk: magasabb RBR jelenlétében nagyobb, míg kevesebb RBR mellett kisebb mérettel osztódó sejteket figyelhettünk meg. A sejtciklus szabályozási gének működésén keresztül,

az RBR szabályozni képes mind G1-S és a G2-M fázisátmeneteket, és így befolyásolhatja a G1 és G2 fázisok hosszát, és végső soron az osztódó sejtek méretét is.

A gázcsere nyílások vagy zárósejtek a levél bőr szövetében található zárósejt merisztémoidokból jönnek létre. Ezek az őssejtek néhány aszimmetrikus osztódást követően szimmetrikus osztódással zárósejtekké formálódhatnak. Az aszimmetrikus osztódások során egyre kisebb méretű merisztéma sejt keletkezik, amíg el nem érnek egy olyan kritikus kis méretet, amely után a szimmetrikus osztódás aktíválódik, és ezt követően a két új sejt zárósejtté differenciálódik. Az RBR szint változtatása lényeges hatással volt az aszimmetrikusan osztódó sejtek méretére és számára. Az RBR fehérje csökkenése fokozta a merisztémoidok osztódását, amely jelentősen kisebb méretű sejtek kialakulásához vezetett, mint amit a kontroll növényekben figyelhettünk meg. Ezzel szemben, az RBR szint emelésével a merisztémoidok kevesebbet osztódtak és nagyobb sejtmérettel, mint a kontroll vad típusú növényekben. Az aszimmetrikus és szimmetrikus osztódásokat különböző bHLH transzkripciós faktorok szabályozzák, és kimutattuk, hogy ezeket a különböző funkciójú géneket az RBR ellentétesen szabályozza. Az aszimmetrikus osztódásokért felelős *SPCH* gént az RBR szint csökkenésével stimulálni tudtuk, míg a szimmetrikus osztódás indukciójáért felelős *MUTE* gén működését a megemelt RBR szint fokozta. Mindkét bHLH faktor specifikus *CYCD* géneket aktivál; az SPCH a *CYCD3;1*, míg a MUTE a *CYCD5;1* és *CYCD7;1* géneket indukálja. Az RBR túltermelésével nemcsak a *MUTE*, hanem a *CYCD5;1* és *CYCD7;1* kifejeződését is fokozni tudtuk. További vizsgálatokra van szükség, annak érdekében, hogy megértsük, hogyan képes az RBR stimulálni a zárósejt merisztémoidok szimmetrikus osztódását.

Összefoglalva, a fejlődő Arabidopsis növényekben a sejtciklus-gátló RBR koncentrációtól függő módon szabályozza a sejtméretet; az állati RB fehérjéhez hasonlóan, kevesebb RBR kisebb sejteket, míg a több RBR nagyobb sejteket eredményez. Eredményeink arra engednek

következtetni, hogy a sejtméret szabályozása az eukaryota élőlényekben konzerválódhatott. Habár a sejtszám és a sejtméret szabályozása között egyértelmű kapcsolat mutatható ki, az RBR a sejtek számát, és a sejtméretet különböző mechanizmusokon keresztül képes szabályozni. Magasabb hőmérsékleten az RBR a növényi növekedési hormon, az auxin-szint változtatásán keresztül szabályozza a sejtméretet, és az auxin normál növekedési hőmérsékleten is fontos szerepet játszik a merisztémák működésében és feltehetően az RBR fehérjével együtt. Ezeknek az RBR-központú molekuláris útvonalaknak a mélyebb megértése lehetőséget kínálhat a növényi növekedés befolyásolására, ami előnyös lehet a növénynemesítési programok számára. További vizsgálatok szükségesek az RBR által közvetített szabályozási folyamatok hátterében álló pontos molekuláris mechanizmusok tisztázásához.

8. References

Abraham, E., P. Miskolczi, F. Ayaydin, et al. 2011. “Immunodetection of Retinoblastoma-Related Protein and Its Phosphorylated Form in Interphase and Mitotic Alfalfa Cells.” Journal of Experimental Botany 62, no. 6: 2155–2168.

Adachi, S., Minamisawa, K., Okushima, Y., Inagaki, S., Yoshiyama, K., Kondou, Y., ... & Umeda, M. (2011). Programmed induction of endoreduplication by DNA double-strand breaks in Arabidopsis. *Proceedings of the National Academy of Sciences*, *108*(24), 10004-10009.

Andriankaja, M., Dhondt, S., De Bodt, S., Vanhaeren, H., Coppens, F., De Milde, L., ... & Inzé, D. (2012). Exit from proliferation during leaf development in Arabidopsis thaliana: a not-so-gradual process. *Developmental cell*, *22*(1), 64-78.

Ai, H., J. Bellstaedt, K. S. Bartusch, et al. 2023. “Auxin-Dependent Regulation of Cell Division Rates Governs Root Thermomorphogenesis.” EMBO Journal 42: e111926.

Amasino, R. (2010). Seasonal and developmental timing of flowering. *The Plant Journal*, *61*(6), 1001-1013.

Anderson, R., P. E. Bayer, and D. Edwards. 2020. “Climate Change and the Need for Agricultural Adaptation.” Current Opinion in Plant Biology 56: 197–202.

Arnell, N. W., J. A. Lowe, A. J. Challinor, and T. J. Osborn. 2019. “Global and Regional Impacts of Climate Change at Different Levels of Global Temperature Increase.” Climatic Change 155: 377–391.

Balasubramanian, S., Sureshkumar, S., Lempe, J., & Weigel, D. (2006). Potent induction of Arabidopsis thaliana flowering by elevated growth temperature. *PLoS genetics*, *2*(7), e106.

Berckmans, B., & De Veylder, L. (2009). Transcriptional control of the cell cycle. *Current opinion in plant biology*, *12*(5), 599-605.

Blázquez, M. A., Ahn, J. H., & Weigel, D. (2003). A thermosensory pathway controlling flowering time in Arabidopsis thaliana. *Nature genetics*, *33*(2), 168-171.

Bellstaedt, J., J. Trenner, and R. Lippmann, et al. 2020. “A Mobile Auxin Signal Connects Temperature Sensing in Cotyledons With Growth Responses in Hypocotyls.” Plant Physiol 180, no. 2: 757–766.

Bian, Y., L. Chu, H. Lin, Y. Qi, Z. Fang, and D. Xu. 2022. “PIFs- and COP1-HY5-Mediated Temperature Signaling in Higher Plants.” Stress Biology 2: 35.

Bianchimano, L., M. B. De Luca, M. B. Borniego, M. J. Iglesias, and J. J. Casal. 2023. “Temperature Regulation of Auxin-Related Gene Expression and Its Implications for Plant Growth.” Journal of Experimental Botany 74: 7015–7033.

Boniotti, M. B., & Gutierrez, C. (2001). A cell-cycle-regulated kinase activity phosphorylates plant retinoblastoma protein and contains, in Arabidopsis, a CDKA/cyclin D complex. *The Plant Journal*, *28*(3), 341-350

Borghi, L., R. Gutzat, J. Fütterer, Y. Laizet, L. Hennig, and W. Gruissem. 2010. “Arabidopsis RETINOBLASTOMA-RELATED Is Required for Stem Cell Maintenance, Cell Differentiation, and Lateral Organ Production.” Plant Cell 22: 1792–1811.

Borniego, M. B., C. Costigliolo-Rojas, and J. J. Casal. 2022. “ShootThermosensors Do Not Fulfil the Same Function in the Root.” NewPhytologist 236: 9–14.

Bouyer, D., M. Heese, P. Chen, et al. 2018. “Genome-Wide Identification ofRETINOBLASTOMA RELATED 1 Binding Sites in Arabidopsis RevealsNovel DNA Damage Regulators.” PLoS Genetics 14, no. 11: e1007797.

Box, M. S., B. E. Huang, M. Domijan, et al. 2015. “ELF3 Controls Ther-moresponsive Growth in Arabidopsis.” Current Biology 25: 194–199.

Bridge, L. J., K. A. Franklin, and M. E. Homer. 2013. “Impact of PlantShoot Architecture on Leaf Cooling: A Coupled Heat and Mass TransferModel.” Journal of the Royal Society, Interface 10: 20130326.

Burgie ES, Vierstra RD **2014**. Phytochromes: an atomic perspective on photoactivation and signaling. *Plant Cell* 26:4568–83

Burko, Y., B. C. Willige, A. Seluzicki, O. Novák, K. Ljung, and J. Chory.2022. “PIF7 Is a Master Regulator of Thermomorphogenesis in Shade.”Nature Communications 13: 4942.

Capovilla, G., Schmid, M., & Posé, D. (2015). Control of flowering by ambient temperature. *Journal of Experimental Botany*, *66*(1), 59-69.

Capovilla, G., Symeonidi, E., Wu, R., & Schmid, M. (2017). Contribution of major FLM isoforms to temperature-dependent flowering in Arabidopsis thaliana. *Journal of Experimental Botany*, *68*(18), 5117-5127.

Casal, J. J., and S. Balasubramanian. 2019. “Thermomorphogenesis.”Annual Review of Plant Biology 70: 321–346.

Casal, J. J., and J. I. Qüesta. 2018. “Light and Temperature Cues: Mul-titasking Receptors and Transcriptional Integrators.” New Phytologist 217:1029–1034.

Cavallari, N., Nibau, C., Fuchs, A., Dadarou, D., Barta, A., & Doonan, J. H. (2018). The cyclin-dependent kinase G group defines a thermo-sensitive alternative splicing circuit modulating the expression of Arabidopsis ATU 2 AF 65A. *The Plant Journal*, *94*(6), 1010-1022.

Chadha, Y., Khurana, A., & Schmoller, K. M. (2024). Eukaryotic cell size regulation and its implications for cellular function and dysfunction. *Physiological Reviews*, *104*(4), 1679-1717.

Chen, D., M. Lyu, X. Kou, et al. 2022. “Integration of Light and Tem-perature Sensing by Liquid-Liquid Phase Separation of PhytochromeB.” Molecular Cell 82: 3015–3029.e6.

Chung, B. Y. W., M. Balcerowicz, M. Di Antonio, et al. 2020. “An RNAThermoswitch Regulates Daytime Growth in Arabidopsis.” NaturePlants 6: 522–532.

Churchman, M. L., Brown, M. L., Kato, N., Kirik, V., Hulskamp, M., Inze, D., ... & Larkin, J. C. (2006). SIAMESE, a plant-specific cell cycle regulator, controls endoreplication onset in Arabidopsis thaliana. *The Plant Cell*, *18*(11), 3145-3157.

Cockcroft, C. E., B. G. W. den Boer, J. M. S. Healy, and J. A. H. Murray.2000. “Cyclin D Control of Growth Rate in Plants.” Nature 405,no. 6786: 575–579.

Costanzo, M., Nishikawa, J. L., Tang, X., Millman, J. S., Schub, O., Breitkreuz, K., ... & Tyers, M. (2004). CDK activity antagonizes Whi5, an inhibitor of G1/S transcription in yeast. *Cell*, *117*(7), 899-913.

Crawford, A. J., D. H. McLachlan, A. M. Hetherington, andK. A. Franklin. 2012. “High Temperature Exposure Increases PlantCooling Capacity.” Current Biology 22: R396–R397.

Csorba, T., Questa, J. I., Sun, Q., & Dean, C. (2014). Antisense COOLAIR mediates the coordinated switching of chromatin states at FLC during vernalization. *Proceedings of the National Academy of Sciences*, *111*(45), 16160-16165.

Cui, X., Zheng, Y., Lu, Y., Issakidis-Bourguet, E., & Zhou, D. X. (2021). Metabolic control of histone demethylase activity involved in plant response to high temperature. *Plant Physiology*, *185*(4), 1813-1828.

D'Ario, M., R. Tavares, K. Schiessl, et al. 2021. “Cell Size Controlled inPlants Using DNA Content as an Internal Scale.” Science 372: 1176–1181.

De Bruin, R. A., McDonald, W. H., Kalashnikova, T. I., Yates, J., & Wittenberg, C. (2004). Cln3 activates G1-specific transcription via phosphorylation of the SBF bound repressor Whi5. *Cell*, *117*(7), 887-898.

Delker, C., Sonntag, L., James, G. V., Janitza, P., Ibanez, C., Ziermann, H., ... & Quint, M. (2014). The DET1-COP1-HY5 pathway constitutes a multipurpose signaling module regulating plant photomorphogenesis and thermomorphogenesis. *Cell reports*, *9*(6), 1983-1989.

del Pozo, J. C., Diaz-Trivino, S., Cisneros, N., & Gutierrez, C. (2006). The balance between cell division and endoreplication depends on E2FC-DPB, transcription factors regulated by the ubiquitin-SCFSKP2A pathway in Arabidopsis. *The Plant Cell*, *18*(9), 2224-2235.

De Veylder, L. 2019. "The Discovery of Plant D-Type Cyclins." PlantCell 31, no. 6: 1194–1195.

De Veylder, L., Beeckman, T., Beemster, G. T., Krols, L., Terras, F., Landrieu, I., ... & Inzé, D. (2001). Functional analysis of cyclin-dependent kinase inhibitors of Arabidopsis. *The Plant Cell*, *13*(7), 1653-1668.

De Veylder, L., Beeckman, T., Beemster, G. T., de Almeida Engler, J., Ormenese, S., Maes, S., ... & Inzé, D. (2002). Control of proliferation, endoreduplication and differentiation by the Arabidopsis E2Fa–DPa transcription factor. *The EMBO journal*.

De Veylder, L., Beeckman, T., & Inzé, D. (2007). The ins and outs of the plant cell cycle. *Nature Reviews Molecular Cell Biology*, *8*(8), 655-665.

Desvoyes, B., and C. Gutierrez. 2020. "Roles of Plant RetinoblastomaProtein: Cell Cycle and Beyond." EMBO Journal 39: e105802.

Dewitte, W., S. Scofield, A. A. Alcasabas, et al. 2007. "Arabidopsis CYCD3 D-Type Cyclins Link Cell Proliferation and Endocycles and Are Rate-Limiting for Cytokinin Responses." Proceedings of the National Academy of Sciences 104, no. 36: 14537–14542.

Dick, F. A., & Rubin, S. M. (2013). Molecular mechanisms underlying RB protein function. *Nature reviews Molecular cell biology*, *14*(5), 297-306.

Dong, J., C. A. MacAlister, and D. C. Bergmann. 2009. "BASL Controls Asymmetric Cell Division in Arabidopsis." Cell 137: 1320–1330.

Dubois, M., Selden, K., Bediée, A., Rolland, G., Baumberger, N., Noir, S., ... & Genschik, P. (2018). SIAMESE-RELATED1 is regulated posttranslationally and participates in repression of leaf growth under moderate drought. *Plant physiology*, *176*(4), 2834-2850.

Feraru, E., M. I. Feraru, E. Barbez, et al. 2019. "PILS6 Is a Temperature- Sensitive Regulator of Nuclear Auxin Input and Organ Growth in Arabidopsis thaliana." Proceedings of the National Academy of Sciences 116: 3893–3898.

Fiorucci, A.-S., V. C. Galvão, Y. Ç. Ince, et al. 2020. “Phytochrome Interacting Factor 7 Is Important for Early Responses to Elevated Temperature in Arabidopsis Seedlings.” New Phytologist 226: 50–58.

Fischer, M., & DeCaprio, J. A. (2015). Does Arabidopsis thaliana DREAM of cell cycle control?. *The EMBO journal*, *34*(15), 1987-1989.

Fonseca de Lima, C. F., J. Kleine-Vehn, I. De Smet, and E. Feraru. 2021. “Getting to the Root of Belowground High Temperature Responses in Plants.” Journal of Experimental Botany 72: 7404–7413.

Fornara, F., deMontaigu, A. and Coupland, G. (2010) SnapShot: control of flowering in Arabidopsis. *Cell*, **141**, 550, 550 e551-552.

Franklin, K. A., S. H. Lee, D. Patel, et al. 2011. “Phytochrome- Interacting Factor 4 (PIF4) Regulates Auxin Biosynthesis at High Temperature.” Proceedings of the National Academy of Sciences 108: 20231–20235.

Fujii, Y., Tanaka, H., Konno, N., Ogasawara, Y., Hamashima, N., Tamura, S., ... & Kodama, Y. (2017). Phototropin perceives temperature based on the lifetime of its photoactivated state. *Proceedings of the National Academy of Sciences*, *114*(34), 9206-9211.

Gaillochet, C., Y. Burko, and M. P. Platre, et al. 2020. “HY5 and Phytochrome Activity Modulate Shoot-to-Root Coordination During Thermomorphogenesis in Arabidopsis.” Development 147, no. 24: dev192625

Gombos, M., C. Raynaud, Y. Nomoto, et al. 2023. “The Canonical E2Fs Together With RETINOBLASTOMA-RELATED Are Required to Establish Quiescence During Plant Development.” Communications Biology 6: 903.

Gong, Y., Dale, R., Fung, H. F., Amador, G. O., Smit, M. E., & Bergmann, D. C. (2023). A cell size threshold triggers commitment to stomatal fate in Arabidopsis. *Science Advances*, *9*(38), eadf3497.

Hachez, C., Ohashi-Ito, K., Dong, J., & Bergmann, D. C. (2011). Differentiation of Arabidopsis guard cells: analysis of the networks incorporating the basic helix-loop-helix transcription factor, FAMA. *Plant Physiology*, *155*(3), 1458-1472.

Halliday, K. J., Salter, M. G., Thingnaes, E., & Whitelam, G. C. (2003). Phytochrome control of flowering is temperature sensitive and correlates with expression of the floral integrator FT. *The Plant Journal*, *33*(5), 875-885.

Han, S. K., & Torii, K. U. (2016). Lineage-specific stem cells, signals and asymmetries during stomatal development. *Development*, *143*(8), 1259-1270.

Han, S. K., Herrmann, A., Yang, J., Iwasaki, R., Sakamoto, T., Desvoyes, B., ... & Torii, K. U. (2022). Deceleration of the cell cycle underpins a switch from proliferative to terminal divisions in plant stomatal lineage. *Developmental Cell*, *57*(5), 569-582.

Han, X., H. Yu, R. Yuan, Y. Yang, F. An, and G. Qin. 2019. "Arabidopsis Transcription Factor TCP5 Controls Plant Thermomorphogenesis by Positively Regulating PIF4 Activity." iScience 15: 611–622.

Hanzawa, T., K. Shibasaki, T. Numata, Y. Kawamura, T. Gaude, and A. Rahman. 2013. "Cellular Auxin Homeostasis Under High Temperature Is Regulated Through a SORTING NEXIN1–Dependent Endosomal Trafficking Pathway." Plant Cell 25: 3424–3433.

Harashima, H., and K. Sugimoto. 2016. "Integration of Developmental and Environmental Signals Into Cell Proliferation and Differentiation Through RETINOBLASTOMA-RELATED 1." Current Opinion in Plant Biology 29: 95–103.

Hayes, S. (2020). Interaction of light and temperature signalling in plants. In *ELS* (1st ed.Chichester, England:). John Wiley & Sons Ltd.

Hayes, S., J. Schachtschabel, M. Mishkind, T. Munnik, and S. A. Arisz. 2021. "Hot Topic: Thermosensing in Plants." Plant, Cell & Environment 44: 2018–2033.

Hayes, S., Sharma, A., Fraser, D. P., Trevisan, M., Cragg-Barber, C. K., Tavridou, E., ... & Franklin, K. A. (2017). UV-B perceived by the UVR8 photoreceptor inhibits plant thermomorphogenesis. *Current Biology*, *27*(1), 120-127.

Hendrix, S. (2022). Remembering a warm day: daytime temperature influences nighttime hypocotyl growth in Arabidopsis.

Henley, S., and F. A. Dick. 2012. "The Retinoblastoma Family of Proteins and Their Regulatory Functions in the Mammalian Cell Division Cycle." Cell Division 7, no. 1: 10.

Ibañez, C., Y. Poeschl, T. Peterson, et al. 2017. "Ambient Temperature and Genotype Differentially Affect Developmental and Phenotypic Plasticity in Arabidopsis thaliana." BMC Plant Biology 17, no. 1: 114.

Ibañez, C., Delker, C., Martinez, C., Bürstenbinder, K., Janitza, P., Lippmann, R., ... & Quint, M. (2018). Brassinosteroids dominate hormonal regulation of plant thermomorphogenesis via BZR1. *Current Biology*, *28*(2), 303-310.

Ito, M. (2005). Conservation and diversification of three-repeat Myb transcription factors in plants. *Journal of plant research*, *118*, 61-69.

Iwata, E., S. Ikeda, S. Matsunaga, et al. 2011. “GIGAS CELL1, a Novel Negative Regulator of the Anaphase-Promoting Complex/Cyclosome, Is Required for Proper Mitotic Progression and Cell Fate Determination in Arabidopsis.” Plant Cell 23: 4382–4393.

Jaakola, L., A. M. Pirttilä, M. Halonen, and A. Hohtola. 2001. “Isolation of High Quality RNA From Bilberry (Vaccinium myrtillus L.) Fruit.” Molecular biotechnology 19, no. 2: 201–203. https://doi.org/10.1385/ MB:19:2:201.

Jang, S., Torti, S., & Coupland, G. (2009). Genetic and spatial interactions between FT, TSF and SVP during the early stages of floral induction in Arabidopsis. *The Plant Journal*, *60*(4), 614-625.

John, A., Smith, E. S., Jones, D. S., Soyars, C. L., & Nimchuk, Z. L. (2023). A network of CLAVATA receptors buffers auxin-dependent meristem maintenance. *Nature plants*, *9*(8), 1306-1317.

Joubès, J., & Chevalier, C. (2000). Endoreduplication in higher plants. *The plant cell cycle*, 191-201.

Jung, J. H., Barbosa, A. D., Hutin, S., Kumita, J. R., Gao, M., Derwort, D., ... & Wigge, P. A. (2020). A prion-like domain in ELF3 functions as a thermosensor in Arabidopsis. *Nature*, *585*(7824), 256-260.

Jung, J.-H., M. Domijan, C. Klose, et al. 2016. “Phytochromes Function as Thermosensors in Arabidopsis.” Science 354: 886–889.

Jung, J.-H., P. J. Seo, E. Oh, and J. Kim. 2023. “Temperature Perception by Plants.” Trends in Plant Science 28: 924–940.

Kazda, A., S. Akimcheva, J. M. Watson, and K. Riha. 2016. “Cell Proliferation Analysis Using EdU Labeling in Whole Plant and Histological Samples of Arabidopsis.” Methods Mol Biol 1370: 169–182.

Kim, S., Hwang, G., Kim, S., Thi, T. N., Kim, H., Jeong, J., ... & Oh, E. (2020). The epidermis coordinates thermoresponsive growth through the phyB-PIF4-auxin pathway. *Nature communications*, *11*(1), 1053.

Kim, C., Kwon, Y., Jeong, J., Kang, M., Lee, G. S., Moon, J. H., ... & Choi, G. (2023). Phytochrome B photobodies are comprised of phytochrome B and its primary and secondary interacting proteins. *Nature Communications*, *14*(1), 1708.

Kobayashi, K., Suzuki, T., Iwata, E., Magyar, Z., Bögre, L., & Ito, M. (2015). MYB3Rs, plant homologs of Myb oncoproteins, control cell cycle-regulated transcription and form DREAM-like complexes. *Transcription*, *6*(5), 106-111.

Koini, M. A., L. Alvey, T. Allen, et al. 2009. “High Temperature- Mediated Adaptations in Plant Architecture Require the bHLH Transcription Factor PIF4.” Current Biology 19: 408–413.

Komaki, S., & Sugimoto, K. (2012). Control of the plant cell cycle by developmental and environmental cues. *Plant and Cell Physiology*, *53*(6), 953-964.

Kono, A., C. Umeda-Hara, S. Adachi, et al. 2007. “The Arabidopsis D-Type Cyclin CYCD4 Controls Cell Division in the Stomatal Lineage of the Hypocotyl Epidermis.” Plant Cell 19, no. 4: 1265–1277.

Kostaki, K. I., Coupel-Ledru, A., Bonnell, V. C., Gustavsson, M., Sun, P., McLaughlin, F. J., ... & Franklin, K. A. (2020). Guard cells integrate light and temperature signals to control stomatal aperture. *Plant Physiology*, *182*(3), 1404-1419.

Kumar, N., Dale, R., Kemboi, D., Zeringue, E. A., Kato, N., & Larkin, J. C. (2018). Functional analysis of short linear motifs in the plant cyclin-dependent kinase inhibitor SIAMESE. *Plant physiology*, *177*(4), 1569-1579.

Kumar, N., Harashima, H., Kalve, S., Bramsiepe, J., Wang, K., Sizani, B. L., ... & Larkin, J. C. (2015). Functional conservation in the SIAMESE-RELATED family of cyclin-dependent kinase inhibitors in land plants. *The Plant Cell*, *27*(11), 3065-3080.

Kumar, S. V., & Wigge, P. A. (2010). H2A. Z-containing nucleosomes mediate the thermosensory response in Arabidopsis. *Cell*, *140*(1), 136-147.

Lai, L. B., Nadeau, J. A., Lucas, J., Lee, E. K., Nakagawa, T., Zhao, L., ... & Sack, F. D. (2005). The Arabidopsis R2R3 MYB proteins FOUR LIPS and MYB88 restrict divisions late in the stomatal cell lineage. *The Plant Cell*, *17*(10), 2754-2767.

Lang, L., Pettkó-Szandtner, A., Elbaşı, H. T., Takatsuka, H., Nomoto, Y., Zaki, A., ... & Schnittger, A. (2021). The DREAM complex represses growth in response to DNA damage in Arabidopsis. *Life Science Alliance*, *4*(12).

Lang, L., & Schnittger, A. (2020). Endoreplication—a means to an end in cell growth and stress response. *Current opinion in plant biology*, *54*, 85-92.

Larson-Rabin, Z., Li, Z., Masson, P. H., & Day, C. D. (2009). FZR2/CCS52A1 expression is a determinant of endoreduplication and cell expansion in Arabidopsis. *Plant Physiology*, *149*(2), 874-884.

Lau, O. S., & Bergmann, D. C. (2012). Stomatal development: a plant's perspective on cell polarity, cell fate transitions and intercellular communication. *Development*, *139*(20), 3683-3692.

Lau, O. S., Davies, K. A., Chang, J., Adrian, J., Rowe, M. H., Ballenger, C. E., & Bergmann, D. C. (2014). Direct roles of SPEECHLESS in the specification of stomatal self-renewing cells. *Science*, *345*(6204), 1605-1609.

Lee, R., Baldwin, S., Kenel, F., McCallum, J., & Macknight, R. (2013). FLOWERING LOCUS T genes control onion bulb formation and flowering. *Nature communications*, *4*(1), 2884.

Lee, S., I. Paik, and E. Huq. 2020. "SPAs Promote Thermomorphogenesis by Regulating the phyB-PIF4 Module in Arabidopsis." Development (Cambridge, England) 147.

Lee, H. J., Jung, J. H., Cortés Llorca, L., Kim, S. G., Lee, S., Baldwin, I. T., & Park, C. M. (2014). FCA mediates thermal adaptation of stem growth by attenuating auxin action in Arabidopsis. *Nature communications*, *5*(1), 5473.

Lee, J. H., Yoo, S. J., Park, S. H., Hwang, I., Lee, J. S., & Ahn, J. H. (2007). Role of SVP in the control of flowering time by ambient temperature in Arabidopsis. *Genes & development*, *21*(4), 397-402.

Legris, M. 2023. "Light and Temperature Regulation of Leaf Morphogenesis in Arabidopsis." New Phytologist 240: 2191–2196. https://doi. org/10.1111/nph.19258.

Legris, M., C. Klose, E. S. Burgie, et al. 2016. "Phytochrome B Integrates Light and Temperature Signals in Arabidopsis." Science 354, no. 6314: 897–900.

Leviczky, T., E. Molnár, C. Papdi, et al. 2019. "E2FA and E2FB Transcription Factors Coordinate Cell Proliferation With Seed Maturation." Development 146: dev179333.

Li, D., Liu, C., Shen, L., Wu, Y., Chen, H., Robertson, M., ... & Yu, H. (2008). A repressor complex governs the integration of flowering signals in Arabidopsis. *Developmental cell*, *15*(1), 110-120.

Lippmann, R., S. Babben, A. Menger, C. Delker, and M. Quint. 2019. "Development of Wild and Cultivated Plants Under Global Warming Conditions." Current Biology 29: R1326–R1338.

MacAlister, C. A., Ohashi-Ito, K., & Bergmann, D. C. (2007). Transcription factor control of asymmetric cell divisions that establish the stomatal lineage. *Nature*, *445*(7127), 537-540.

Ma, D., X. Li, Y. Guo, et al. 2016. "Cryptochrome 1 Interacts With PIF4 to Regulate High Temperature-Mediated Hypocotyl Elongation in Response to Blue Light." Proceedings of the National Academy of Sciences 113: 224–229.

Magyar, Z., B. Horváth, S. Khan, et al. 2012. "Arabidopsis E2FA Stimulates Proliferation and Endocycle Separately Through RBR-Bound and RBR-Free Complexes." EMBO Journal 31: 1480–1493.

Magyar, Z., Bögre, L., & Ito, M. (2016). DREAMs make plant cells to cycle or to become quiescent. *Current Opinion in Plant Biology*, *34*, 100-106.

Magyar, Z., L. De Veylder, A. Atanassova, L. Bakó, D. Inzé, and L. Bögre. 2005. "The Role of the Arabidopsis E2FB Transcription Factor in Regulating Auxin-Dependent Cell Division." The Plant Cell 17, no. 9: 2527–2541. https://doi.org/10.1105/tpc.105.033761.

Martínez, C., C. Nieto, and S. Prat. 2018. "Convergent Regulation of PIFs and the E3 Ligase COP1/SPA1 Mediates Thermosensory Hypocotyl Elongation by Plant Phytochromes." Current Opinion in Plant Biology 45: 188–203.

Martínez, C., Espinosa-Ruíz, A., de Lucas, M., Bernardo-García, S., Franco-Zorrilla, J. M., & Prat, S. (2018). PIF 4-induced BR synthesis is critical to diurnal and thermomorphogenic growth. *The EMBO journal*, *37*(23), e99552.

Martins, S., A. Montiel-Jorda, A. Cayrel, et al. 2017. "Brassinosteroid Signaling-Dependent Root Responses to Prolonged Elevated Ambient Temperature." Nature Communications 8: 309.

McClung, C. R., Lou, P., Hermand, V., & Kim, J. A. (2016). The importance of ambient temperature to growth and the induction of flowering. *Frontiers in Plant Science*, *7*, 1266.

Miettinen, T. P., Caldez, M. J., Kaldis, P., & Björklund, M. (2017). Cell size control–a mechanism for maintaining fitness and function. *Bioessays*, *39*(9), 1700058.

Medina, E. M., Turner, J. J., Gordâ N, R., Skotheim, J. M., & Buchler, N. E. (2016). Punctuated evolution and transitional hybrid network in an ancestral cell cycle of fungi.

Mirón, I. J., C. Linares, and J. Díaz. 2023. "The Influence of Climate Change on Food Production and Food Safety." Environmental Research 216: 114674.

Murcia, G., Nieto, C., Sellaro, R., Prat, S., & Casal, J. J. (2022). Hysteresis in PHYTOCHROME-INTERACTING FACTOR 4 and EARLY-FLOWERING 3 dynamics dominates warm daytime memory in Arabidopsis. *The Plant Cell*, *34*(6), 2188-2204.

Nibau, C., Gallemí, M., Dadarou, D., Doonan, J. H., & Cavallari, N. (2020). Thermo-sensitive alternative splicing of FLOWERING LOCUS M is modulated by cyclin-dependent kinase G2. *Frontiers in plant science*, *10*, 1680.

Nieto, C., Luengo, L. M., & Prat, S. (2020). Regulation of COP1 function by Brassinosteroid signaling. *Frontiers in Plant Science*, *11*, 1151.

Nomoto, Y., H. Takatsuka, K. Yamada, et al. 2022. “A Hierarchical Transcriptional Network Activates Specific CDK Inhibitors That Regulate G2 to Control Cell Size and Number in Arabidopsis.” Nature Communications 13: 1660.

Nowack, M. K., H. Harashima, N. Dissmeyer, et al. 2012. “Genetic Framework of Cyclin-Dependent Kinase Function in Arabidopsis.” Developmental Cell 22: 1030–1040. https://doi.org/10.1016/j.devcel.2012. 02.015.

Oh, E., Zhu, J. Y., Bai, M. Y., Arenhart, R. A., Sun, Y., & Wang, Z. Y. (2014). Cell elongation is regulated through a central circuit of interacting transcription factors in the Arabidopsis hypocotyl. *elife*, *3*, e03031.

Ortiz-Bobea, A., T. R. Ault, C. M. Carrillo, R. G. Chambers, and D. B. Lobell. 2021. “Anthropogenic Climate Change has Slowed Global Agricultural Productivity Growth.” Nature Climate Change 11: 306–312.

Őszi, E., C. Papdi, B. Mohammed, et al. 2020. “E2FB Interacts With RETINOBLASTOMA RELATED and Regulates Cell Proliferation During Leaf Development.” Plant Physiology 182: 518–533.

Pardi, S. A., & Nusinow, D. A. (2021). Out of the dark and into the light: a new view of phytochrome photobodies. *Frontiers in Plant Science*, *12*, 732947.

Park, Y.-J., H.-J. Lee, K.-E. Gil, et al. 2019. “Developmental Programming of Thermonastic Leaf Movement.” Plant Physiology 180: 1185–1197.

Peres, A., Churchman, M. L., Hariharan, S., Himanen, K., Verkest, A., Vandepoele, K., ... & De Veylder, L. (2007). Novel plant-specific cyclin-dependent kinase inhibitors induced by biotic and abiotic stresses. *Journal of Biological Chemistry*, *282*(35), 25588-25596.

Perilli, S., J. M. Perez-Perez, R. Di Mambro, et al. 2013. “RETINOBLASTOMA-RELATED Protein Stimulates Cell Differentiation in the Arabidopsis Root Meristem by Interacting With Cytokinin Signaling.” The Plant Cell 25: 4469–4478.

Perrella, G., I. Bäurle, and M. van Zanten. 2022. “Epigenetic Regulation of Thermomorphogenesis and Heat Stress Tolerance.” New Phytologist 234: 1144–1160.

Pettkó-Szandtner, A., Mészáros, T., Horváth, G. V., Bakó, L., Csordás-Tóth, É., Blastyák, A., ... & Dudits, D. (2006). Activation of an alfalfa cyclin-dependent kinase inhibitor by calmodulin-like domain protein kinase. *The Plant Journal*, *46*(1), 111-123.

Pillitteri, L. J., Sloan, D. B., Bogenschutz, N. L., & Torii, K. U. (2007). Termination of asymmetric cell division and differentiation of stomata. *Nature*, *445*(7127), 501-505.

Polyn, S., Willems, A., & De Veylder, L. (2015). Cell cycle entry, maintenance, and exit during plant development. *Current Opinion in Plant Biology*, *23*, 1-7.

Posé, D., Yant, L. & Schmid, M. The end of innocence: flowering networks explode in complexity. *Curr. Opin. Plant Biol.* **15**, 45–50 (2012)

Press, M. O., A. Lanctot, and C. Queitsch. 2016. "PIF4 and ELF3 Act Independently in Arabidopsis thaliana Thermoresponsive Flowering." PloS One 11: e0161791.

Qi, F., & Zhang, F. (2020). Cell cycle regulation in the plant response to stress. *Frontiers in plant science*, *10*, 1765.

Qi, L., Y. Shi, W. Terzaghi, S. Yang, and J. Li. 2022. "Integration of Light and Temperature Signaling Pathways in Plants." Journal of Integrative Plant Biology 64: 393–411.

Qiu, Y. 2020. "Regulation of PIF4-Mediated Thermosensory Growth." Plant Science 297: 110541.

Qiu, Y., E. K. Pasoreck, C. Y. Yoo, et al. 2021. "Rcb Initiates Arabidopsis Thermomorphogenesis by Stabilizing the Thermoregulator PIF4 in the Daytime." Nature Communications 12: 2042.

Quint, M., C. Delker, K. A. Franklin, P. A. Wigge, K. J. Halliday, and M. van Zanten. 2016. "Molecular and Genetic Control of Plant Thermomorphogenesis." Nature Plants 2: 15190.

Quint, M., H. Ito, W. Zhang, and W. M. Gray. 2005. "Characterization of a Novel Temperature-Sensitive Allele of the CUL1/AXR6 Subunit of SCF Ubiquitin-Ligases." Plant Journal 43, no. 3: 371–383. https://doi.org/10.1111/j.1365-313X.2005.02449.x.

Quint, M., L. Barkawi, K. -T. Fan, J. D. Cohen, and W. M. Gray. 2009. "Arabidopsis IAR4 Modulates Auxin Response by Regulating Auxin Homeostasis." Plant physiology 150, no 2: 748–758.

Raschke, A., C. Ibañez, K. K. Ullrich, et al. 2015. "Natural Variants of ELF3 Affect Thermomorphogenesis by Transcriptionally Modulating PIF4-Dependent Auxin Response Genes." BMC Plant Biology 15: 197.

Ray, D. K., P. C. West, M. Clark, J. S. Gerber, A. V. Prishchepov, and S. Chatterjee. 2019. "Climate Change has Likely Already Affected Global Food Production." PLoS One 14: e0217148.

Riou-Khamlichi, C., Huntley, R., Jacqmard, A., & Murray, J. A. (1999). Cytokinin activation of Arabidopsis cell division through a D-type cyclin. *Science*, *283*(5407), 1541-1544.

Riou-Khamlichi, C., M. Menges, J. M. S. Healy, and J. A. H. Murray. 2000. “Sugar Control of the Plant Cell Cycle: Differential Regulation of Arabidopsis D-Type Cyclin Gene Expression.” Molecular and Cellular Biology 20, no. 13: 4513–4521.

Rockwell, N. C., Su, Y. S., & Lagarias, J. C. (2006). Phytochrome structure and signaling mechanisms. *Annu. Rev. Plant Biol.*, *57*(1), 837-858.

Roeder, A. H., Chickarmane, V., Cunha, A., Obara, B., Manjunath, B. S., & Meyerowitz, E. M. (2010). Variability in the control of cell division underlies sepal epidermal patterning in Arabidopsis thaliana. *PLoS biology*, *8*(5), e1000367.

Romero-Montepaone, S., R. Sellaro, C. Esteban Hernando, et al. 2021. “Functional Convergence of Growth Responses to Shade and Warmth in Arabidopsis.” New Phytologist 231: 1890–1905.

Sablowski, R., and C. Gutierrez. 2022. “Cycling in a Crowd: Coordination of Plant Cell Division, Growth, and Cell Fate.” Plant Cell 34: 193–208.

Sage, J., Mulligan, G. J., Attardi, L. D., Miller, A., Chen, S., Williams, B., ... & Jacks, T. (2000). Targeted disruption of the three Rb-related genes leads to loss of G1 control and immortalization. *Genes & development*, *14*(23), 3037-3050.

Saitoh, A., T. Takase, H. Abe, M. Watahiki, Y. Hirakawa, and T. Kiyosue. 2021. “Zeitlupe Enhances Expression of PIF4 and YUC8 in the Upper Aerial Parts of Arabidopsis Seedlings to Positively Regulate Hypocotyl Elongation.” Plant Cell Reports 40: 479–489.

Sánchez-Lamas, M., Lorenzo, C. D., & Cerdán, P. D. (2016). Bottom-up assembly of the phytochrome network. *PLoS genetics*, *12*(11), e1006413.

Sanidas, I., R. Morris, K. A. Fella, et al. 2019. “A Code of Mono.Phosphorylation Modulates the Function of RB.” Molecular Cell 73, no. 5: 985–1000.e6.

Schmoller, K. M., J. J. Turner, M. Kõivomägi, and J. M. Skotheim. 2015. “Dilution of the Cell Cycle Inhibitor Whi5 Controls Budding-Yeast Cell Size.” Nature 526: 268–272.

Scortecci, K. C., Michaels, S. D., & Amasino, R. M. (2001). Identification of a MADS-box gene, FLOWERING LOCUS M, that represses flowering. *The Plant Journal*, *26*(2), 229-236.

Shimotohno, A., Aki, S. S., Takahashi, N., & Umeda, M. (2021). Regulation of the plant cell cycle in response to hormones and the environment. *Annual review of plant biology*, *72*(1), 273-296.

Seo, D., Park, J., Park, J., Hwang, G., Seo, P. J., & Oh, E. (2023). ZTL regulates thermomorphogenesis through TOC1 and PRR5. *Plant, Cell & Environment*, *46*(5), 1442-1452.

Seo, E., Lee, H., Jeon, J., Park, H., Kim, J., Noh, Y. S., & Lee, I. (2009). Crosstalk between cold response and flowering in Arabidopsis is mediated through the flowering-time gene SOC1 and its upstream negative regulator FLC. *The Plant Cell*, *21*(10), 3185-3197.

Shimotohno, A., Aki, S. S., Takahashi, N., & Umeda, M. (2021). Regulation of the plant cell cycle in response to hormones and the environment. *Annual review of plant biology*, *72*(1), 273-296.

Smaczniak, C., Immink, R. G., Muiño, J. M., Blanvillain, R., Busscher, M., Busscher-Lange, J., ... & Kaufmann, K. (2012). Characterization of MADS-domain transcription factor complexes in Arabidopsis flower development. *Proceedings of the National Academy of Sciences*, *109*(5), 1560-1565.

Song, Y. H., Shim, J. S., Kinmonth-Schultz, H. A., & Imaizumi, T. (2015). Photoperiodic flowering: time measurement mechanisms in leaves. *Annual review of plant biology*, *66*(1), 441-464.

Stavang, J. A., J. Gallego-Bartolomé, M. D. Gómez, et al. 2009. “Hormonal Regulation of Temperature-Induced Growth in Arabidopsis.” Plant Journal 60: 589–601.

Sun, J., L. Qi, Y. Li, J. Chu, and C. Li. 2012. “PIF4-Mediated Activation of YUCCA8 Expression Integrates Temperature Into the Auxin Pathway in Regulating Arabidopsis Hypocotyl Growth.” PLoS Genetics 8: e1002594.

Swaffer, M. P., Kim, J., Chandler-Brown, D., Langhinrichs, M., Marinov, G. K., Greenleaf, W. J., ... & Skotheim, J. M. (2021). Transcriptional and chromatin-based partitioning mechanisms uncouple protein scaling from cell size. *Molecular cell*, *81*(23), 4861-4875.

Takahashi, I., S. Kojima, N. Sakaguchi, C. Umeda-Hara, and M. Umeda. 2010. “Two Arabidopsis Cyclin A3s Possess G1 Cyclin-Like Features.” Plant Cell Reports 29, no. 4: 307–315.

Talbot, M. J., and R. G. White. 2013. “Methanol Fixation of Plant Tissue for Scanning Electron Microscopyimproves Preservation of Tissue Morphology and Dimensions.” Plant Methods 9, no. 1: 36.

Tasset, C., Singh Yadav, A., Sureshkumar, S., Singh, R., van der Woude, L., Nekrasov, M., ... & Balasubramanian, S. (2018). POWERDRESS-mediated histone deacetylation is essential for thermomorphogenesis in Arabidopsis thaliana. *PLoS genetics*, *14*(3), e1007280.

Van Der Woude, L. C., Perrella, G., Snoek, B. L., Van Hoogdalem, M., Novák, O., Van Verk, M. C., ... & Van Zanten, M. (2019). HISTONE DEACETYLASE 9 stimulates auxin-dependent thermomorphogenesis

in Arabidopsis thaliana by mediating H2A. Z depletion. *Proceedings of the National Academy of Sciences*, *116*(50), 25343-25354.

Van Leene, J., J. Boruc, G. De Jaeger, E. Russinova, and L. De Veylder. 2011. "A Kaleidoscopic View of the Arabidopsis Core Cell Cycle Interactome." Trends in Plant Science 16: 140–150.

Valverde, F., Mouradov, A., Soppe, W., Ravenscroft, D., Samach, A., & Coupland, G. (2004). Photoreceptor regulation of CONSTANS protein in photoperiodic flowering. *Science*, *303*(5660), 1003-1006.

Verma, N., D. Singh, L. Mittal, G. Banerjee, S. Noryang, and A. K. Sinha. 2023. "MPK4 Mediated Phosphorylation of PHYTOCHROME INTERACTING FACTOR4 Controls Thermosensing by Regulation of H2A.Z Deposition in Arabidopsis." Plant Cell 36, no. 10: 4535–4556.

Vu, L. D., Gevaert, K., & De Smet, I. (2019). Feeling the heat: Searching for plant thermosensors. *Trends in Plant Science*, **24**(3), 210–219.

Wang, Q., and Z. Zhu. 2022. "Light Signaling-Mediated Growth Plasticity in Arabidopsis Grown Under High-Temperature Conditions." Stress Biology 2: 53.

Wang, S., Y. Gu, S. G. Zebell, et al. 2014. "A Noncanonical Role for the CKI-RB-E2F Cell-Cycle Signaling Pathway in Plant Effector-Triggered Immunity." Cell Host & Microbe 16: 787–794.

Wang, R., Y. Zhang, M. Kieffer, H. Yu, S. Kepinski, and M. Estelle. 2016. "HSP90 Regulates Temperature-Dependentseedling Growth in Arabidopsis by Stabilizing the Auxin Co-Receptor F-Boxprotein TIR1." Nature communications 7: 10269.

Weimer, A. K., Matos, J. L., Sharma, N., Patell, F., Murray, J. A., Dewitte, W., & Bergmann, D. C. (2018). Lineage-and stage-specific expressed CYCD7; 1 coordinates the single symmetric division that creates stomatal guard cells. *Development*, *145*(6).

Wildwater, M., A. Campilho, J. M. Perez-Perez, et al. 2005. "The RETINOBLASTOMA-RELATED Gene Regulates Stem Cell Maintenance in Arabidopsis Roots." Cell 123, no. 7: 1337–1349.

Wu, J., P. Liu, and Y. Liu. 2023. "Thermosensing and Thermal Responses in Plants." Trends in Biochemical Sciences 48, no. 11: 923–926. https://doi.org/10.1016/j.tibs.2023.08.002

Wyrzykowska, J., M. Schorderet, S. Pien, W. Gruissem, and A. J. Fleming. 2006. "Induction of Differentiation in the Shoot Apical Meristem by Transient Overexpression of a Retinoblastoma-Related Protein." Plant Physiology 141: 1338–1348.

Xie, Z., Lee, E., Lucas, J. R., Morohashi, K., Li, D., Murray, J. A., ... & Grotewold, E. (2010). Regulation of cell proliferation in the stomatal lineage by the Arabidopsis MYB FOUR LIPS via direct targeting of core cell cycle genes. *The Plant Cell*, *22*(7), 2306-2321.

Xu, Y., and Z. Zhu. 2021. "PIF4 and PIF4-Interacting Proteins: At the Nexus of Plant Light, Temperature and Hormone Signal Integrations." International Journal of Molecular Sciences 22: 10304.

Yang, X., G. Dong, K. Palaniappan, G. Mi, and T. I. Baskin. 2017. "Temperature-Compensated Cell Production Rate and Elongation Zone Length in the Root of Arabidopsis thaliana." Plant, Cell & Environment 40, no. 2: 264–276.

Yi, D., Alvim Kamei, C. L., Cools, T., Vanderauwera, S., Takahashi, N., Okushima, Y., ... & De Veylder, L. (2014). The Arabidopsis SIAMESE-RELATED cyclin-dependent kinase inhibitors SMR5 and SMR7 regulate the DNA damage checkpoint in response to reactive oxygen species. *The Plant Cell*, *26*(1), 296-309.

Zatulovskiy, E., S. Zhang, D. F. Berenson, B. R. Topacio, and J. M. Skotheim. 2020. "Cell Growth Dilutes the Cell Cycle Inhibitor Rb to Trigger Cell Division." Science 369: 466–471.

Zhang, L. L., Luo, A., Davis, S. J., & Liu, J. X. (2021). Timing to grow: roles of clock in thermomorphogenesis. *Trends in Plant Science*, *26*(12), 1248-1257.

Zhao, H., and Y. Bao. 2021. "PIF4: Integrator of Light and Temperature Cues in Plant Growth." Plant Science 313: 111086.

9. List of publications

The publications constitute the foundation of the thesis:

1, Hamid RSB, Nagy F, Kaszler N, Domonkos I, Gombos M, Marton A, Vizler Cs, Molnár E, Pettkó-Szandtner A, Bögre L, Fehér A., Magyar Z. (2025) RETINOBLASTOMA-RELATED Has Both Canonical and Noncanonical Regulatory Functions During Thermomorphogenesis Responses in Arabidopsis Seedlings. **PLANT CELL AND ENVIRONMENT** 48: (2) 1217-1231. doi: 10.1111/pce.15202. Epub 2024 Oct 17

2, Fehér A, Hamid RSB, Magyar Z. (2025) How Do Arabidopsis Seedlings Sense and React to Increasing Ambient Temperatures? **Plants – Basel,** 14(2):248. https://doi.org/10.3390/plants14020248

Additional publication:

1, Janib Y, Aamir R, Hamid RSB, Zubair A, Durre S. (2023) Comparative effects of caffeine and lead nitrate on the bio-physiological and yield associated traits of lentil (*Lens culinaris* Medik.). Heliyon. 9(6):e16351. doi: 10.1016/j.heliyon.2023.e16351.

10. Declaration

I declare that the data used in the thesis written by SHIEKH RASIK BIN HAMID reflect the contribution of the doctoral candidate to the article: RETINOBLASTOMA-RELATED has both canonical and non-canonical regulatory functions during thermo-morphogenic responses in Arabidopsis seedlings, Plant cell and environment 2025. The results reported in the Ph.D. thesis and the publication were not used to acquire any Ph.D. degree previously. I further declare that the candidate has made significant contribution to the creation of the above-mentioned publication.

Dr. Magyar Zoltán

Institute of Plant Biology

HUN-REN Biological Research Centre Szeged

11. Supplementary data

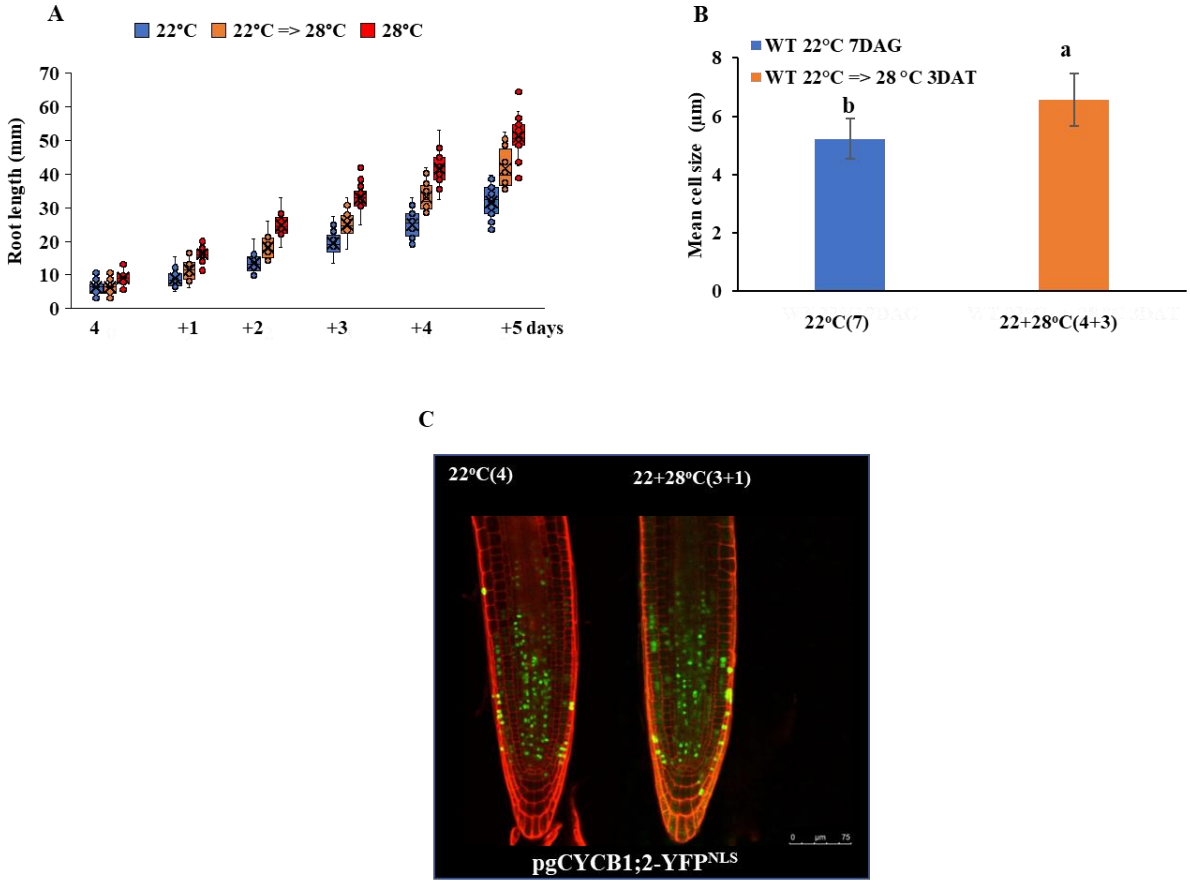

Supplemental Figure 1. Effect of temperature shift on root length, cortex cell size and mitotic activity in Arabidospis seedlings. A) Root length of WT seedlings was followed in continuous 22ºC or 28ºC or days after transfer from 22ºC to 28ºC as indicated. T0 represents 4 DAG old seedlings. **B**) Mean cortex cell size in the root meristem of WT seedlings grow at 22ºC for 7DAG or 3DAT of 4 DAG old seedlings from 22ºC to 28ºC. **C**)

pgCYCB1;2-YFP^{NLS} in WT background were grown at 22ºC for 4 DAG or 1 DAT of 3DAG old seedlings to 28ºC. Scale bar is indicated at the right corner.

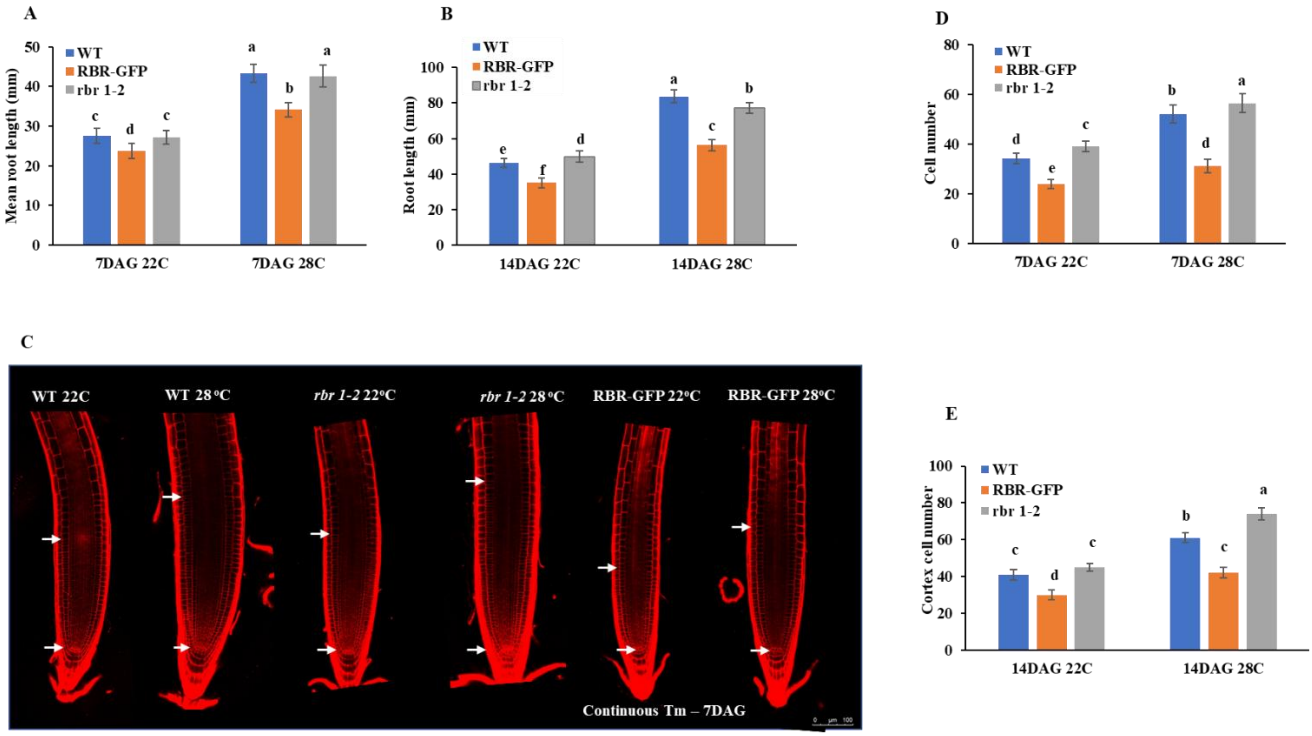

Supplemental Figure S2. Warm temperature induces root growth by regulating meristem cell size and cell proliferation in RBR dependent manner. A-B) Warm temperature increases root length at both 7 and 14 days after germintion and its effect was partially suppressed or enhanced by high and low RBR levels presented in *rbr1-2* mutant and ectopic RBR lines, respectively . **C**) Representative root meristems of WT, *rbr1-2* and RBR-GFP seedlings grow continuously at 22ºC or 28ºC for 7DAG. Arrows mark quiescent centre and the last small cortex cells representing the boundary of the root meristem. **D**) Cortex cell numbers were also counted in the root meristems of these lines at both temperatures. **E**) Cortex cell numbers were increased in all the three root meristems at 28ºC in comparison to the 22ºC in two weeks old seedlings.

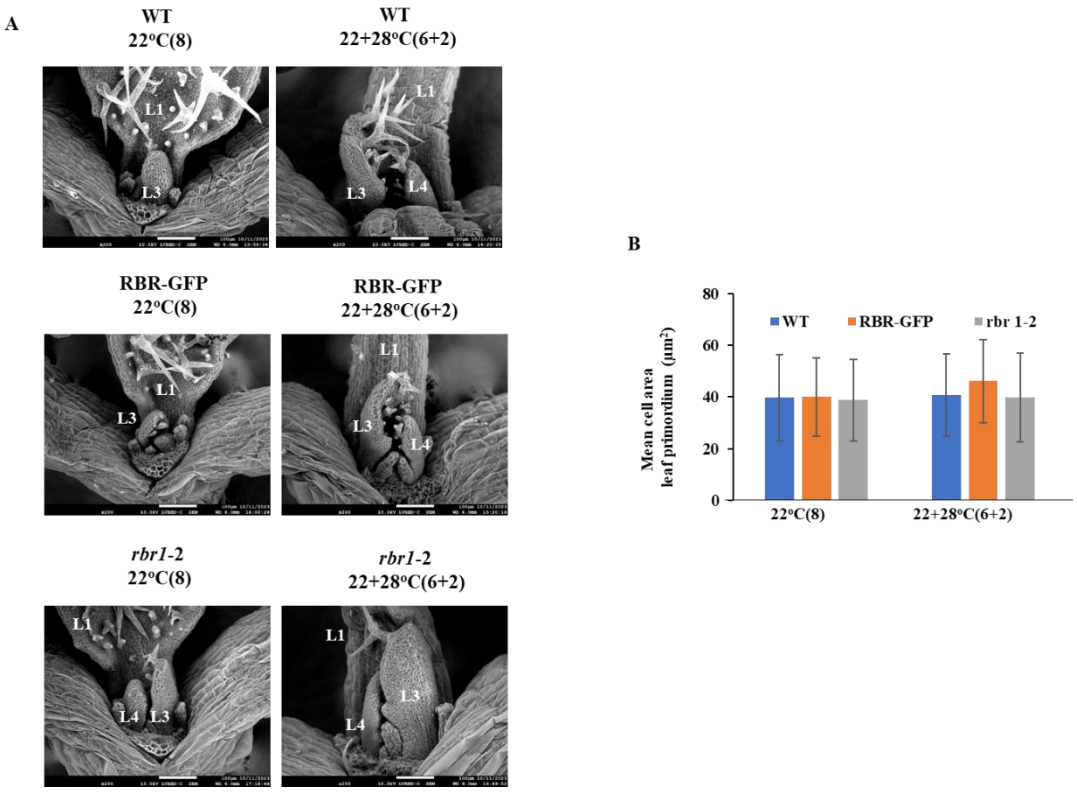

Supplemental Figure S3. Warm temperature accelerates shoot and leaf development and its effect was regulated by RBR. A) Scanning electron microscopic images of shoot apex of WT, RBR-GFP and *rbr1-2* seedlings. Leaf primordium size increased in all the three genotypes 2DAT from 22°C to 28°C in comparison to the seedlings grow at continuous 22°C. Order of leaf primordium (L) is marked by numbers. Scale bar is indicated. **B**) Cell size of the 3rd leaf primordium was measured in all the three lines at the indicated temperature and developmental time.

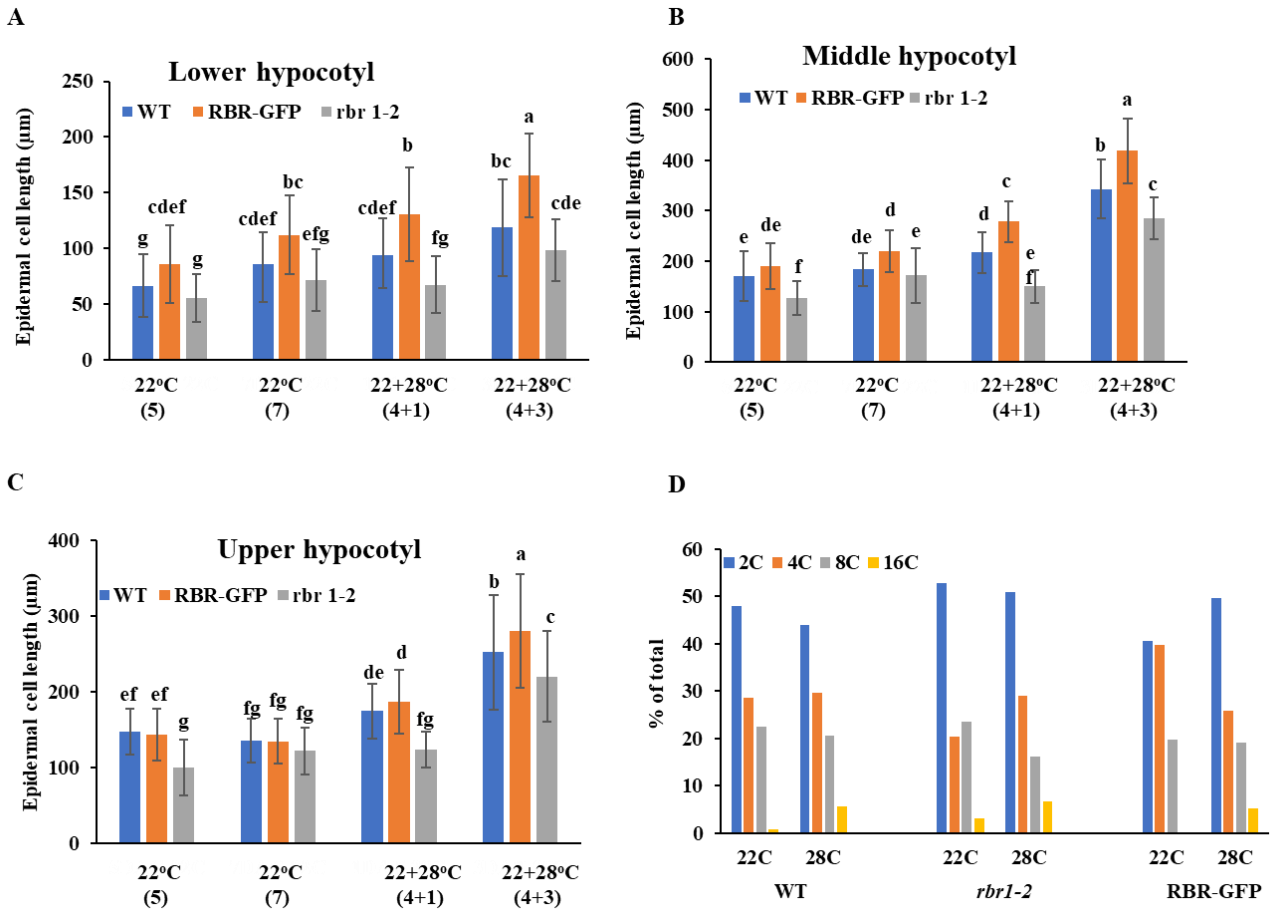

Supplemental Figure S4. Ectopic RBR level increases epidermal size of the hypocotyl with warm temperature without affecting ploidy level. A-C) Epidermal cells of the hypocotyl of WT, *rbr1-2* and RBR-GFP lines were measured in three regions of the hypocotyl (upper-**A**, middle-**B** and the bottom-**C** part) at continuous 22°C and after transfer to 28°C as indicated. **D**) Ploidy level of hypocotyls of these lines were determined by flow cytometer at both temperatures.

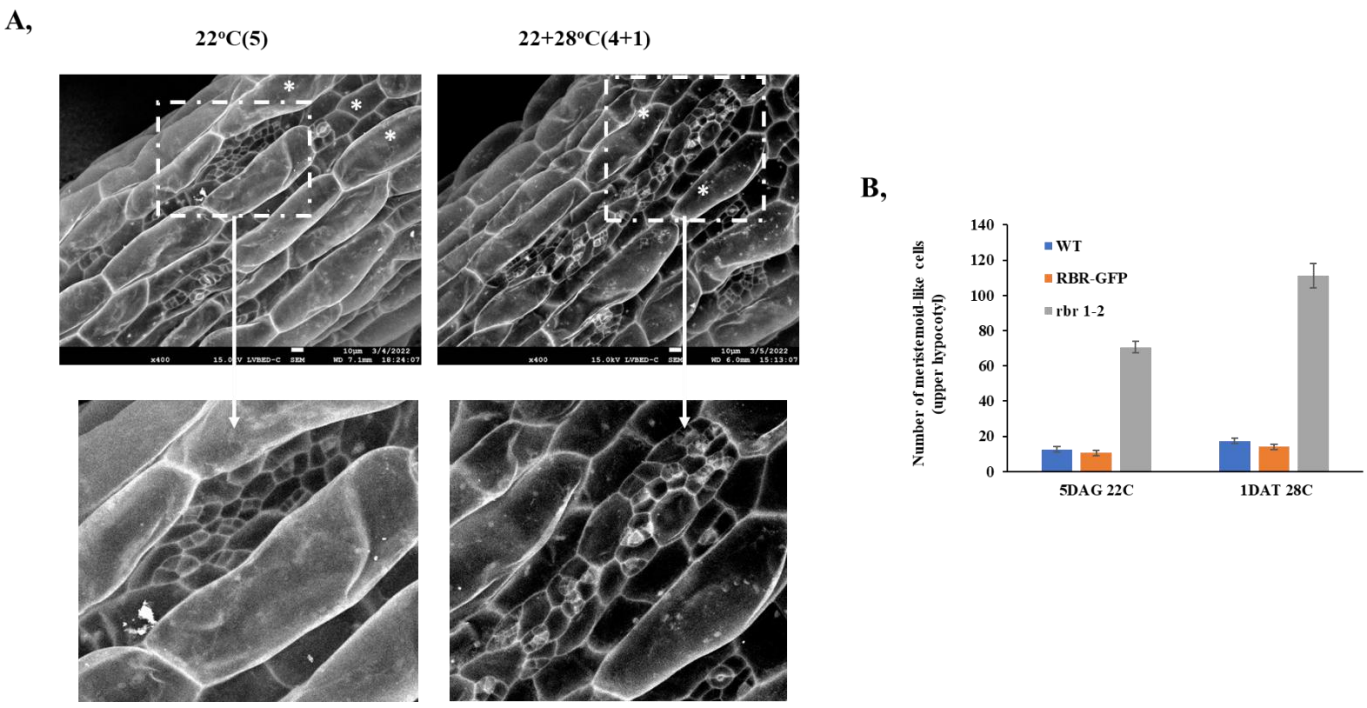

Supplemental Figure S5. Stomatal meristemoid cells in the *rbr1-2* mutant hypocotyl show increased proliferation activity under warm temperature resulted in the formation of small cell clusters. **A**) Representative SEM picture of the hypocotyl of *rbr1-2* seedlings grow at continuous 22°C and 1 DAT of 4 DAG seedlings to 28°C. Meristemoid cells observed in the non-protruding cell files. **B**) Number of stomatal meristemoid-like cells increased the most in the rbr1-2 mutant line, and warm temperature further increased its number.

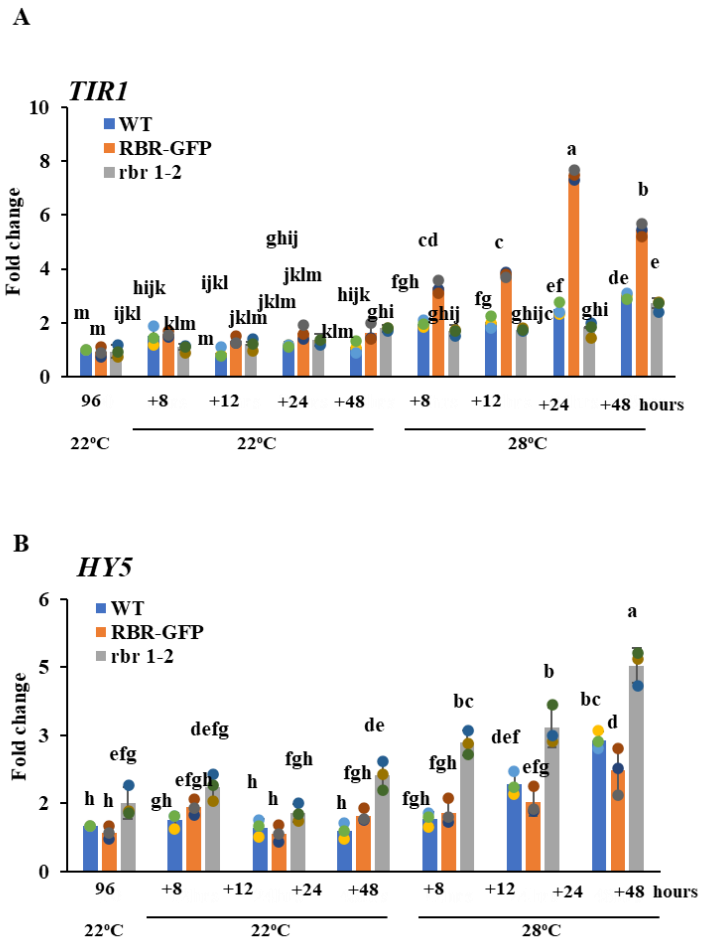

Supplemental Figure S6. RBR oppositely regulates auxin receptor gene *TIR1* and the photomorphogen *HY5* at warm temperature. A-B) Expression of *TIR1* and *HY5* was monitored by qRT-PCR at continuous 22ºC or after transfer to 28ºC as indicated. **A**) F-box and auxin receptor TIR1 was induced by warm temperature, and it was further stimulated by ectopic RBR. **B**) Expression of *HY5* was also increased by warm temperature but the reduced RBR level in the *rbr1-2* mutant resulted in a higher transcript level, while the ectopic RBR in the RBR-GFP seedlings suppresses the effect of warmth. T0 represents 4 DAG old seedlings, and they were kept growing at 22ºC or transferred to 28ºC, and samples were taken at 8, 12, 24 and 48 hours (hrs) afterwards. Values represent fold change normalized to the value of the relevant transcript of the seedlings at T0 (4 DAG), which was set arbitrarily at 1. Data are means +/- sd. N=3 biological replicates.

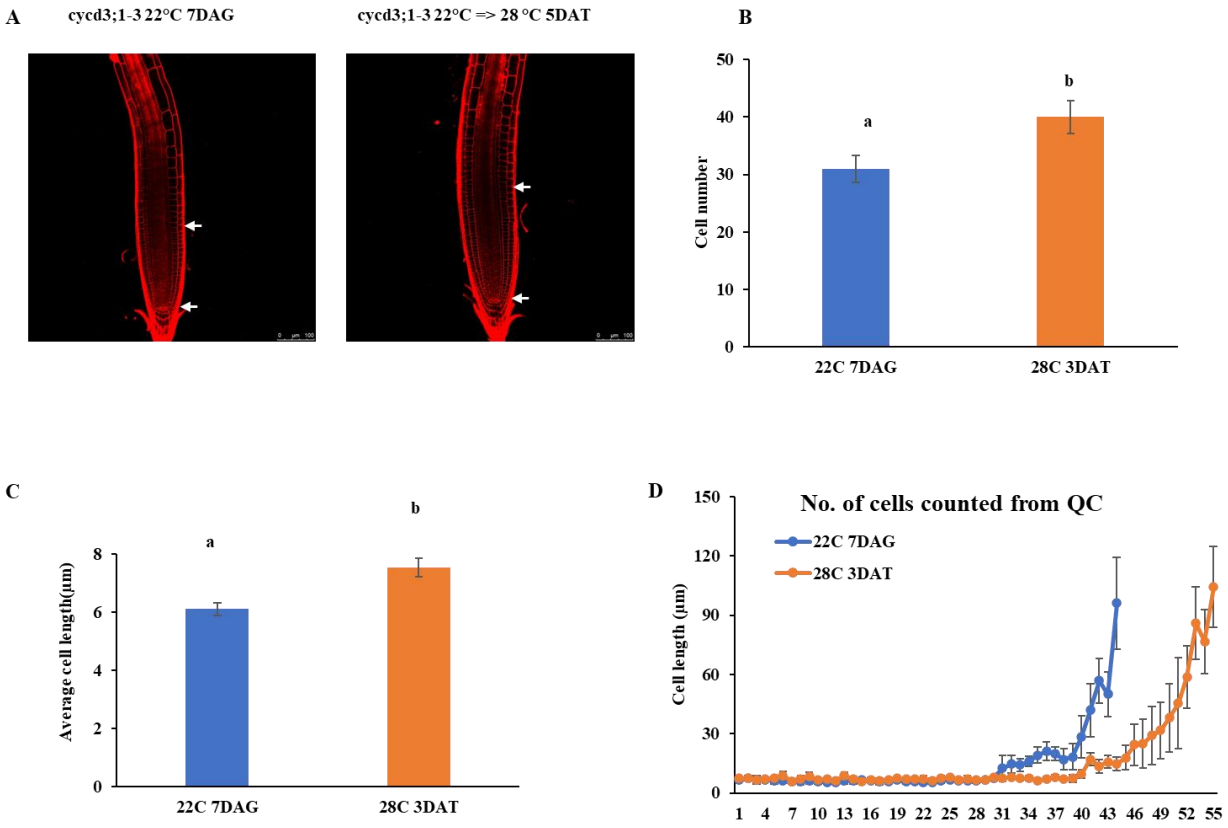

Supplemental Figure S7. The *cycd3;1-3* mutants reveal a temperature-dependent regulation of root meristem size and cell elongation. A) The representative images of the root meristems of *cycd3;1-3* seedlings grown for 7 days after germination (DAG) at 22ºC or 3 days after transfer (DAT) of 4 DAG old seedlings from 22ºC to 28ºC. Arrows mark quiescent centre and the last small cortex cells, which delineate the boundary of the root meristem. **B**) The number of cortex cells was quantified in the root meristems at both temperatures. **C**) The average cell length was also assessed, revealing an increase in the root meristems at 28ºC compared to the 22ºC. **D**) The spatial distribution of cell length across root meristems in *cycd3,1-3* was analysed for 7 DAG at 22ºC or 3 DAT of 4 DAG old seedlings from 22ºC to 28ºC.

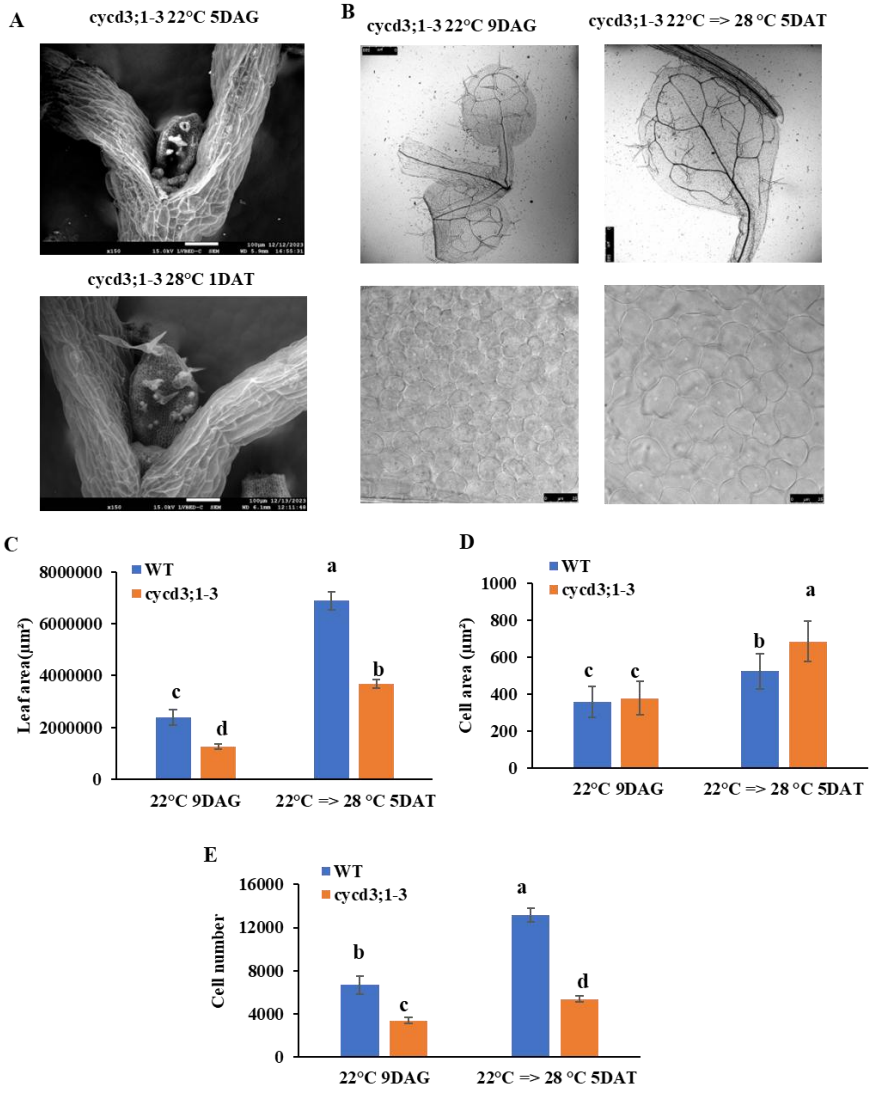

Supplemental Figure S8. The *cycd3,1-3* mutation positively affect hypocotyl elongation by promoting cell elongation, akin to the effects seen in the ectopic RBR-GFP line. **A**) Scanning electron microscopy (SEM) images depict the shoot apex of *cycd3,1-3* seedlings. An increase in leaf primordium size was noted 2 days after transfer (DAT) from 22ºC to 28ºC, compared to seedlings maintained at a constant 22ºC. The scale bar is indicated. **B**) The first leaf of *cycd3,1-3* mutant seedlings was imaged using a confocal laser microscope at both 22ºC and 28ºC, as indicated. The scale bar is indicated. Palisade cells of the first leaf of WT, RBR-GFP and *rbr1-2* seedlings were grown continuously at 22ºC for 9 days after germination (DAG) or for 4 DAG followed by 5 DAT at 28ºC. **C-E**)

Measurements were taken of the first leaf size (**C**), and the palisade cell area (**D**) for each genotype at both temperatures, and cell number was calculated (**E**).

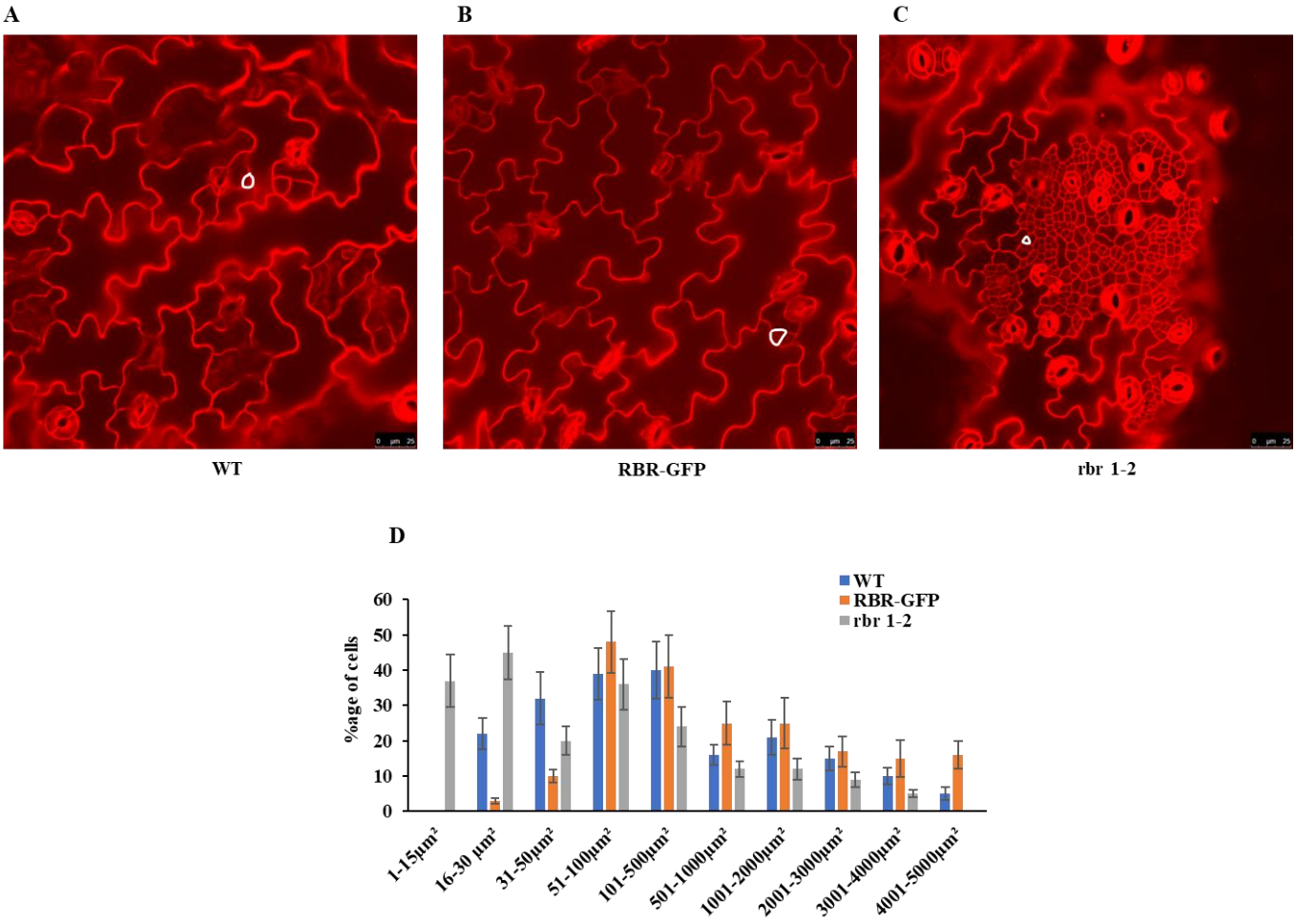

Supplemental Figure S9. The RBR regulates mersitemoid cell divison and cell size in post embryonic cotyledon. **A-C**) Representative images of propidium iodide-stained post-embryonic cotyledon at 7 days post-germination. The triangular cells highlighted in the images indicate the stomatal meristemoid cells. **D**) the spatial distribution of cell area is depicted across the whole cotyledon in all the three lines, with a minimum 200 cells counted.

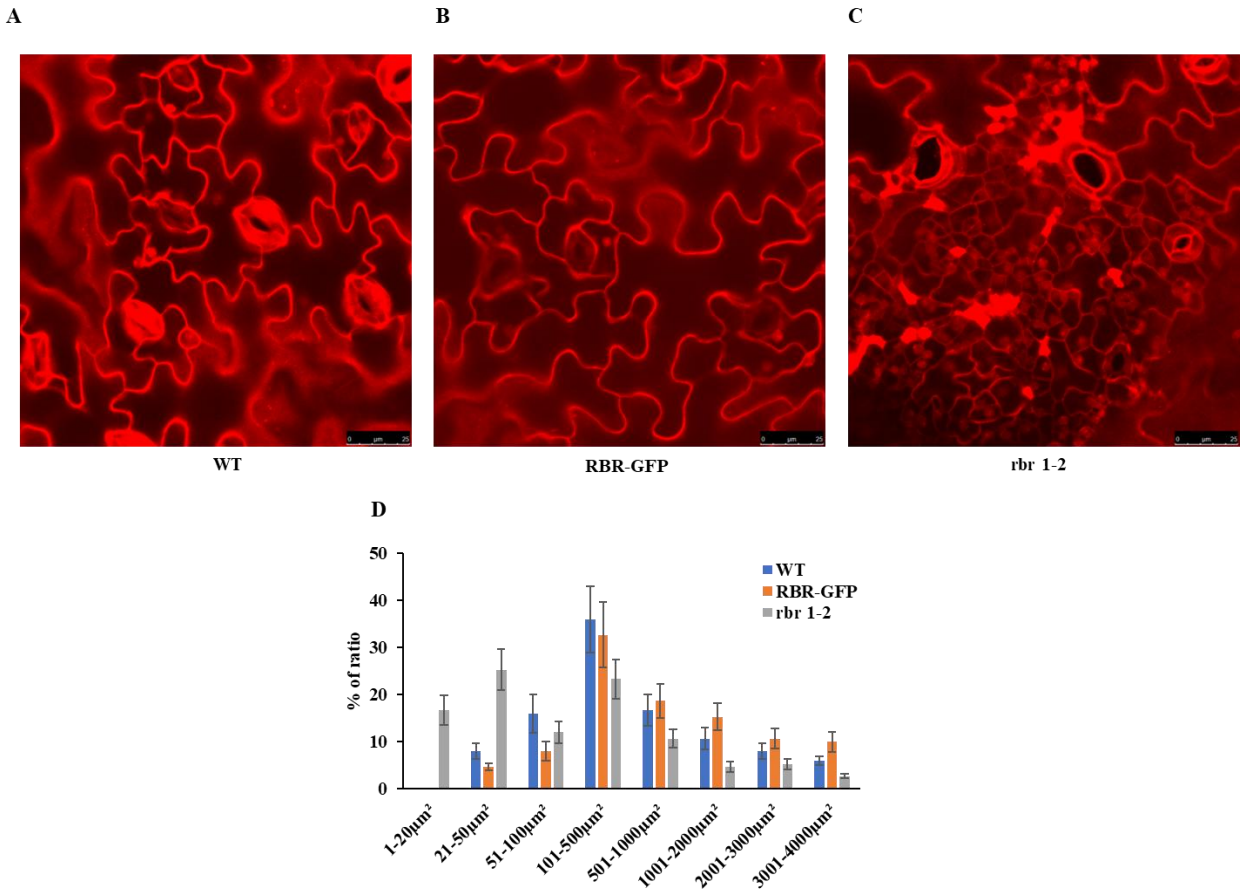

Supplemental Figure S10. The distribution of epidermal cell size indicates a pattern in *Arabidopsis* leaves that is dependent on RBR concentration. A-C) Representative images of the first leaf pair stained with propidium iodide, taken 14 days post germination. **D**) The spatial distribution of cell area across the whole cotyledon for all three lines, with a minimum of 150 cells counted.

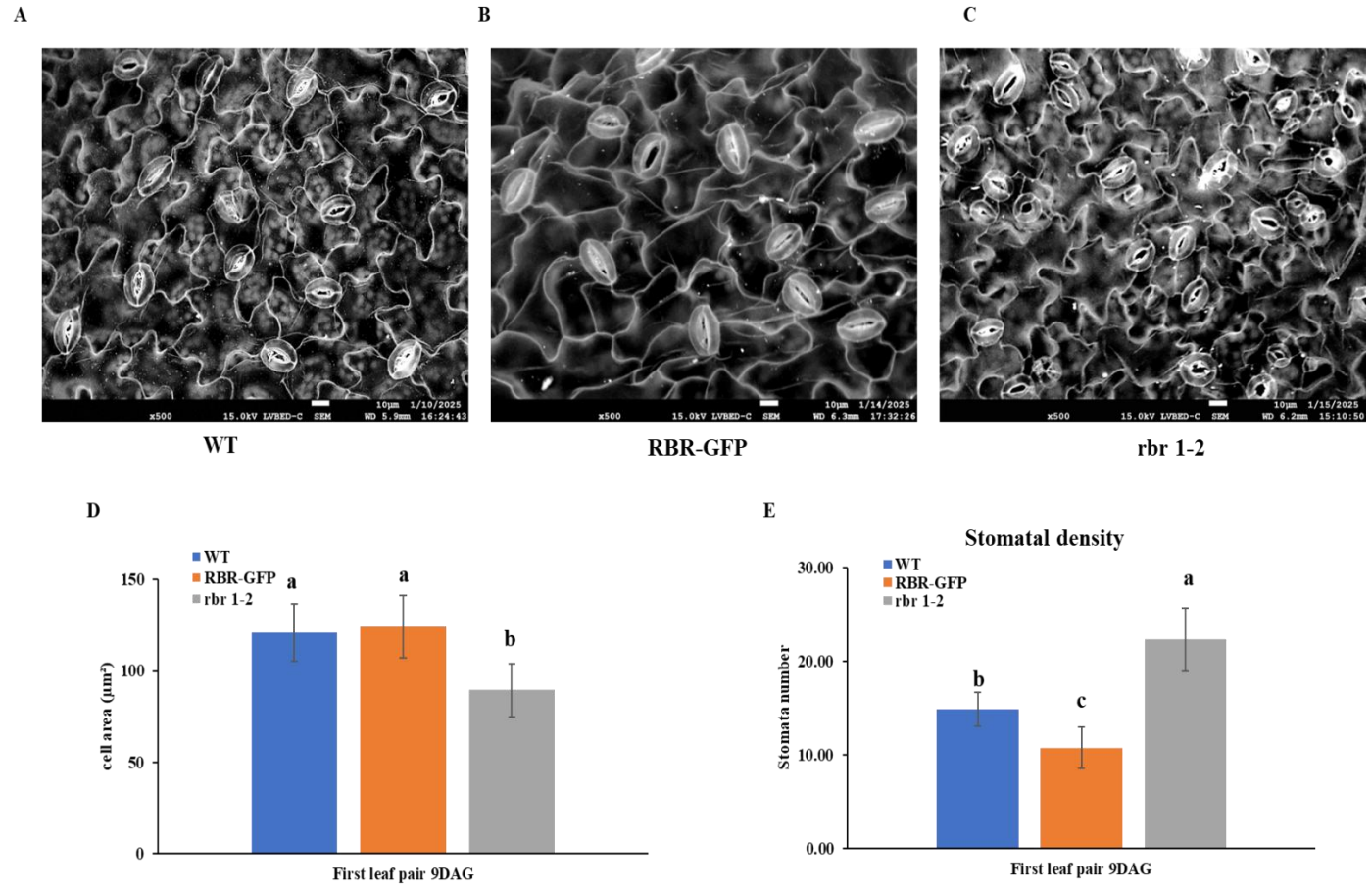

Supplemental Figure S11. The concentration of RBR is inversely correlated with stomatal density. A-C) Scanning Electron Microscopy (SEM) images of the first leaf pair, 9 days post-germination, are presented for the specified lines. The scale bar is indicated in the figure. **D**) The area of the guard cell was measured and plotted**. E**) the number of stomata per unit area was counted and plotted.

NAME	FWD Primer	REV Primer
ORC2	TCGACATTGTATGGTGCAAA	ACCATGTCAACGCTCCATTA
CDKB1;1	TCTGTTGGTTGTATCTTTGCTGA	CATTGCTGCTCAGTTGGTGT
CYCD3;1	GGCAACTACTGATGGGAGGT	TCACTGGGATTTCCTCAACA
CYCA3;1	CTCAGACACTCTTTACCTCGCT	AGCATTGAAGTAACTGCCAAAAGC
PIF4	TCAGGATCAAACCGAAGGAG	GAGGTATTAGTTCTTGCAAAGCC
PIF7	GAGCAGCTCGCTAGGTACATG	GTTGTTGTTGCACGGTCTG
YUCCA1	TGGTCTTGCCACTTCAGCAT	GGGAAGTCCAGGAGGGGTAA
YUCCA2	CCTTGAGTCTTACGCCGAAC	CCATAACCCACACCGCCTAT
YUCCA8	GTCGAACTTGTCAATGGAGAACA	CAATATGGGACGTTGCTGCG
YUCCA9	ATTTCTCAGAGCGGCCGATGT	ACAACGAATGGGACTCCTTGA
TIR1	CCCATATAATCGTGTTCCGGT	ATGAAGCAGCCGAGATTCAAA
HY5	CAGGCGACTGTCGGAGAAAGTCAAAGG	TCAACAACCTCTTCAGCCGCTTGTTCTC
SPCH	GCTGCTCTTGAAGATTTGGCT	CACTCAATTCCAATCTTGATGGTG
MUTE	CACGATTCGCCTAGAGACAAC	GCTGTAACTCCCCTCATGCTA
CYCD5;1	GACACCTCCACCGGAAATAG	TCTTGGCTGGTGGAGAACTT
CYCD7;1	CGGTATGGTTGGGGATCATA	ACGCTTGGTGGGTATTGAAG

Supplementary Table 1. Primer sequences

10. Declaration

I declare that the data used in the thesis written by SHIEKH RASIK BIN HAMID reflect the contribution of the doctoral candidate to the article: RETINOBLASTOMA-RELATED has both canonical and non-canonical regulatory functions during thermo-morphogenic responses in Arabidopsis seedlings, Plant cell and environment 2024. The results reported in the Ph.D. thesis and the publication were not used to acquire any Ph.D. degree previously. I further declare that the candidate has made significant contribution to the creation of the above-mentioned publication.